A New Approach for Studying Carbon Content of Urban Trees Using Non-Destructive Measurements of Tree Structure and Wood Traits.

by

Samit Kafle

A thesis submitted to the Graduate Faculty of
Auburn University
in partial fulfillment of the
requirements for the Degree of
Master of Science in Forestry

Auburn, Alabama
May 2, 2026

Keywords: urban trees; aboveground carbon; terrestrial laser scanning; carbon fraction; quantitative structure models; xylem vessel anatomy

Approved by

Dr. Georgios Arseniou, Chair, Assistant Professor & Extension Specialist, College of Forestry, Wildlife and Environment, Auburn University
Dr. Zhaofei (Joseph) Fan, Professor, College of Forestry, Wildlife and Environment, Auburn University
Dr. David W. MacFarlane, Professor, Department of Forestry, Michigan State University
Dr. Brian Via, Professor, College of Forestry, Wildlife and Environment, Auburn University

ABSTRACT

Accurate quantification of urban tree carbon is important for climate change mitigation. However, many estimates rely on allometric equations developed in natural forests, published wood density values, and a standard assumption that dry biomass is 50% carbon. These assumptions may not represent urban trees, which grow under very different and heterogeneous conditions. For example, street trees often face greater site constraints and stress than park trees, which can affect physiological processes and carbon accumulation.

In this study, we combined terrestrial laser scanning (TLS) for aboveground woody volume estimation with direct measurements of wood density, elemental analysis of wood carbon concentration (C%), and microscopic analysis of xylem vessel anatomy from increment cores. We sampled 90 trees of three species: *Quercus falcata*, *Quercus lyrata*, and *Taxodium distichum*, equally from street and park environments in Auburn, Alabama, USA.

The first chapter provides the conceptual and methodological foundation for the thesis. In the second chapter, we examined how species and growing environment affect wood C%, total aboveground carbon (AGC) biomass, and xylem vessel anatomy. Wood C% differed among species, with *T. distichum* having the highest and *Q. falcata* the lowest. In the two oak species, park trees had higher wood C% than street trees, whereas *T. distichum* showed no significant difference between environments. AGC scaled similarly with diameter across environments, but park trees accumulated more carbon at a given age than street trees. Microscopic analysis showed that park-grown oaks developed fewer but larger vessels, while street-grown oaks had more but smaller vessels. Vessel size was positively related to main-stem carbon biomass, but it explained only a small portion of the overall variation.

In the third chapter, we used TLS to quantify carbon allocation within sampled trees and compared TLS-based estimates with i-Tree-based estimates. Using measured wood density and carbon content instead of published defaults significantly affected AGC estimates in a species-dependent manner. TLS enabled component-level analysis, which showed that carbon allocation between the main stem and branches was species dependent, with *Q. lyrata* showing higher branch carbon relative to stem carbon than *Q. falcata* and *T. distichum*. Branch carbon decreased sharply with increasing branch order and was concentrated in large, low-order branches in the lower crown. TLS-based and i-Tree estimates were strongly correlated, but absolute agreement varied by species and was sensitive to the Crown Light Exposure (CLE) adjustment (open-grown biomass adjustment factor in i-Tree), which improved estimates for some species but worsened them for others.

Collectively, this study demonstrates that species and growing environment significantly influence both the biology of carbon storage and the precision of carbon estimation methods. The findings support the use of species-specific wood properties and TLS-based structural measurements for improving urban forest carbon accounting, developing urban-specific allometric equations, and guiding species selection and management strategies that enhance urban forest carbon sequestration.

Artificial Intelligence (AI) Use Disclosure Statement

In the preparation of this thesis, the following Artificial Intelligence (AI) tools were used: Microsoft 365 Copilot. This tool was used only to support the presentation and readability of the text. The author acknowledges full responsibility for the intellectual content of this work and has ensured that all AI-assisted sections have been reviewed and revised for accuracy and appropriate academic style. All AI-generated content was reviewed and validated for relevance, appropriateness, and accuracy before incorporation into the final document to maintain scholarly integrity of this research.

Digital Accessibility Disclosure Statement

In the preparation of this thesis, the following digital accessibility tools were used to ensure this document complies with federal requirements: Microsoft Word Accessibility Checker. The author acknowledges full responsibility for the intellectual content of this work and has made a good faith effort to comply with digital accessibility requirements in publishing, wherein the nature of the content does not significantly change in order to do so. Furthermore, all content has been reviewed and revised to meet these requirements prior to final publication.

Acknowledgments

This dissertation would not have been possible without the support, guidance, and encouragement of many individuals to whom I owe my deepest gratitude.

First, I want to sincerely thank my major advisor, Dr. Georgios Arseniou, for his constant mentorship, support, and patience throughout this journey. His passion for urban forests and commitment to high standards have greatly influenced my growth as a researcher. I feel fortunate to have had a mentor who valued this work and encouraged me to pursue it at the highest level.

I also want to thank my committee members for their valuable insights, helpful feedback, and generous time. Their diverse expertise enhanced both the scope and depth of this research. I am thankful to Dr. David MacFarlane for his thoughtful contributions as a co-author, especially for strengthening the analytical frameworks that support this work.

I thank the City of Auburn for coordinating access and logistical support for data collection across the city. I also thank the Donald E. Davis Arboretum at Auburn University for facilitating sampling on campus and for providing information about the study trees. I further acknowledge the College of Forestry, Wildlife, and Environment for providing access to the sample processing laboratory used in this study. In addition, I sincerely appreciate Dr. John Kush for making essential coring equipment available when needed.

To my colleagues and fellow graduate students in the College of Forestry, Wildlife, and Environment at Auburn University: thank you for the friendship, conversations, and shared resilience. You all made the days in the lab and the field meaningful.

This research was made possible by the resources and support from Auburn University, and I appreciate the opportunities I received as a Graduate Research and Teaching Assistant.

I also want to thank Divya Thapa, whose steady presence during the toughest moments meant more than I can express. Your support and encouragement helped me during uncertain times, and I am deeply grateful to have had you by my side.

Finally, I want to thank my family for their unconditional love and endless faith in my goals. To my beloved parents, Guru Prasad Kafle and Sarada Kafle, and my dear sister, Shreedhi Kafle: your belief in me across the miles has been the foundation of everything I have accomplished. This work is as much yours as it is mine, and I dedicate it to you with all my love and gratitude.

Table of Contents

ABSTRACT ii
Artificial Intelligence (AI) Use Disclosure Statement iv
Digital Accessibility Disclosure Statement v
Acknowledgments vi
Table of Contents viii
List of Tables xi
List of Figures xii
CHAPTER 1 1
INTRODUCTION 1
1.1 Urban Forests in the Context of Climate Change 1
1.2 Challenges in Quantifying Urban Tree Carbon 2
1.3 The Influence of Urban Growing Environments on Tree Carbon Dynamics 5
1.4 Xylem Vessel Anatomy as a Mechanistic Link Between Environment and Carbon Storage 6
1.5 Terrestrial Laser Scanning: A Non-Destructive Approach to Tree Carbon Quantification 8
1.6 The Need for Integrated Approaches 10
1.7 Thesis Objectives and Organization 10
References 12
CHAPTER 2 19
Species-specific characteristics and growing environment affect the carbon content and xylem structure of urban trees 19
Abstract 19
2.1 Introduction 20
2.2 Materials and methods 24
2.2.1 Study area 24
2.2.2 Terrestrial Laser Scanning (TLS) Data Collection and Processing 25
2.2.3 Wood density calculations 26
2.2.4 Carbon concentration - Quantification of Sampled Wood Cores 27

2.2.5 TLS-based carbon biomass estimation 28
2.2.6 Tree age quantification 28
2.2.7 Calculations of wood vessel metrics 29
2.2.8 Statistical analysis 30
2.3 Results 32
2.3.1 Differences in the carbon concentration of increment cores across species and growing environments 32
2.3.2 Relationship between total aboveground carbon biomass and DBH across growing environments 34
2.3.3 Relationship between total above-ground carbon biomass and age across growing environments 35
2.3.4 Relationship between DBH and age across growing environments 36
2.3.5 Differences in xylem vessel metrics across growing environments and the relationship between vessel metrics and the main stem carbon biomass 37
2.4 Discussion 40
2.4.1 Variation in the carbon concentration of increment cores among different species 40
2.4.2 Variation in the carbon concentration of increment cores in different growing environments 41
2.4.3 Allometric relationship between total aboveground carbon biomass, tree DBH, and age in different growing environments 43
2.4.4 Growing environment shapes xylem hydraulic architecture and stem carbon accumulation 45
2.5 Conclusions 47
References 48
CHAPTER 3 61
Enhancing the quantification of urban tree carbon stocks with the use of terrestrial laser scanning technology. 61
Abstract 61
3.1 Introduction 62
3.2 Materials and Methods 67

3.2.1 Study Area 67
3.2.2 Wood density and carbon content calculation from cores 68
3.2.3 Terrestrial Laser Scanning (TLS) and Quantitative Structure Models Generation 69
3.2.4 TLS-based total above-ground carbon estimates 71
3.2.5 i-Tree Carbon Estimation 72
3.2.6 Statistical analyses 73
3.3 Results 76
3.3.1 Measured Wood Properties 76
3.3.2 Effect of conversion parameters on TLS-based AGC 77
3.3.3 Leaf-off versus leaf-on TLS-based carbon estimates and rTwig correction 78
3.3.4 Total above-ground carbon biomass in main stem and branches 80
3.3.5 Carbon biomass distribution in branches 81
3.3.6 i-Tree versus -TLS-based carbon biomass estimates 85
3.4 Discussion 87
3.4.1 Implications of wood density and carbon concentration for AGC estimation 87
3.4.2 Leaf-on versus leaf-off AGC estimates 89
3.4.3 Stem–branch carbon allocation 92
3.4.4 TLS versus i-Tree-based carbon estimates 94
3.5 Conclusions 96
References 96
CHAPTER 4 105
OVERALL DISCUSSION AND CONCLUSIONS 105
4.1 Discussion 105
4.2 Limitations and Future Research 111
4.3 Conclusions 113
References 114

List of Tables

Table 2.1 Summary statistics of the size of the study trees..... 24

Table 2.2 Wood vessel metrics 30

Table 2.3 Comparison of xylem vessel metrics between park trees and street trees. 39

Table 3.1 Summary statistics of the size of study trees. 67

Table 3.2 Summary of wood trait values used for TLS volume to carbon conversion. 76

Table 3.3 Comparison of leaf-on versus leaf-off TLS-derived above-ground carbon biomass (AGC) estimates with and without rTwig correction for each species and across all species combined..... 80

Table 3.4 Comparison statistics between TLS-based above-ground carbon (AGC) and i-Tree-based AGC estimates, with and without the Crown Light Exposure (CLE) adjustment..... 86

List of Figures

Figure 2.1 Comparison of carbon concentration (C%) in increment cores collected from the study species *Quercus falcata, Quercus lyrata,* and *Taxodium distichum*. The boxes show the interquartile range with median lines. Different letters indicate significant ($p < 0.05$) differences in group means according to Tukey's post-hoc pairwise comparison. 33

Figure 2.2 Comparison of carbon concentration (C%) in increment cores between park and street trees across the three study species Quercus falcata, Quercus lyrata, and Taxodium distichum. Boxes show the interquartile range with median lines. 34

Figure 2.3 Relationship between total aboveground carbon biomass (AGC) and diameter at breast height (DBH) on a log scale for park and street trees. The 95% confidence interval has been plotted around the regression lines. 35

Figure 2.4 Relationship between total aboveground carbon biomass (AGC) and tree age on log-scale for park and street trees. The 95% confidence interval has been plotted around the regression lines..... 36

Figure 2.5 Relationship between diameter at breast height (DBH) and tree age on log-scale for park and street trees. The 95% confidence interval has been plotted around the regression lines. 37

Figure 2.6 Xylem vessel metrics in street versus park trees of Quercus falcata and Quercus lyrata combined. Boxplots show (a) mean lumen area (μm²), (b) vessel frequency (VFreq; number of vessels/mm^2), (c) hydraulically weighted diameter (HWD, μm), and (d) vulnerability index, across growing environments. 38

Figure 2.7 Relationships between main stem carbon biomass and xylem vessel metrics: a) Mean lumen area (μm²) and b) Hydraulically weighted diameter (μm) of two oak species. The 95% confidence interval has been plotted around the regression lines. 39

Figure 3.1 Species-specific sensitivity of TLS-derived above-ground carbon (AGC) to conversion parameters. Points show the mean percent difference, with standard deviations, in

AGC for Scenarios A–C relative to Scenario D (measured wood density and measured carbon concentration). The dashed vertical line indicates zero difference from Scenario D. 78

Figure 3.2 Leaf-on vs leaf-off TLS-based above-ground carbon (AGC) estimates with and without rTwig correction, shown for all species combined and by each species separately. Points indicate individual trees; red color indicates the use of rTwig, blue color indicates no use of rTwig. Solid lines represent linear regressions with 95% confidence intervals plotted around them. The dashed line indicates the 1:1 relationship. 79

Figure 3.3 Relationship between main-stem carbon biomass and total branch carbon biomass for all species combined and for individual species separately. The 95% confidence interval is plotted around the regression lines. Dashed lines indicate the 1:1 relationship. 81

Figure 3.4 Distribution of branch carbon biomass per branch order for all species combined and for individual species. 82

Figure 3.5 Distribution of branch carbon biomass across branch base diameter classes, shown for all species combined and for each species separately. 83

Figure 3.6 Relative vertical distribution (branch base height divided by total tree height) of branch carbon biomass (proportion of total branch carbon biomass) within crowns, shown for all trees combined and by species. The dashed horizontal line marks the mid-crown. 84

Figure 3.7 Regression comparisons of above-ground carbon biomass estimate from i-Tree Eco versus TLS-derived estimates shown for all trees combined and by species. Blue points and lines indicate i-Tree estimates without the CLE adjustment; red points and lines indicate i-Tree estimates with the CLE adjustment. Solid lines are fitted linear regressions with 95% confidence intervals plotted around them. The dashed black line indicates the 1:1 relationship. 85

CHAPTER 1

INTRODUCTION

1.1 Urban Forests in the Context of Climate Change

Urban forest refers to all trees in and around urban areas, including street trees, park trees, remnant woodlands, and trees on private property (Vogt 2020). It is one of the few nature-based solutions that can be implemented directly in built environments. Trees help mitigate climate change by absorbing carbon dioxide from the atmosphere through photosynthesis. They convert CO_2 into organic carbon compounds, which get stored in wood, bark, roots, and leaves (Nowak 1994). As long as a tree is alive and growing, it continues to gather carbon in its woody material. This process functions as both a carbon sink through new growth and a carbon pool through the storage of existing carbon biomass (Ariluoma et al. 2021; Bherwani et al. 2024).

In addition to capturing carbon, urban trees provide many other benefits that support the argument for investing in them as climate infrastructure. Trees cool the air through evapotranspiration and shading, which helps reduce the urban heat island effect and lower the energy needs for cooling buildings (Akbari et al. 2001; Zhao et al. 2010). Their canopies catch rainfall, reducing the amount and speed of stormwater runoff while easing the burden on drainage systems (Berland et al. 2017). They filter out airborne particulate matter and absorb harmful gases like ozone, nitrogen dioxide, and sulphur dioxide, which improves local air quality (Escobedo et al. 2011; Nowak et al. 2014). Urban forests promote biodiversity by offering habitats and ecological connections in otherwise fragmented landscapes (Lepczyk et al. 2017). Additionally, urban greenery enhances human physical and mental health by reducing stress and

improving cognitive function (Roy et al. 2012; Kuo 2015). These benefits are key reasons cities plant and maintain trees, making it essential for carbon accounting associated with urban forests to be credible. Unreliable carbon estimates could weaken the overall argument for urban greening.

As awareness of these benefits grows, cities are more explicitly including urban forests in climate action plans, sustainability frameworks, and greenhouse gas reporting guidelines. Cities throughout the United States and around the world now make specific commitments about the carbon value of their tree canopies (Churkina et al. 2020; Piana et al. 2021). They use quantitative estimates to support planting targets, set emissions offsets, or claim carbon credits (Piana et al. 2021). This means the success of urban forestry as a climate strategy relies on the accuracy and reliability of the carbon data that supports it. If the methods for estimating urban tree carbon are unclear, inconsistent, or biased, the resulting numbers can mislead policymakers, misallocate resources, and erode public trust in nature-based climate solutions (Nowak et al. 2013). Getting these figures right is not just an academic task; it is a practical necessity for responsible urban environmental management.

1.2 Challenges in Quantifying Urban Tree Carbon

The carbon content of a tree is the product of three quantities: the volume of its woody structure, the density of its wood, and the concentration of carbon within that wood (Chave et al. 2005; Martin et al. 2018). Estimating any one of these quantities accurately for a living tree is nontrivial, and errors in any single component propagate directly into the final carbon estimate (Vorster et al. 2020).

The standard method for estimating tree biomass relies on allometric equations; statistical models that predict total aboveground biomass (or volume) from simple field measurements such as diameter at breast height (DBH) and total tree height (Jenkins et al. 2003; Stovall et al. 2018; Arseniou et al. 2023). These equations are developed by destructively sampling trees: felling them, drying and weighing their components, and then fitting regression models that relate biomass to easily measurable dimensions (Chave et al. 2014; Weiskittel et al. 2015; Arseniou et al. 2023). The resulting equations can then be applied non-destructively to standing trees in inventories and monitoring programs. The fundamental problem for urban applications is that the vast majority of available allometric equations were developed from trees grown in closed-canopy forests, where competition for light drives tall, narrow growth forms with relatively small crowns (Jenkins et al. 2003; McHale et al. 2009). Urban trees, particularly those growing in open conditions, develop very different architectures like shorter trunks, wider crowns, heavier branching, and more spreading forms, that do not conform to the structural assumptions embedded in forest-derived equations (McHale et al. 2009; McPherson et al. 2016). When these equations are applied to urban trees, the mismatch between assumed and actual architecture can produce errors at the individual tree level (McHale et al. 2009). Even urban-specific equations, where they exist, are limited in the number of species they cover and the range of sizes and conditions they represent, making generalization difficult.

Many biomass estimation approaches require a value for wood density to convert volume estimates into mass. Wood density varies substantially among species, among individuals within a species, and even within a single tree: radially from pith to bark, vertically from base to crown, and between heartwood and sapwood (Williamson and Wiemann 2010; Demol et al. 2021). The common practice is to source a single representative wood density value from published

databases or literature compilations and then apply it uniformly across the tree (Nowak and Crane 2002; Miles and Smith 2009; Arseniou et al. 2023). While practical and sometimes unavoidable, this approach introduces systematic bias whose magnitude and direction depend on the species, the source of the published value, and how well it represents the specific population of trees being studied. For urban trees, which may grow under conditions quite different from the forest-grown individuals on which published densities are based, this mismatch can be especially consequential.

The final step in converting biomass to carbon requires a value for the fraction of dry wood mass that is elemental carbon. The Intergovernmental Panel on Climate Change (IPCC, 2006) recommends a default carbon fraction of 0.50 (i.e., 50%) for all tree species, and this value is embedded in widely used tools such as i-Tree Eco (Nowak 2024). However, measured wood carbon concentrations vary substantially across species, ranging from approximately 42% to 55%, with systematic differences between angiosperms (hardwoods) and gymnosperms (softwoods) driven largely by differences in lignin content and extractive chemistry (Lamlom and Savidge 2003; Thomas and Martin 2012; Martin et al. 2018).

The critical point is that these sources of error are not independent in practice. Each assumption layered onto the previous one either amplifies or, occasionally, compensates for the error already present, but the net effect is difficult to predict without measuring all three components directly. In the context of urban forests, where tree populations are highly heterogeneous in species, size, age, condition, and growing environment, the cumulative uncertainty can be substantial and can vary in unpredictable ways across the urban landscape. This is the methodological problem that motivates the present research.

1.3 The Influence of Urban Growing Environments on Tree Carbon Dynamics

Urban trees grow across a wide spectrum of site conditions, from highly constrained street corridors to relatively spacious park settings. These environments differ in ways that can significantly affect tree growth, physiology, and wood formation.

Street trees occupy some of the most challenging growing environments found in any landscape. Their rooting space is typically restricted by sidewalks, curbs, utility trenches, and building foundations, creating soil volumes that are often far too small to support the full root development of a mature tree (Randrup et al. 2001). The hard, impervious surfaces that surround them reduce rainfall infiltration and increase surface runoff, so that less water reaches the root zone even during adequate rainfall events (Yao et al. 2016). Soil compaction from foot traffic, vehicle loading, and construction activity reduces pore space, limits aeration, and further impedes root penetration and function (Moore et al. 2019). Street trees are exposed to de-icing salts in winter, elevated air temperatures from the urban heat island effect, reflected and re-radiated heat from pavement and buildings, mechanical damage from vehicles and pedestrians, and higher concentrations of gaseous and particulate air pollutants from vehicle exhaust (Randrup et al. 2001; Tang et al. 2024; Alonzo et al. 2025). Collectively, these stressors can reduce photosynthetic capacity, slow radial growth, alter patterns of carbon allocation, change wood chemistry, and shorten tree lifespans relative to trees of the same species growing in less constrained settings (Czaja et al. 2020; Patel et al. 2024).

Park trees, by contrast, generally grow in larger soil volumes with better structure, improved water infiltration, lower concentrations of pollutants, and substantially more room for both root and canopy development (North et al. 2018). However, park trees are not free of stress: depending on planting density, they may experience significant competition for light, water, and

nutrients, and they face their own set of management pressures, including mowing damage, compaction from foot traffic along paths, and variable maintenance regimes (Kleiber et al. 2019; Kraemer and Kabisch 2022).

The consequence of these environmental differences is that trees of the same species and the same age can exhibit markedly different sizes, growth rates, crown architectures, and health conditions depending on whether they grow on a street or in a park (Gregg et al. 2003; Pretzsch et al. 2017). They translate directly into differences in the total volume of wood produced, the rate at which that wood is deposited, the density and chemical composition of the wood itself, and therefore the total quantity of carbon stored in the tree.

1.4 Xylem Vessel Anatomy as a Mechanistic Link Between Environment and Carbon Storage

Recognizing that street trees and park trees store different amounts of carbon is an important observation. It becomes even more meaningful when we can connect it to underlying physiological mechanisms. One promising way to establish this connection is by studying xylem vessel anatomy.

Wood is a type of tissue that can move water. Its main role is to transport water and dissolved minerals from the roots to the leaves, where photosynthesis occurs (Sperry et al. 2002; Tyree and Zimmermann 2002). In angiosperm species, this transport happens through specialized cells called vessels. These vessels are elongated, hollow tubes formed by the fusion of individual vessel elements. The size, number, and arrangement of these vessels affect how well the wood can convey water (Tyree and Zimmermann 2002; Hacke et al. 2017). This ability, known as hydraulic conductivity, determines how quickly water can move to the leaves. This

regulates the rate of transpiration and gas exchange during photosynthesis (Whitehead 1998). Photosynthesis is how trees turn atmospheric carbon into organic compounds, so the wood's hydraulic architecture determines how fast the tree can absorb carbon (Cruiziat et al. 2002; Pfautsch 2016).

The link between hydraulic architecture and carbon absorption follows a well-known physical principle. According to the Hagen-Poiseuille equation, the flow rate through a cylindrical tube depends on the fourth power of its radius. So, a vessel that is twice as wide can carry sixteen times more water in the same amount of time, assuming everything else is equal (Tyree et al. 1994). Even small changes in vessel diameter can significantly impact the wood's total water transport capacity and subsequently affect the tree's photosynthetic ability and carbon fixation capacity.

This principle is relevant for urban trees, particularly considering the hydraulic efficiency-safety trade-off. Urban trees face various stresses, like limited water, soil compaction, and higher temperatures. Under these conditions, they tend to develop xylem with smaller, more numerous vessels (Pittermann et al. 2006; Hacke et al. 2017). Smaller vessels are less prone to cavitation, which is when air bubbles form and block water flow. This makes the hydraulic system more resilient to drought (Rissanen et al. 2025). However, this safety comes at the expense of efficiency. Smaller vessels move less water per unit area, leading to less water reaching the leaves, lower transpiration rates, more frequent stomatal closure, and reduced photosynthetic carbon gain.

Research has shown changes in xylem anatomy along urban-rural gradients and in response to specific urban challenges (Savi et al. 2015; Rissanen et al. 2025). This confirms that

the urban environment can alter the hydraulic structure of trees. However, no studies have directly looked at the relationship between xylem vessel features and carbon biomass in urban trees. This gap is significant because it allows us to see that street trees store less carbon than park trees without understanding the physiological mechanism behind this difference. Closing this gap, by measuring xylem vessel anatomy and carbon biomass in the same trees in different growing environments, could help explain the variations in carbon storage and guide the selection of species for urban planting programs that aim to maximize carbon benefits under challenging conditions.

1.5 Terrestrial Laser Scanning: A Non-Destructive Approach to Tree Carbon Quantification

The limitations of allometric equations for urban trees create a need for alternative methods that can capture the actual three-dimensional structure of individual trees without requiring destructive sampling (Weiskittel et al. 2015). Terrestrial laser scanning (TLS) offers precisely this capability.

TLS is an active remote sensing technology that emits millions of laser pulses to measure distances to surfaces and create a dense point cloud that represents tree structure in three-dimensions (Liang et al. 2016; Calders et al. 2020). TLS systems commonly use two measurement principles: time-of-flight (TOF) and phase-shift. In TOF systems, distance is calculated as a function of the time required for the laser pulse to reach the target and be recorded by the scanner. On the other hand, phase-shift systems estimate distance from the phase difference between a continuously modulated laser beam and its reflected signal (Calders et al., 2020). To convert these raw point clouds into volumetric estimates, we need to reconstruct quantitative structure models (QSMs). A QSM reconstructs the tree's woody skeleton as a

connected network of geometric primitives, typically cylinders, that are fitted sequentially along the stem and branches, following the branching topology of the tree from the base to the tips of the crown (Raumonen et al. 2013). Each cylinder in the model has a known position, orientation, length, and radius, so the total volume of the tree (or of any specified subset, such as the main stem, primary branches, or fine branches) can be calculated directly by summing the volumes of the constituent cylinders.

Multiple studies have validated TLS-derived biomass estimates against destructive reference measurements and have demonstrated that, with appropriate data collection and processing protocols, TLS can achieve accuracies comparable to or better than the best available allometric models, while eliminating the need for species- or region-specific equation calibration (Calders et al. 2015; Gonzalez de Tanago et al. 2018; Demol et al. 2022). Beyond accuracy, TLS offers several practical advantages for urban applications. Scanning is non-destructive, which is essential in urban settings where trees are valued community assets that cannot be felled for measurement. It captures structural detail, such as branch-level carbon allocation and crown architecture, that is simply inaccessible through traditional inventory methods (McHale et al. 2009; Lee et al. 2025). And it produces a permanent digital record of tree structure that can be revisited, reanalyzed, and compared with future scans to assess growth and change over time.

Despite these advantages, TLS is not a complete solution on its own. A QSM provides volume, but converting volume to carbon still requires wood density and carbon concentration values. If generic literature values are used for these conversions, the final carbon estimate inherits the same biases discussed earlier, biases that can negate the structural precision gained through TLS. Realizing the full potential of TLS for carbon quantification, therefore, requires pairing it with direct measurements of wood density and carbon concentration from the same

trees, creating an internally consistent measurement chain from three-dimensional structure to elemental carbon.

1.6 The Need for Integrated Approaches

Addressing the shortcomings of current urban tree carbon estimation methods requires an integrated approach that measures each component of the volume-to-carbon conversion chain as directly and accurately as possible. This thesis adopts such an approach. It combines TLS for non-destructive, three-dimensional volume quantification; basic wood density measurement from increment cores extracted from the study trees; elemental analysis (using a CHN analyzer) for direct determination of wood carbon concentration; and microscopic analysis of xylem vessel anatomy to understand the physiological drivers of carbon storage differences between growing environments. By applying all these methods to the same study trees across contrasting urban settings, the research provides an internally consistent dataset that can be used to evaluate where existing estimation tools perform well, where common assumptions break down, and what the practical consequences of those breakdowns are for urban forest carbon accounting.

1.7 Thesis Objectives and Organization

The overall goal of this thesis is to advance both the understanding and the quantification of aboveground carbon content in urban trees. To achieve this goal, the thesis is organized into four chapters, including two main study chapters, each addressing a complementary set of research objectives.

Chapter 1: This chapter provides the conceptual and methodological rationale for the thesis. It reviews the importance of urban forests in climate-change mitigation, outlines the major challenges associated with quantifying carbon in urban trees, and introduces the biological and

methodological factors that motivate this research, including urban growing environment, wood traits, xylem anatomy, and terrestrial laser scanning (TLS). The chapter concludes by defining the research objectives and the overall structure of the thesis.

Chapter 2: Species-specific characteristics and growing environment effects on the carbon content of urban trees. This chapter examines: (1) how species and growing environment (street versus park) influence the carbon concentration of woody tissue; (2) how total aboveground carbon biomass scales with tree size and age across species and growing environments; and (3) how xylem vessel anatomy differs between park and street trees of the two ring-porous oak species and whether vessel metrics are related to carbon biomass.

Chapter 3: Enhancing the quantification of urban tree carbon content through terrestrial laser scanning. This chapter examines: (1) how the choice of conversion parameters affects TLS-derived carbon estimates; (2) how urban trees allocate carbon in the main stem and branches, and how this allocation varies by species, branch order, branch size class, and position within the crown; and (3) how TLS-based carbon estimates compare with i-Tree-based estimates.

Chapter 4: Overall Discussion and Conclusions. The findings from Chapters 2 and 3 are synthesized in a final chapter that brings together the biological and methodological threads of the thesis. This chapter discusses the broader implications of the findings for urban forest management practices, carbon accounting policy, and greenhouse gas reporting, species selection for urban tree planting programs, along with limitations and future research directions. Together, these chapters provide a comprehensive assessment of both the biological factors and the measurement methods that determine the accuracy of urban forest carbon estimates.

References

Akbari, H., M. Pomerantz, and H. Taha. 2001. Cool surfaces and shade trees to reduce energy use and improve air quality in urban areas. *Solar Energy* 70(3):295–310. https://doi.org/10.1016/S0038-092X(00)00089-X.

Alonzo, M., P. C. Ibsen, and D. H. Locke. 2025. Urban Trees and Cooling: A Review of the Recent Literature (2018 to 2024). *Arboriculture & Urban Forestry* 51(5):420–444. https://doi.org/10.48044/JAUF.2025.023.

Ariluoma, M., J. Ottelin, R. Hautamäki, E. M. Tuhkanen, and M. Mänttäri. 2021. Carbon sequestration and storage potential of urban green in residential yards: A case study from Helsinki. *Urban Forestry & Urban Greening* 57:126939. https://doi.org/10.1016/J.UFUG.2020.126939.

Arseniou, G., D. W. MacFarlane, K. Calders, and M. Baker. 2023. Accuracy differences in aboveground woody biomass estimation with terrestrial laser scanning for trees in urban and rural forests and different leaf conditions. *Trees - Structure and Function* 37(3):761–779. https://doi.org/10.1007/S00468-022-02382-1/.

Berland, A., S. A. Shiflett, W. D. Shuster, A. S. Garmestani, H. C. Goddard, D. L. Herrmann, and M. E. Hopton. 2017. The role of trees in urban stormwater management. *Landscape and Urban Planning* 162:167–177. https://doi.org/10.1016/j.landurbplan.2017.02.017.

Bherwani, H., T. Banerji, and R. Menon. 2024. Role and value of urban forests in carbon sequestration: review and assessment in Indian context. *Environment, Development and Sustainability* 26(1):603–626. https://doi.org/10.1007/S10668-022-02725-5/.

Calders, K., J. Adams, J. Armston, H. Bartholomeus, S. Bauwens, L. P. Bentley, J. Chave, et al. 2020. Terrestrial laser scanning in forest ecology: Expanding the horizon. *Remote Sensing of Environment* 251:112102. https://doi.org/10.1016/J.RSE.2020.112102.

Calders, K., G. Newnham, A. Burt, S. Murphy, P. Raumonen, M. Herold, D. Culvenor, et al. 2015. Nondestructive estimates of above-ground biomass using terrestrial laser scanning. *Methods in Ecology and Evolution* 6(2):198–208. https://doi.org/10.1111/2041-210X.12301.

Chave, J., C. Andalo, S. Brown, M. A. Cairns, J. Q. Chambers, D. Eamus, H. Fölster, et al. 2005. Tree allometry and improved estimation of carbon stocks and balance in tropical forests. *Oecologia* 145(1):87–99. https://doi.org/10.1007/S00442-005-0100-X/.

Chave, J., M. Réjou-Méchain, A. Búrquez, E. Chidumayo, M. S. Colgan, W. B. C. Delitti, A. Duque, T. Eid, P. M. Fearnside, and R. C. Goodman. 2014. Improved allometric models to estimate the aboveground biomass of tropical trees. *Global change biology* 20(10):3177–3190.

Churkina, G., A. Organschi, C. P. O. Reyer, A. Ruff, K. Vinke, Z. Liu, B. K. Reck, T. E. Graedel, and H. J. Schellnhuber. 2020. Buildings as a global carbon sink. *Nature Sustainability* 3(4):269–276. https://doi.org/10.1038/s41893-019-0462-4.

Cruiziat, P., H. Cochard, and T. Améglio. 2002. Hydraulic architecture of trees: main concepts and results. *Annals of Forest Science* 59(7):723–752. https://doi.org/10.1051/forest:2002060.

Czaja, M., A. Kołton, and P. Muras. 2020. The Complex Issue of Urban Trees—Stress Factor Accumulation and Ecological Service Possibilities. *Forests 2020, Vol. 11, Page 932* 11(9):932. https://doi.org/10.3390/F11090932.

Demol, M., K. Calders, S. M. Krishna Moorthy, J. Van den Bulcke, H. Verbeeck, and B. Gielen. 2021. Consequences of vertical basic wood density variation on the estimation of aboveground biomass with terrestrial laser scanning. *Trees - Structure and Function* 35(2):671–684. https://doi.org/10.1007/S00468-020-02067-7/.

Demol, M., H. Verbeeck, B. Gielen, J. Armston, A. Burt, M. Disney, L. Duncanson, et al. 2022. Estimating forest above-ground biomass with terrestrial laser scanning: Current status and future directions. *Methods in Ecology and Evolution* 13(8):1628–1639. https://doi.org/10.1111/2041-210X.13906.

Escobedo, F. J., T. Kroeger, and J. E. Wagner. 2011. Urban forests and pollution mitigation: Analyzing ecosystem services and disservices. *Environmental Pollution* 159(8–9):2078–2087. https://doi.org/10.1016/J.ENVPOL.2011.01.010.

Gonzalez de Tanago, J., A. Lau, H. Bartholomeus, M. Herold, V. Avitabile, P. Raumonen, C. Martius, et al. 2018. Estimation of above-ground biomass of large tropical trees with

terrestrial LiDAR. *Methods in Ecology and Evolution* 9(2):223–234. https://doi.org/10.1111/2041-210X.12904.

Gregg, J. W., C. G. Jones, and T. E. Dawson. 2003. Urbanization effects on tree growth in the vicinity of New York City. *Nature 2003 424:6945* 424(6945):183–187. https://doi.org/10.1038/nature01728.

Hacke, U. G., R. Spicer, S. G. Schreiber, and L. Plavcová. 2017. An ecophysiological and developmental perspective on variation in vessel diameter. *Plant Cell and Environment* 40(6):831–845. https://doi.org/10.1111/pce.12777.

Jenkins, J. C., D. C. Chojnacky, L. S. Heath, and R. A. Birdsey. 2003. National scale biomass estimators for United States tree species. *Forest Science. 49: 12-35*.

Kleiber, T., M. Krzyzaniak, D. Swierk, A. Haenel, and S. Galecka. 2019. How does the content of nutrients in soil affect the health status of trees in city parks? *PLOS ONE* 14(9):e0221514. https://doi.org/10.1371/journal.pone.0221514.

Kraemer, R., and N. Kabisch. 2022. Parks Under Stress: Air Temperature Regulation of Urban Green Spaces Under Conditions of Drought and Summer Heat. *Frontiers in Environmental Science* 10:849965. https://doi.org/10.3389/fenvs.2022.849965.

Kuo, M. 2015. How might contact with nature promote human health? Promising mechanisms and a possible central pathway. *Frontiers in Psychology* 6:141022. https://doi.org/10.3389/fpsyg.2015.01093.

Lamlom, S. H., and R. A. Savidge. 2003. A reassessment of carbon content in wood: variation within and between 41 North American species. *Biomass and Bioenergy* 25(4):381–388. https://doi.org/10.1016/S0961-9534(03)00033-3.

Lee, J. M., H. S. Kim, B. Choi, J. Y. Jung, S. Lee, H. Jo, G. Kim, et al. 2025. Enhanced Accuracy in Urban Tree Biomass Estimation: Developing Allometric Equations with Land Use Classifications. *Forests 2025, Vol. 16,* 16(5). https://doi.org/10.3390/f16050841.

Lepczyk, C. A., M. F. J. Aronson, K. L. Evans, M. A. Goddard, S. B. Lerman, and J. S. Macivor. 2017. Biodiversity in the City: Fundamental Questions for Understanding the Ecology of Urban Green Spaces for Biodiversity Conservation. *BioScience* 67(9):799–807. https://doi.org/10.1093/biosci/bix079.

Liang, X., V. Kankare, J. Hyyppä, Y. Wang, A. Kukko, H. Haggrén, X. Yu, et al. 2016. Terrestrial laser scanning in forest inventories. *ISPRS Journal of Photogrammetry and Remote Sensing* 115:63–77. https://doi.org/10.1016/J.ISPRSJPRS.2016.01.006.

Martin, A. R., M. Doraisami, and S. C. Thomas. 2018. Global patterns in wood carbon concentration across the world's trees and forests. *Nature Geoscience 2018 11:12* 11(12):915–920. https://doi.org/10.1038/s41561-018-0246-x.

McHale, M. R., I. C. Burke, M. A. Lefsky, P. J. Peper, and E. G. McPherson. 2009. Urban forest biomass estimates: is it important to use allometric relationships developed specifically for urban trees? *Urban Ecosystems* 12(1):95–113. https://doi.org/10.1007/s11252-009-0081-3.

McPherson, E. G., N. S. van Doorn, and P. J. Peper. 2016. Urban tree database and allometric equations. https://doi.org/10.2737/PSW-GTR-253.

Miles, P. D., and W. Brad. Smith. 2009. *Specific gravity and other properties of wood and bark for 156 tree species found in North America*. U.S. Department of Agriculture, Forest Service, Northern Research Station. https://doi.org/10.2737/nrs-rn-38.

Moore, G. M., A. Fitzgerald, P. B. May, G. M. Moore, A. Fitzgerald, and P. B. May. 2019. Soil Compaction Affects the Growth and Establishment of Street Trees in Urban Australia. *Arboriculture & Urban Forestry* 45(6):239–253. https://doi.org/10.48044/jauf.2019.020.

North, E. A., A. W. D'Amato, and M. B. Russell. 2018. Performance Metrics for Street and Park Trees in Urban Forests. *Journal of Forestry* 116(6):547–554. https://doi.org/10.1093/JOFORE/FVY049.

Nowak, D. J. 1994. Atmospheric carbon dioxide reduction by Chicago's urban forest. *Chicago's urban forest ecosystem: Results of the Chicago urban forest climate project* :83–94.

Nowak, D. J. 2024. *Understanding i-Tree: 2023 summary of programs and methods*. U.S. Department of Agriculture, Forest Service, Northern Research Station. https://doi.org/10.2737/nrs-gtr-200-2023.

Nowak, D. J., and D. E. Crane. 2002. Carbon storage and sequestration by urban trees in the USA. *Environmental Pollution* 116(3):381–389. https://doi.org/10.1016/S0269-7491(01)00214-7.

Nowak, D. J., E. J. Greenfield, R. E. Hoehn, and E. Lapoint. 2013. Carbon storage and sequestration by trees in urban and community areas of the United States. *Environmental Pollution* 178:229–236. https://doi.org/10.1016/J.ENVPOL.2013.03.019.

Nowak, D. J., S. Hirabayashi, A. Bodine, and E. Greenfield. 2014. Tree and forest effects on air quality and human health in the United States. *Environmental Pollution* 193:119–129. https://doi.org/10.1016/j.envpol.2014.05.028.

Patel, V. V., S. Vishwakarma, and R. Gangwar. 2024. Urban Tree Selection and Management Strategies for Climate Adaptation. *Urban Forests, Climate Change and Environmental Pollution* :391–415. https://doi.org/10.1007/978-3-031-67837-0_19.

Pfautsch, S. 2016. Hydraulic Anatomy and Function of Trees—Basics and Critical Developments. *Current Forestry Reports* 2(4):236–248. https://doi.org/10.1007/s40725-016-0046-8.

Piana, M. R., C. C. Pregitzer, and R. A. Hallett. 2021. Advancing management of urban forested natural areas: toward an urban silviculture? *Frontiers in Ecology and the Environment* 19(9):526–535. https://doi.org/10.1002/fee.2389.

Pittermann, J., J. S. Sperry, J. K. Wheeler, U. G. Hacke, and E. H. Sikkema. 2006. Mechanical reinforcement of tracheids compromises the hydraulic efficiency of conifer xylem. *Plant, Cell and Environment* 29(8):1618–1628. https://doi.org/10.1111/J.1365-3040.2006.01539.X;SUBPAGE:STRING:FULL.

Pretzsch, H., P. Biber, E. Uhl, J. Dahlhausen, G. Schütze, D. Perkins, T. Rötzer, et al. 2017. Climate change accelerates growth of urban trees in metropolises worldwide /631/158/858 /704/158/2165 article. *Scientific Reports* 7(1). https://doi.org/10.1038/s41598-017-14831-w.

Randrup, T. B., E. G. McPherson, and L. R. Costello. 2001. A review of tree root conflicts with sidewalks, curbs, and roads. *Urban Ecosystems* 5(3):209–225. https://doi.org/10.1023/a:1024046004731.

Raumonen, P., M. Kaasalainen, M. Åkerblom, S. Kaasalainen, H. Kaartinen, M. Vastaranta, M. Holopainen, M. Disney, and P. Lewis. 2013. Fast Automatic Precision Tree Models from

Terrestrial Laser Scanner Data. *Remote Sensing* 5(2):491–520. https://doi.org/10.3390/rs5020491.

Rissanen, K., V. Vitali, D. Kneeshaw, and A. Paquette. 2025. Vessel anatomy of urban Celtis occidentalis trees varies to favour safety or efficiency depending on site conditions. *Trees 2025 39:1* 39(1):1–15. https://doi.org/10.1007/S00468-025-02603-3.

Roy, S., J. Byrne, and C. Pickering. 2012. A systematic quantitative review of urban tree benefits, costs, and assessment methods across cities in different climatic zones. *Urban Forestry & Urban Greening* 11(4):351–363. https://doi.org/10.1016/J.UFUG.2012.06.006.

Savi, T., S. Bertuzzi, S. Branca, M. Tretiach, and A. Nardini. 2015. Drought-induced xylem cavitation and hydraulic deterioration: risk factors for urban trees under climate change? *New Phytologist* 205(3):1106–1116. https://doi.org/10.1111/NPH.13112.

Sperry, J. S., U. G. Hacke, R. Oren, and J. P. Comstock. 2002. Water deficits and hydraulic limits to leaf water supply. *Plant, Cell & Environment* 25(2):251–263. https://doi.org/10.1046/j.0016-8025.2001.00799.x.

Stovall, A. E. L., H. H. Shugart, A. E. L. Stovall, K. J. Anderson-Teixeira, and K. J. Anderson-Teixeira. 2018. Assessing terrestrial laser scanning for developing non-destructive biomass allometry. *Forest Ecology and Management* 427:217–229. https://doi.org/10.1016/J.FORECO.2018.06.004.

Tang, L., G. Shao, and P. M. Groffman. 2024. Urban trees: how to maximize their benefits for humans and the environment. *Nature* 626(7998):261. https://doi.org/10.1038/D41586-024-00300-8;SUBJMETA.

Thomas, S. C., and A. R. Martin. 2012. Carbon Content of Tree Tissues: A Synthesis. *Forests 2012, Vol. 3, Pages 332-352* 3(2):332–352. https://doi.org/10.3390/f3020332.

Tyree, M. T., S. D. Davis, and H. Cochard. 1994. Biophysical Perspectives of Xylem Evolution: is there a Tradeoff of Hydraulic Efficiency for Vulnerability to Dysfunction? *IAWA Journal* 15(4):335–360. https://doi.org/10.1163/22941932-90001369.

Tyree, M. T., and M. H. Zimmermann. 2002. Xylem Structure and the Ascent of Sap. https://doi.org/10.1007/978-3-662-04931-0.

Vogt, J. 2020. Urban Forests: Biophysical Features and Benefits. P. V5-48-V5-57 in *Encyclopedia of the World's Biomes: Volumes 1-5*, Elsevier. https://doi.org/10.1016/B978-0-12-409548-9.12404-2.

Vorster, A. G., P. H. Evangelista, A. E. L. Stovall, and S. Ex. 2020. Variability and uncertainty in forest biomass estimates from the tree to landscape scale: the role of allometric equations. *Carbon Balance and Management* 15(1):8. https://doi.org/10.1186/s13021-020-00143-6.

Weiskittel, A. R., D. W. MacFarlane, P. J. Radtke, D. L. R. Affleck, H. Temesgen, C. W. Woodall, J. A. Westfall, and J. W. Coulston. 2015. A Call to Improve Methods for Estimating Tree Biomass for Regional and National Assessments. *Journal of Forestry* 113(4):414–424. https://doi.org/10.5849/JOF.14-091.

Whitehead, D. 1998. Regulation of stomatal conductance and transpiration in forest canopies. *Tree Physiology* 18(8–9):633–644. https://doi.org/10.1093/treephys/18.8-9.633.

Williamson, G. B., and M. C. Wiemann. 2010. Measuring wood specific gravity...correctly. *American Journal of Botany* 97(3):519–524. https://doi.org/10.3732/ajb.0900243.

Yao, L., W. Wei, and L. Chen. 2016. How does imperviousness impact the urban rainfall-runoff process under various storm cases? *Ecological Indicators* 60(3):893–905. https://doi.org/10.1016/j.ecolind.2015.08.041.

Zhao, M., Z. hong Kong, F. J. Escobedo, and J. Gao. 2010. Impacts of urban forests on offsetting carbon emissions from industrial energy use in Hangzhou, China. *Journal of Environmental Management* 91(4):807–813. https://doi.org/10.1016/J.JENVMAN.2009.10.010.

CHAPTER 2

Species-specific characteristics and growing environment affect the carbon content and xylem structure of urban trees.

Abstract

Urban trees grow under a wide range of conditions, which can affect their biomass and wood carbon concentration, thus affecting estimates of urban forest carbon storage. This study aims to determine how species characteristics and the local growing environment (street versus park) influence the carbon content of urban trees, including an assessment of how xylem vessel metrics help explain differences in carbon content accumulation. We sampled 90 trees of three species (*Quercus falcata*, *Quercus lyrata*, and *Taxodium distichum;* 30 trees per species) in Auburn, Alabama, at street and park sites. We scanned all study trees using a Terrestrial Laser Scanner (TLS) to obtain precise aboveground, woody volume estimates, which were converted to total aboveground carbon (AGC) using measured wood density and carbon concentration (C%) from wood increment core samples. We found that the wood C% in cores varied significantly by species and growing environment. *T. distichum* had significantly higher wood C% than the two oak species, and oak trees exhibited higher wood C% in parks compared to streets. The total aboveground carbon (AGC) showed similar scaling relationships with tree size in both street and park environments, but park trees accumulated more AGC at a given age, because of both faster growth rates and greater carbon concentrations in the wood. Microscopic analyses of increment cores from the two oak species revealed that xylem vessel metrics differ significantly between urban growing environments. Park-grown oaks developed fewer, larger vessels (promoting hydraulic efficiency), whereas street-grown oaks had many small vessels

(favoring hydraulic safety). These results have important implications for effective urban forest management and tree species selection to strengthen the role of urban forests in atmospheric carbon sequestration under a changing climate.

2.1 Introduction

As global urbanization accelerates, the role of urban forests in atmospheric carbon sequestration becomes more important. Urban areas cover only about 3% of Earth's land surface. Yet they contain more than 55% of the world's population, projected to rise to 68% by 2050 (UN DESA, 2018) and account for an estimated 70% of global carbon dioxide (CO_2) emissions (Nations 2012; Crippa et al. 2021). At the same time, atmospheric CO_2 concentrations exceeded 420 ppm in 2023 (Muller-Feuga 2024), reinforcing the need for effective climate change mitigation strategies. In this context, urban forests are increasingly recognized as a key component of climate action (Nowak and Crane 2002; Roy et al. 2012; IPCC 2023; Hutt-Taylor et al. 2024). In addition to providing ecosystem services such as temperature regulation, stormwater management, and air quality improvement (Zhao et al. 2010; Escobedo et al. 2011), urban trees directly contribute to climate change mitigation by sequestering atmospheric CO_2 and storing it in woody biomass (Hoover and Riddle 2020).

Carbon sequestration in urban trees varies widely. An individual tree may store approximately 0.5 to 3.0 kg of carbon per year, depending on species, age, size, and local growing conditions (Nowak et al. 2013; McPherson et al. 2013), and urban forests can store substantial carbon at the city level. For example, urban trees in the United States collectively sequester about 22.8 million tons of atmospheric CO_2 annually (Nowak and Crane 2002). However, estimates of urban tree and urban forest carbon sequestration remain highly uncertain, in part because many assessments rely on methods developed for rural forest conditions rather

than the urban environment. Since tree carbon capture is the product of (1) tree biomass and (2) the carbon concentration of that biomass (C%), new research needs to focus on understanding how urban environments affect both elements.

Uncertainty in urban tree biomass estimates is largely driven by differences in tree form and biomass allocation between urban and forest settings. Urban trees often experience reduced competition, altered light environment, routine management (e.g., pruning), and site constraints, which can produce different stem form, crown architecture, and allocation patterns than forest-grown trees of the same species (McPherson et al. 2016; Ngo and Lum 2018). This generally results in urban trees having a different 'allometry', meaning the relationship between the growth of different parts of the tree. As a result, forest-derived allometric equations can produce large errors in biomass estimation when applied in cities. For instance, McHale et al. (2009) reported that biomass predictions for urban trees using forest-derived equations could vary by up to 300%. More generally, several studies have emphasized that biomass models are frequently used outside the conditions under which they were developed and have called for improved approaches and calibration data to reduce systematic error in biomass and carbon assessments (Chave et al. 2014; Weiskittel et al. 2015; Radtke et al. 2017; Vorster et al. 2020). This points to a need to create new biomass equations for urban conditions.

Improving biomass equations traditionally requires destructive sampling and weighing, but tree removal is typically not feasible in urban settings due to cost, permitting, and public concerns (McHale et al. 2009; Lee et al. 2025). Given these constraints, terrestrial laser scanning (TLS) has emerged as a powerful tool for non-destructive biomass quantification (Weiskittel et al. 2015; Disney et al. 2018; Arseniou et al. 2023). TLS is an active remote sensing technology that emits millions of laser pulses to measure distances to surfaces and create a dense point cloud

that represents tree structure in three-dimensional space (Liang et al. 2016; Calders et al. 2020). Recent applications of TLS have demonstrated its effectiveness for providing consistent accuracy in biomass estimation across different DBH sizes, unlike allometric equations, where error increased with tree size (Disney et al. 2018, 2020; Wilkes et al. 2018; Krause et al. 2023). TLS, therefore, offers a robust, non-destructive pathway to quantify the structural component of above-ground biomass.

Even with very good estimates of tree biomass, urban tree carbon stocks depend on converting biomass to carbon using an appropriate C%. The assumption that tree biomass contains 50% carbon by mass has become a standard value in carbon accounting protocols (IPCC 2006; Klein et al. 2021). However, studies have demonstrated that wood C% varies substantially across growing environments and among species, ranging from about 41% to 51% (Lamlom and Savidge 2003; Martin and Thomas 2011). Street trees are exposed to multiple environmental stressors, including limited space for root growth, impervious surfaces that reduce water infiltration, soil compaction, higher local atmospheric temperatures associated with the urban heat island effect, deicing salts, air pollution, and mechanical damage (Randrup et al. 2001; Tang et al. 2024; Alonzo et al. 2025). These stressors may reduce photosynthetic capacity, shift carbon allocation patterns, and alter wood formation processes (Czaja et al. 2020; Patel et al. 2024). By contrast, park trees may experience less harsh growing conditions, including greater available soil volume, better soil quality, and lower exposure to pollution, although they may face greater competition for resources depending on tree crowding (North et al. 2018). So, differences in urban tree growing conditions might alter the C% by influencing tree growth rates, crown architecture, and stress responses (Gregg et al. 2003; Pretzsch et al. 2017). In general, the net effect of the urban growing conditions on tree C% remains poorly understood.

Xylem vessel characteristics may provide a mechanistic link between urban growing conditions and tree carbon dynamics. Vessel anatomy influences hydraulic conductivity, which determines water delivery to leaves and can therefore affect photosynthetic carbon assimilation (Brodribb and Feild 2000; Santiago et al. 2004). Because urban trees frequently experience chronic water stress, they may develop a wood anatomy that balances hydraulic efficiency with resistance to hydraulic cavitation (Savi et al. 2015; Rissanen et al. 2025). Such anatomical adjustments can influence wood density, carbon allocation, and ultimately wood carbon biomass. While some studies have documented altered xylem characteristics in urban trees, including reduced vessel diameters under stress, the relationship between vessel anatomy and carbon biomass in urban trees remains unexplored (Savi et al. 2015; Rissanen et al. 2025).

In this study, we employed an integrated approach combining terrestrial laser scanning (TLS) for precise aboveground biomass quantification of urban trees, elemental analysis for direct measurement of C% in woody core samples, and microscopic wood vessel metrics analysis to understand mechanistic drivers of urban tree carbon storage. The objectives of this study were: (1) to examine differences in carbon concentration (C%) of woody cores sampled from street trees and park trees of different species, (2) to quantify and compare total aboveground carbon biomass (AGC, kg) of street trees and park trees using TLS, and (3) to quantify wood vessel metrics that may explain differences in the carbon biomass captured in street and park trees. This comprehensive approach provides essential insights for improving urban forest carbon quantification while examining the underlying physiological mechanisms of urban tree carbon storage.

2.2 Materials and methods

2.2.1 Study area

The study was conducted in Auburn, Alabama, USA. We sampled a total of 90 trees, comprising 30 individuals from each of the three species: southern red oak (*Quercus falcata*), overcup oak (*Quercus lyrata*), and bald cypress (*Taxodium distichum*). These species were selected to represent a gradient of drought tolerance capabilities (Niinemets and Valladares 2006). On a standardized scale of 0 (least drought tolerance) to 5 (highly drought-tolerant), *Q. lyrata* has the least drought tolerance (value: 1), *T. distichum* has moderate drought tolerance (value: 3.25±0.38), and *Q. falcata* has high drought tolerance (value: 5).

For each species, 15 park-grown trees and 15 street-grown trees were sampled. Measurements were collected on all study trees, including diameter at breast height (DBH) and total tree height. The study trees were sampled to represent a range of DBH and height values (see Table 2.1). All sampled trees were healthy, showing no major signs of disease, pest infestation, or significant structural damage that could affect the carbon estimates.

Table 2.1 Summary statistics of the size of the study trees

Species	Height(m) (mean [min, max])		DBH (m) (mean [min, max])	
	Park Trees	Street Trees	Park Trees	Street Trees
Quercus falcata	18.79 [7.18, 25.75]	18.35 [8.96, 29.15]	0.76 [0.21, 1.35]	0.59 [0.28, 1.00]
Quercus lyrata	11.78 [7.75, 18.45]	13.23 [9.37, 18.89]	0.54 [0.33, 1.13]	0.49 [0.32, 0.76]
Taxodium distichum	10.78 [5.90, 27.51]	13.86 [8.31, 21.43]	0.34 [0.21, 0.82]	0.43 [0.22, 0.62]

2.2.2 Terrestrial Laser Scanning (TLS) Data Collection and Processing

We used a FARO Focus Premium terrestrial laser scanner (FARO Technologies, 2024) to laser scan the study trees. Following the single-tree scanning protocol established by Wilkes et al. (2017), each tree was scanned from four to six positions to minimize occlusion. Four spherical reference targets were placed around each tree for accurate registration of scans from multiple positions. All scans were conducted during the leaf-off period to obtain an unobstructed view of the tree's woody structure. Scanning was performed under low-wind conditions (wind speed < 5 m/s) to reduce noise and occlusion caused by swaying stems and branches in the resulting point clouds (Seidel et al. 2012).

Individual scans were co-registered and merged using FARO Scene 2023.1.0 software using automatic target-based registration with spherical targets. After registration, the point clouds were exported and analyzed in CloudCompare v2.13.2 (http://www.cloudcompare.org/). We removed noise from the point clouds using the statistical outlier removal tool in CloudCompare v2.13.2.

We generated quantitative structure models (QSMs) for each tree's point cloud using the *TreeQSM* 2.4.1 algorithm (Raumonen et al. 2013). The algorithm begins by segmenting the woody point cloud into small surface patches that conform to the local surface geometry (Raumonen et al. 2013; Calders et al. 2018). These patches are formed based on a cover-set approach, where points are grouped based on both spatial proximity and similarity in surface normal characteristics. Next, the algorithm performs component recognition by identifying and classifying different tree parts. The main stem is identified based on criteria such as the apical position, vertical orientation, and minimal curvature (Arseniou et al. 2021). Branches of various orders are then determined through a hierarchical analysis of the spatial relationships and

connectivity among segments. Finally, the algorithm fits cylinders to these segmented components via least-squares optimization. This process typically begins at the base of the tree and proceeds upward, carefully maintaining connectivity and enforcing biological constraints such as branch tapering, thereby ensuring that the reconstructed model accurately reflects the tree's architecture (Raumonen et al. 2013). Tree woody volume is then estimated as the sum of the volumes of all fitted cylinders. The algorithm generates multiple QSM iterations for each tree's point cloud by testing different values for the minimum and maximum cover-set sizes, as the stochastic nature of the initial clustering can influence final volume estimates. From these iterations, the algorithm selects an optimal QSM for each tree point cloud (Raumonen et al. 2013).

QSMs commonly overestimate the volume of small branches and twigs < 5 cm in diameter due to limitations of TLS technology, such as beam divergence, occlusion, co-registration errors, and wind (Wilkes et al. 2017; Abegg et al. 2021; Demol et al. 2022; Morales and MacFarlane 2025a). To correct such overestimation, the *rTwig* package in R uses species-specific twig diameter to enforce the QSM cylinder to follow realistic branch tapering (Morales and MacFarlane 2025b). Therefore, we applied a correction to the optimal QSM using the *rTwig* package in R. Finally, we derived the total aboveground wood volume and component volumes (main stem and branches) of all trees from the corrected QSMs.

2.2.3 Wood density calculations

From each study tree, 5.15 mm diameter increment cores were extracted on the main stem at breast height (1.37 m above the ground) using an increment borer. Extracting woody cores is an effective approach for measuring wood density and actual wood C% with minimum impact on trees (Williamson and Wiemann 2010).

Each core was then immediately placed in a sealed, labeled bag to prevent moisture loss. We measured the diameter of the cores with a caliper (±0.01 mm precision), and the core length with a standard engineer's ruler. The green volume of each core sample was calculated as the volume of a cylinder based on the core dimensions. Each core was then oven-dried at 100°C until a constant weight. The basic wood density of the core sample was calculated using equation (1).

$$Basic\ wood\ density = \frac{oven - dry\ mass\ (g)}{green\ volume\ (cm^3)} \quad (1)$$

2.2.4 Carbon concentration - Quantification of Sampled Wood Cores

We determined the carbon concentration (C%) of the sampled wood core for each tree via high-temperature combustion using a Flash Smart CHNS/O elemental analyzer (Thermo Fisher Scientific, Massachusetts, USA). The elemental analyzer quantifies total carbon (as a percentage of its dry mass) with an integrated thermal conductivity detector (Bird et al. 2017). This approach provides more accurate estimates than assuming a fixed wood C%, particularly when comparing the trees growing in contrasting urban environments and across different species. Each dried increment core was divided into three segments along the radius: pith, mid-radius (center), and bark. Approximately 2-3 mg of wood from each segment was weighed into tin capsules for combustion analysis. Carbon concentration was reported as percent dry mass for each radial segment.

We calculated a weighted average wood carbon concentration (C%) of increment cores per study tree (see equation 2). This weighted average was based on the relative volumetric proportions of bark and wood, using species-specific values derived from Miles and Smith (2009).

$$C\% = (C_{wood} \times \%Vol_{wood}) + (C_{bark} \times \%Vol_{bark}) \quad (2)$$

where,

C% = weighted average carbon concentration of the woody core,

C_{wood} = average carbon concentration at the core center and pith,

C_{bark} = carbon concentration of the bark,

$\%Vol_{wood}$ = percentage of wood volume [80% for *T. distichum*; 78% for *Q. falcata* and *Q. lyrata* (Miles and Smith 2009)]

$\%Vol_{bark}$ = percentage of bark volume [20% for *T. distichum*; 22% for *Q. falcata* and *Q. lyrata* (Miles and Smith 2009)].

2.2.5 TLS-based carbon biomass estimation

QSM-derived woody volumes were converted to dry biomass for each tree using the corresponding measured basic wood density. The resulting biomass estimates were then multiplied by the tree-specific wood carbon concentration (C%) obtained from core samples to calculate total aboveground carbon biomass (AGC, kg). Using this approach, we quantified total AGC and component carbon biomass values of the main stem and branches of all study trees.

2.2.6 Tree age quantification

We extracted a second increment core sample from each tree at DBH to estimate the tree's age by counting the annual rings. Cores were dried and sanded with fine grit to clearly expose ring boundaries for ring identification and counting. For the partial cores (i.e., cores not reaching the pith), the number of missing rings was estimated by following the approach proposed by Altman et al. (2016), averaging radial growth extrapolation and mean basal area increment. The

final age of partial cores was then determined as a sum of the number of partial rings and the estimated number of missing rings.

2.2.7 Calculations of wood vessel metrics

Xylem vessel metrics were quantified using the second increment core samples collected from study trees of the two ring-porous species (*Q. falcata* and *Q. lyrata*). The cross sections of increment core samples were prepared for vessel measurement (Von Arx et al. 2016). We cleaned the core surface and took images with an AmScope digital microscope (AmScope, Irvine, CA, USA) at 45× magnification. We captured digital images of the 10 most recent annual rings per core. We focused on earlywood vessels, as they play a key role in water transport in ring-porous species (Fonti et al. 2010). In each ring, we manually identified and measured the lumen area of individual vessels using the AmScope 3.0.1. software. We excluded any vessels smaller than 5000 μm^2 from the analysis. This was done to avoid confusion with latewood vessels or other wood structures (Castagneri et al. 2017; Rissanen et al. 2025).

From these measurements, we calculated four key hydraulic metrics that characterize xylem hydraulic architecture (see Table 2.2). Mean vessel lumen area (LA) was calculated as the average cross-sectional area of all measured vessels, providing insight into the water transport capacity of individual conduits (Castagneri et al. 2020). Vessel frequency (VFreq) was calculated as the number of vessels per unit area (n mm^{-2}), reflecting the density of water-conducting elements and the tree's investment in hydraulic redundancy (Fonti and García-González 2004). The hydraulically weighted vessel diameter was calculated based on Sperry and Saliendra (1994), where D represents individual vessel diameters (see Table 2.2). This metric places greater emphasis on larger vessels, reflecting their disproportionate contribution to hydraulic conductivity according to the Hagen-Poiseuille equation. The vulnerability index (VI) was

calculated as the ratio of mean vessel diameter to vessel frequency, characterizing drought susceptibility because higher VI values suggest greater vulnerability to cavitation under water stress conditions (Carlquist 1977). These vessel metrics were used to compare xylem anatomy between park and street trees and to test their relationships with main-stem carbon biomass.

Table 2.2 Wood vessel metrics

Vessel Trait	**Formula (Unit)**
Mean vessel lumen area (LA)	(μm2)
Vessel frequency (VFreq)	no. of vessels/aoi (n mm−2)
Hydraulically weighted vessel diameter (HWD)	∑D5/∑D4 (μm)
Vulnerability index (VI)	mean D/VFreq

Vessel lumen area (μm²) was measured directly from increment-core surface images (captured with a microscope) using AmScope software. Vessel frequency (VFreq, vessels mm^{-2}) was calculated as the number of measured earlywood vessels (n) divided by the analyzed area of interest (AOI, mm^2). D refers to the vessel lumen diameter (μm) (i.e., equivalent diameter derived from lumen area).

2.2.8 Statistical analysis

Differences in carbon concentration (C%) in woody cores were tested using analysis of variance (ANOVA) with species as a fixed effect. When significant, species differences were evaluated using Tukey's post-hoc pairwise comparisons (Williams and Applegate 1992). Differences in C% between growing environments within each species were evaluated using independent samples *t*-tests. Assumptions of normality and homoscedasticity were assessed visually (Q–Q plots; residual vs fitted values).

To quantify how aboveground carbon biomass (AGC, kg) scales with tree size and age across growing environments, we modeled AGC as a power function of DBH (m) and tree age (years).

$$AGC = a \times DBH^{b}$$

$$AGC = a' \times Age^{b'}$$

Variables were log-transformed to linearize the relationships:

$$\ln(AGC) = \ln(a) + b \ln(DBH)$$

$$\ln(AGC) = \ln(a') + b' \ln(Age)$$

where a is a normalization constant, and b is the scaling exponent.

Log–log relationships were analyzed using standardized major axis (SMA) regression in the *smatr* package in R (Warton et al. 2012). SMA was selected to estimate biological scaling rather than to generate predictive models. We first tested whether slopes differed between environments; where slopes did not differ significantly, we tested for differences in intercepts (elevation) along a common slope to assess whether AGC differed between environments for trees of equivalent DBH or age.

To compare xylem vessel metrics between growing environments, we conducted Welch's *t*-tests for each vessel metric (West 2021), comparing park trees and street trees for the combined oak species.

The relationship between xylem vessel metrics and carbon biomass in the main stem was examined using Pearson's correlation coefficient (r) and simple linear regression. The regression analysis was used descriptively to characterize the direction and slope of the linear trend and to

visualize the fitted relationship, rather than to develop a predictive model. Pearson's correlation coefficient (r) was used to describe the strength and direction of association between individual vessel metrics and main-stem carbon biomass, and the corresponding R^2 from the simple linear regression was reported as a descriptive measure of the variation associated with the fitted linear trend. We focused on the main stem carbon biomass because the vessel metrics were calculated from wood cores extracted at DBH. All analyses were performed in R version 4.3.1 (R Core Team, 2023).

2.3 Results

2.3.1 Differences in the carbon concentration of increment cores across species and growing environments

The carbon concentration (C%) in increment cores differed significantly among the three study species ($p < 0.01$). *T. distichum* had the highest mean wood C% (49.82%), which was statistically greater than the mean wood C% of the two oak species. *Q. falcata* and *Q. lyrata* had nearly identical mean wood C% (45.52% and 45.67%, respectively), with no statistically significant difference between them (see Figure 2.1).

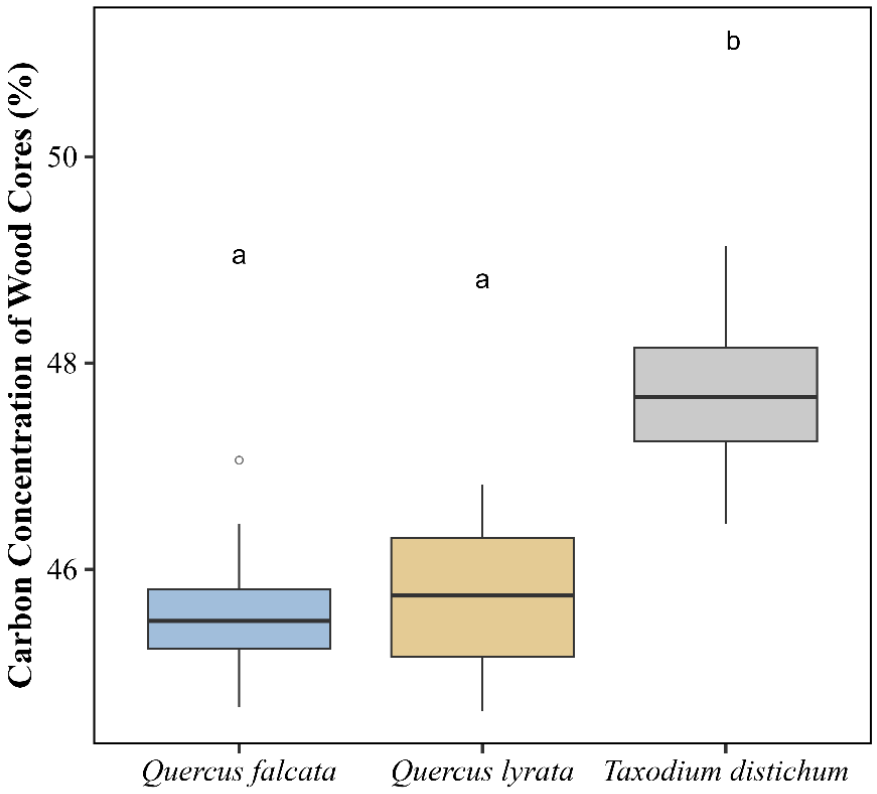

Figure 2.1 Comparison of carbon concentration (C%) in increment cores collected from the study species *Quercus falcata, Quercus lyrata,* and *Taxodium distichum*. The boxes show the interquartile range with median lines. Different letters indicate significant ($p < 0.05$) differences in group means according to Tukey's post-hoc pairwise comparison.

Significant differences were also found in the C% in increment cores between park and street trees (see Figure 2.2). For *Q. falcata*, trees in parks had significantly greater wood C% than street trees ($p = 0.036$). A similar pattern was found for *Q. lyrata*, where wood C% was greater in park trees compared to street trees ($p = 0.015$). However, *T. distichum* did not show any significant difference in wood C% between park and street trees ($p = 0.24$).

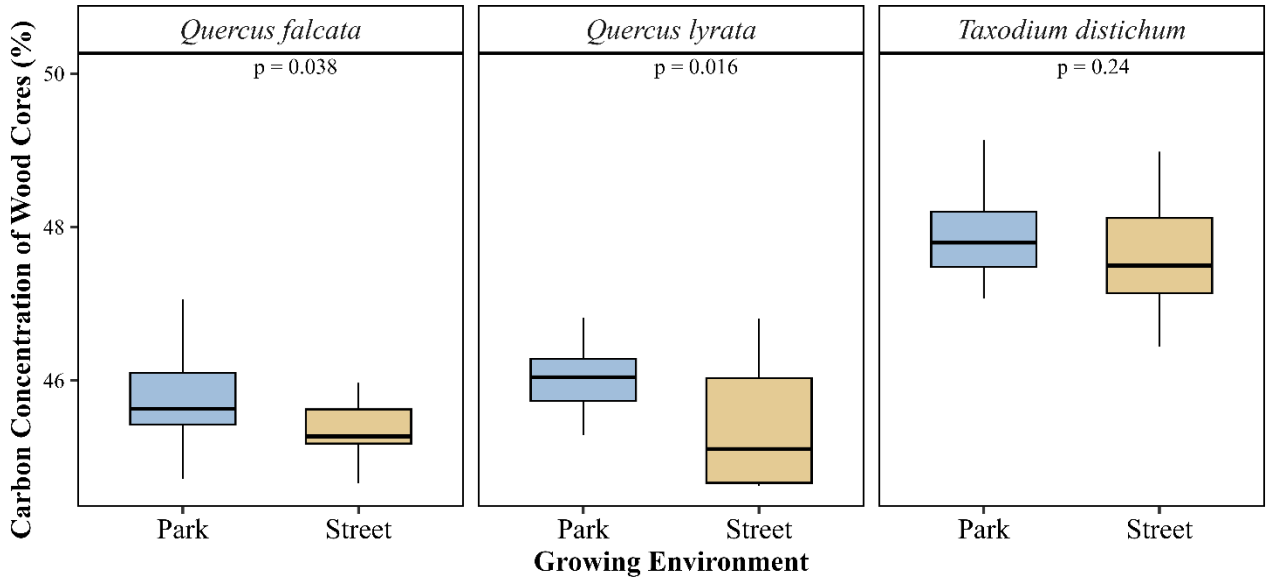

Figure 2.2 Comparison of carbon concentration (C%) in increment cores between park and street trees across the three study species *Quercus falcata, Quercus lyrata*, and *Taxodium distichum*. Boxes show the interquartile range with median lines.

2.3.2 Relationship between total aboveground carbon biomass and DBH across growing environments

The relationship between AGC and DBH on a log scale was positive in both park and street growing environments (see Figure 2.3). The SMA regression on a log scale showed that the slope and intercept of the park and street trees regression lines were not statistically different ($p > 0.05$). This indicates that for trees of the same DBH, estimated AGC did not differ systematically between street and park environments.

The model explained less variance for street trees ($R^2 = 0.70$) than for park trees ($R^2 = 0.90$), indicating greater residual variability in AGC at a given DBH under street growing conditions (see Figure 2.3)

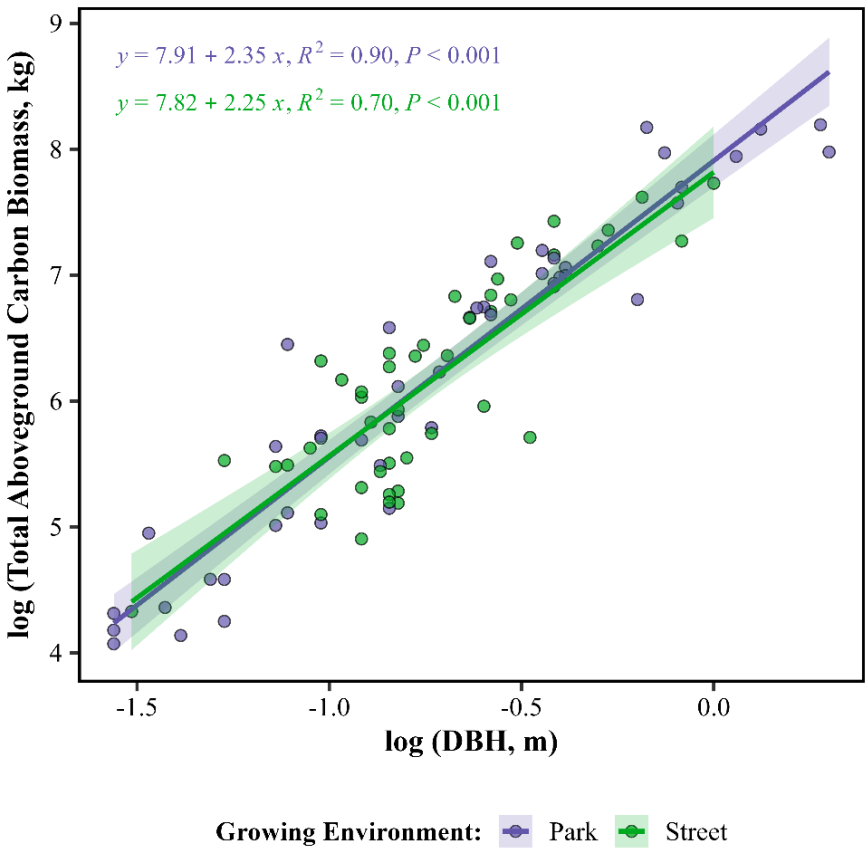

Figure 2.3 Relationship between total aboveground carbon biomass (AGC) and diameter at breast height (DBH) on a log scale for park and street trees. The 95% confidence interval has been plotted around the regression lines.

2.3.3 Relationship between total above-ground carbon biomass and age across growing environments

AGC increased with tree age in both park and street growing environments (see Figure 2.4). The SMA regression on a log scale revealed no significant difference in the slope of park and street trees' regression lines (p = 0.58). However, the intercepts of the two regression lines were statistically different (p = 0.0018). These differences were due to both faster growth rates and higher C% (Figure 2, above) in the wood of trees growing in parks versus on streets.

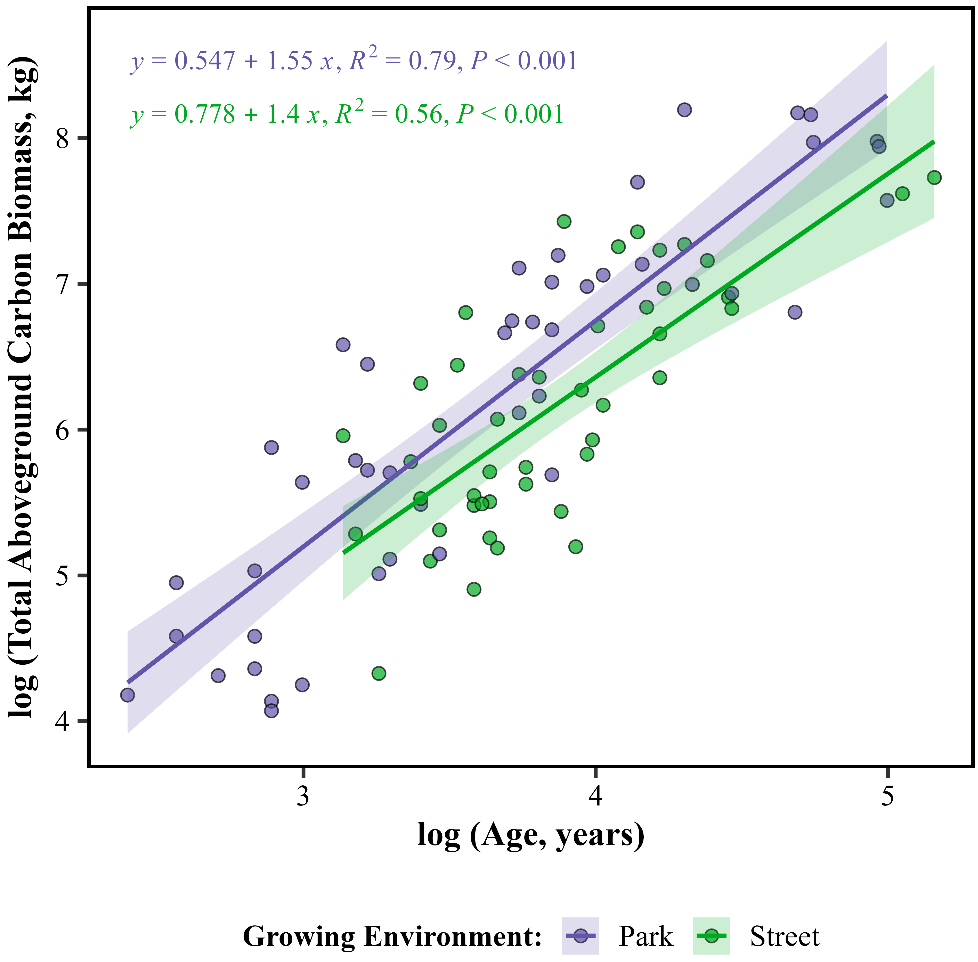

Figure 2.4 Relationship between total aboveground carbon biomass (AGC) and tree age on log-scale for park and street trees. The 95% confidence interval has been plotted around the regression lines.

2.3.4 Relationship between DBH and age across growing environments

Tree diameter at breast height (DBH) increased significantly with tree age in both park and street environments (see Figure 2.5). On the log-transformed scale, both relationships were positive and statistically significant. There was no significant difference in slope, but the intercept differed significantly (p=0.0023). Park trees generally had larger DBH values than

street trees of similar age, indicating an upward shift in the DBH-age relationship for park-grown trees.

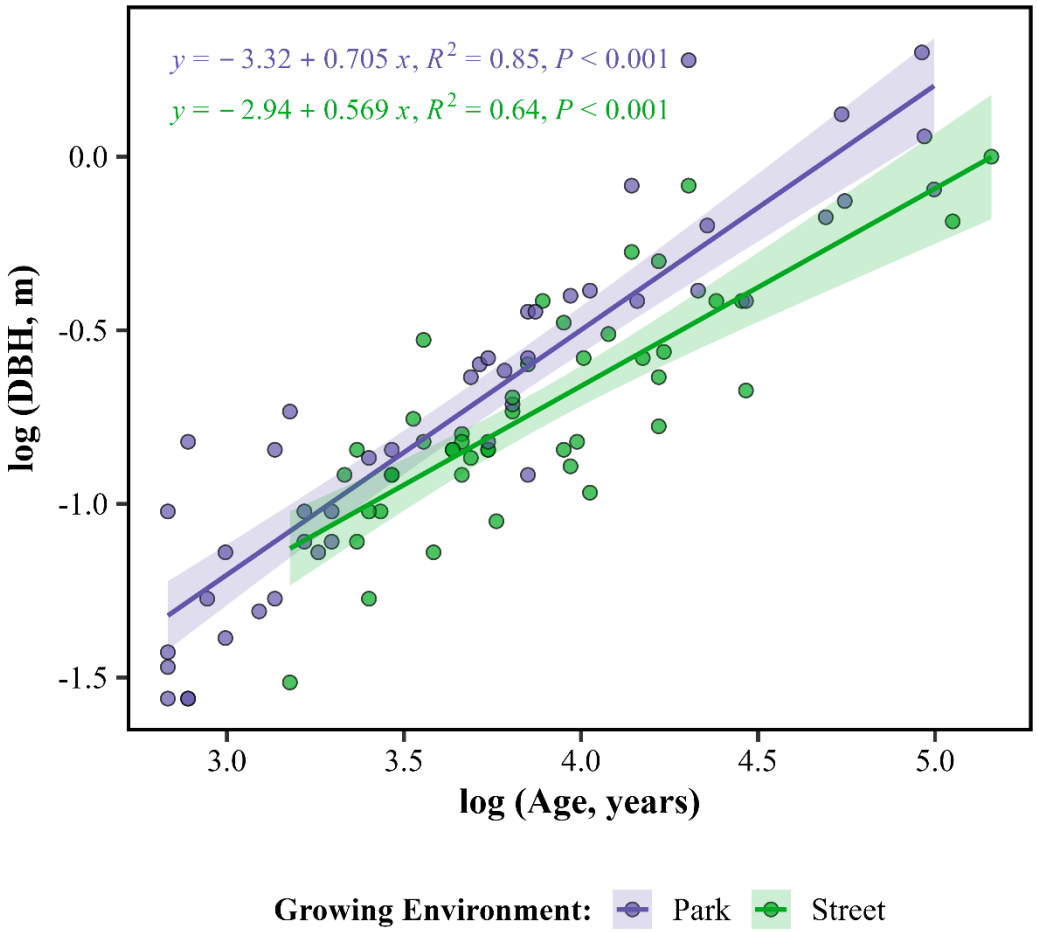

Figure 2.5 Relationship between diameter at breast height (DBH) and tree age on log-scale for park and street trees. The 95% confidence interval has been plotted around the regression lines.

2.3.5 Differences in xylem vessel metrics across growing environments and the relationship between vessel metrics and the main stem carbon biomass

All xylem vessel metrics were statistically different between park and street trees of *Q. falcata* and *Q. lyrata* species combined (see Figure 2.6; Table 2.3). Lumen area (LA), hydraulically weighted diameter (HWD), and vulnerability index (VI) were significantly greater

in park trees compared to street trees. Vessel frequency (VFreq) was greater in street trees compared to park trees (see Figure 2.6; Table 2.3).

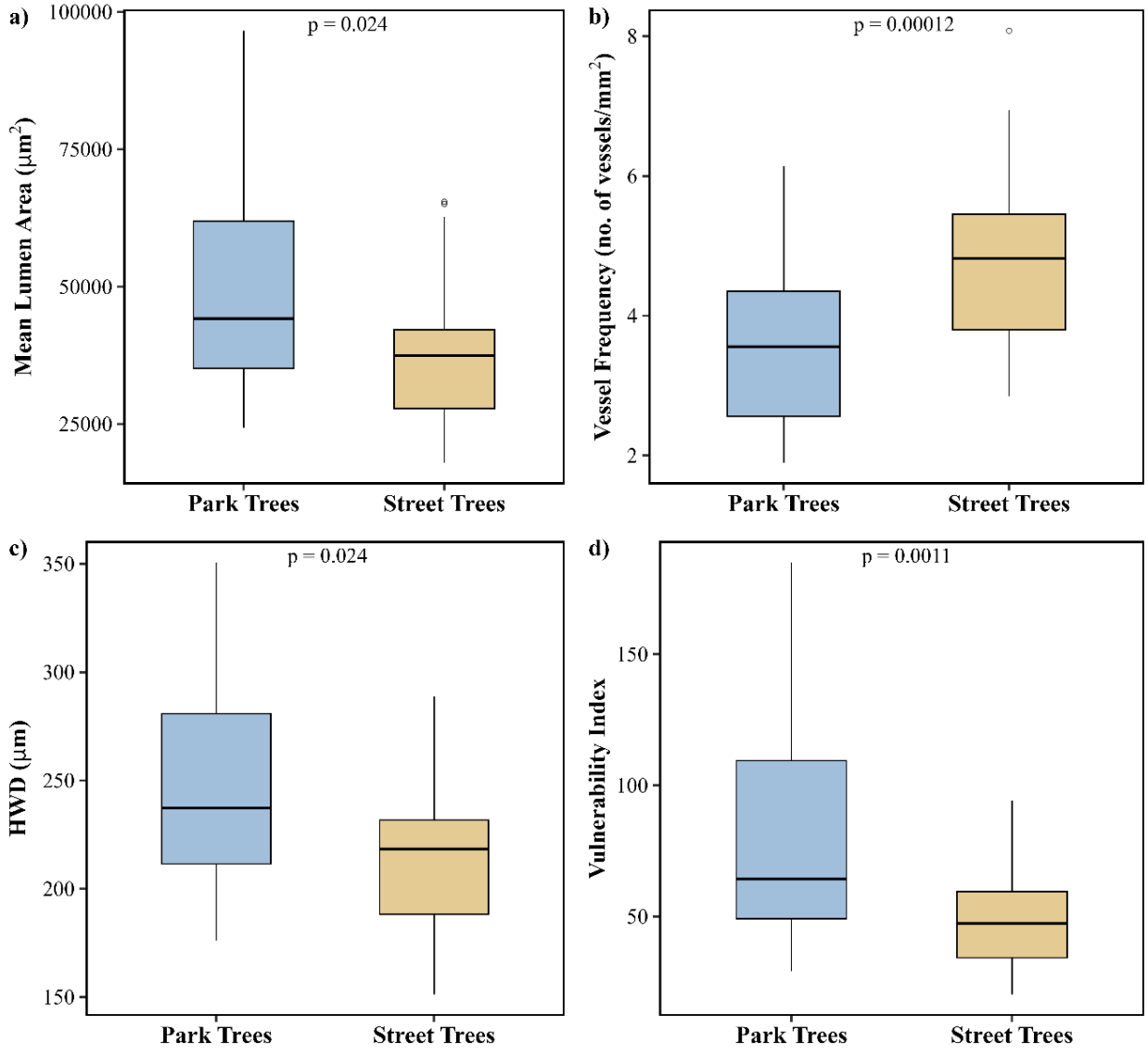

Figure 2.6 Xylem vessel metrics in street versus park trees of *Quercus falcata* and *Quercus lyrata* combined. Boxplots show (a) mean lumen area (μm²), (b) vessel frequency (VFreq; number of vessels/mm^2), (c) hydraulically weighted diameter (HWD, μm), and (d) vulnerability index, across growing environments.

Table 2.3 Comparison of xylem vessel metrics between park trees and street trees.

Vessel trait	p-value	Park trees, mean (standard deviation)	Street trees, mean (standard deviation)
Mean vessel lumen area (LA, μm²)	0.024	50097.3 (20692.6)	37955.1 (13117.1)
Vessel frequency (VFreq, number of vessels/mm²)	0.001	3.5 (1.1)	4.8 (1.3)
Hydraulically weighted diameter (μm)	0.024	247.6 (50.6)	216.7 (37.6)
Vulnerability index (VI)	0.001	47.6 (13.1)	36.8 (13.4)

There was a statistically significant relationship between the main stem carbon biomass and the mean lumen area of xylem vessels (Pearson's r = 0.33; adj. R^2= 0.11, p< 0.05), and between the main stem carbon biomass and the hydraulically-weighted diameter of vessels (Pearson's r =0.35; adj. R^2= 0.12, p<0.05) of the species *Q. falcata* and *Q. lyrata* (see Figure 2.7).

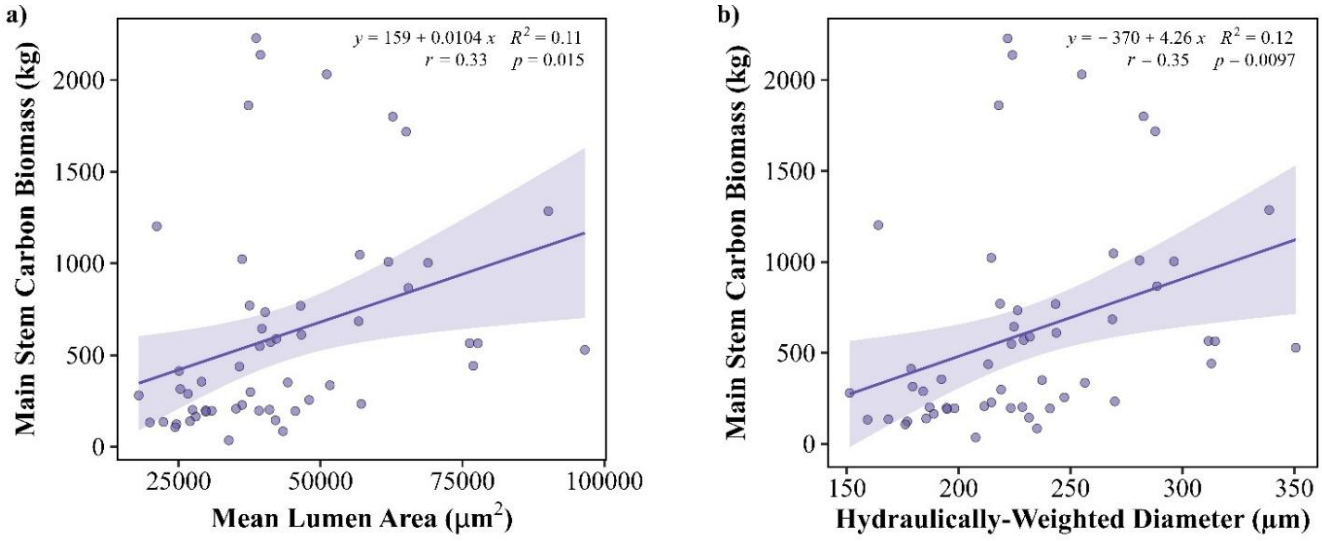

Figure 2.7 Relationships between main stem carbon biomass and xylem vessel metrics: a) Mean lumen area (μm²) and b) Hydraulically weighted diameter (μm) of two oak species. The 95%

confidence interval has been plotted around the regression lines. Pearson's correlation coefficient is represented by *r*.

2.4 Discussion

2.4.1 Variation in the carbon concentration of increment cores among different species

This study demonstrated that the carbon concentration of wood core samples (C%) varied among species, aligning with previous studies that indicate that the commonly assumed 50% carbon concentration of dried wood is inaccurate (Martin et al. 2015; Gao et al. 2016). Doraisami et al. (2024) reported that the wood C% of different tree species in different biomes varies greatly and that the use of species-specific values can significantly improve the accuracy of forest carbon estimates. Similarly, Ma et al. (2020) reported that the assumption of a fixed 50% wood carbon concentration can introduce errors in carbon estimation ranging from −2.5% to +5.9% at the tree level.

The finding that *T. distichum* had significantly greater wood C% compared to the two oak species is consistent with wood chemistry patterns that reflect fundamental phylogenetic differences between gymnosperms and angiosperms. Lamlom and Savidge (2003) suggested that gymnosperms generally contain 47.2–55.2% carbon in their wood biomass, whereas wood carbon concentration in angiosperms ranges between 46.3–50.0%. Similarly, Wu et al. (2017) reported significant differences in subtropical forests, where gymnosperms have, on average, 47.4 ± 2.6% wood carbon concentration, whereas angiosperms have 43.8 ± 2.4% wood carbon concentration.

In the above-mentioned studies, the observed differences in wood C% between gymnosperms and angiosperms were attributed to greater lignification of wood tissues and

differences in lignin chemistry in gymnosperms. Lignin is composed of approximately 72% carbon, which is much greater than the 44-45% carbon that is found in cellulose and hemicellulose (Lamlom and Savidge 2003; Bengtsson et al. 2019). Gymnosperms typically produce only guaiacyl (G) lignin and have a relatively high lignin content (approximately 30% of their wood mass). On the other hand, angiosperms produce guaiacyl and syringyl (S) lignin, but in relatively small amounts (approximately 20% of their wood mass; Lamlom and Savidge 2003). Consequently, the wood of gymnosperms contains more lignin and therefore a higher overall wood C%.

The variation of wood C% among species has important implications for carbon quantification, especially given the widespread use of standardized conversion factors. The Intergovernmental Panel on Climate Change (IPCC, 2006) suggested a standard C% of 50% for the conversion of tree biomass to carbon. This assumption has been broadly utilized in forest inventories, urban tree carbon assessments, and the development of municipal greenhouse gas reporting frameworks. Nowak et al. (2013) estimated that urban forests in the United States store approximately 643 million tons of carbon, largely based on default conversion factors. While the use of standard conversion factors simplifies calculations and promotes comparability across studies, it overlooks species-level variability. Considering the diversity of urban tree populations that include both gymnosperm and angiosperm species, species-level variation in wood C% could lead to highly biased estimates across different spatial scales.

2.4.2 Variation in the carbon concentration of increment cores in different growing environments

This study showed that the carbon concentration of increment cores (C%) sampled from urban trees can differ based on the growing environment. The higher wood C% in park oaks

compared to street oaks may indicate varying levels of growth stress among urban trees across different environments.

Urban street environments expose trees to chronic, multifactorial stress that can disrupt normal physiological processes (Patel et al. 2024). Street trees often grow in compacted soils with limited available growing space for root expansion; they may experience elevated soil temperature and pH, and they can be exposed to soil and air pollution, and water scarcity (Iakovoglou et al. 2001, 2002; Mullaney et al. 2015). These combined stressors affect tree biological processes and can alter wood chemistry and structure. Studies have showed that impervious surfaces and water stress combined suppress tree radial growth (McClung and Ibáñez 2017), reduce photosynthetic activity (Wang et al. 2018), and reduce hydraulic safety margins, increasing vulnerability to cavitation (Savi et al. 2015). In contrast, park environments typically provide large soil volumes available for root growth, better soil structure and aeration, greater water infiltration, moderate soil temperatures, and lower pollutant exposure, all of which promote physiological stability and sustained tree growth (Sarah et al. 2015). Water availability has emerged as a key factor of wood formation in urban trees (Meineke and Frank 2018). When water availability is limited, cambial activity ceases even when the carbon supply remains adequate (Deslauriers et al. 2016). Chronic water deficits can thus shorten the period of wood formation despite potential favorable photosynthetic conditions, suggesting that growth may be constrained more by a tree's ability to use carbon (sink limitation) than by its capacity to produce it (Brzostek et al. 2014).

In addition to reduced growth activity, drought stress in street trees can also reduce atmospheric CO_2 uptake through stomatal regulation. To avoid hydraulic failure during water stress, trees close their stomata to resist xylem embolism (Pivovaroff et al. 2016). While this

response conserves water, it also restricts CO_2 uptake as gas exchange is curtailed. Prolonged stomatal closure or leaf loss during drought therefore reduces carbohydrate production. When respiration and phloem transport continue under these conditions, trees may experience carbon starvation as available carbohydrates are progressively depleted (Chen et al. 2022). Over time, this imbalance further limits the carbon available for wood formation, contributing to the lower wood C% observed in street-grown oaks.

Notably, *T. distichum* had no significant difference in wood C% between street and park environments. Unlike ring-porous oaks that transport water through vessels and adjust vessel size and frequency depending on growing conditions, *T. distichum* transports water mainly through tracheids, which are smaller, more uniform conduits with reinforced walls that provide inherently greater resistance to cavitation (Pittermann et al. 2006; Choat et al. 2012). *T. distichum* also shows an ability to tolerate reduced oxygen availability for its roots due to soil waterlogging or soil compaction through specialized aerenchyma tissue that allows oxygen to reach the roots (Hook 1984). As a result, *T. distichum* may exhibit stability in physiological processes and growth across varying environments in urban settings.

2.4.3 Allometric relationship between total aboveground carbon biomass, tree DBH, and age in different growing environments

The relationship between the total aboveground carbon biomass (AGC, kg) of the study trees and their DBH was similar in street and park environments, aligning with previous studies that show that stem diameter is typically the most important predictor of aboveground biomass and carbon in urban trees (McHale et al. 2009; Kükenbrink et al. 2021; Arseniou et al. 2023; Arseniou et al. 2025).

Greater variability in street-tree AGC at a given DBH suggests that factors beyond stem diameter may be more influential in street environments than in parks. While DBH-based models remain practical, future work could explicitly test incorporating other variables that might improve prediction accuracy for street trees, where growing conditions and management intensity are highly heterogeneous (Radtke et al. 2017; Lee et al. 2025; Parhizgar et al. 2025).

The greater carbon storage of oak trees in parks relative to street trees was a combination of greater carbon concentrations in the wood of the park trees and faster growth rates. Our DBH–age analysis (see Figure 2.5) shows a significant intercept difference, such that park trees attained larger DBH at a given age. Because AGC scales strongly with stem size, greater DBH at a given age directly translates into greater biomass and AGC. This pattern aligns with previous findings that street environments suppress diameter growth relative to less constrained sites.

A study by Quigley (2004) found that street trees were often smaller in trunk diameter than nearby woodlot trees of the same age, and that proximity to impervious surfaces was associated with reduced growth rates. Reduced growth in street settings is commonly attributed to rooting-volume limitation and fragmented planting spaces, which constrain water and nutrient supply and can limit canopy development (Sanders and Grabosky 2014). Street trees also experience compacted soils from streetscape infrastructure, which can restrict root proliferation and reduce aeration and infiltration (Moore et al. 2019). In addition, street corridors often impose chronic disturbance and management constraints, including pruning to maintain clearance around infrastructure and obstructions, which can reduce leaf area and carbon gain, contributing to slower growth (Speak and Salbitano 2023; Egerer et al. 2024). At broader scales, Lin et al. (2022) similarly found that urban tree carbon density decreases with increasing development intensity (i.e., more impervious surfaces, more constrained environments). Together, these

findings support the interpretation that constrained environments like streets shift DBH–age trajectories downward, thereby reducing AGC at comparable ages.

Although street trees are often exposed to chronic, multifactorial stress, all park sites should not be assumed to provide uniformly lower physical stress, as some parks can also develop compacted soils under repeated trampling and equipment traffic (Rompato et al. 2025). In the southeastern United States, rainfall shows strong temporal variability, and convective rainfall can be highly localized over small spatial scales so that nearby sites may differ meaningfully in water availability (Wei et al. 2018). Because precipitation was not monitored at the site level, its effects could not be separated from those of other environmental factors. Future work would benefit from direct measurements of soil bulk density, soil moisture, and local precipitation to better identify the mechanisms underlying site-related variation in carbon biomass.

2.4.4 Growing environment shapes xylem hydraulic architecture and stem carbon accumulation

We found that park-grown oaks developed fewer, larger earlywood vessels, while street-grown oaks produced many smaller vessels. Similar patterns have been reported in *Celtis occidentalis* along an urban gradient, where park trees showed larger vessel lumen areas and lower vessel frequency, whereas inner-city street trees had smaller vessel lumen areas and higher vessel frequency (Rissanen et al. 2025). This pattern aligns with the well-documented trade-off between hydraulic efficiency and hydraulic safety in xylem architecture (Pittermann et al. 2006; Hoeber et al. 2014). Under stressful growing environments like the street, trees often shift toward conservative xylem designs with smaller conduits to reduce embolism risk (Hacke et al. 2017). Our finding that street trees exhibited smaller vessel diameters and a lower vulnerability index

supports this adaptive strategy, indicating a safety-oriented xylem configuration under recurrent environmental stress.

We also observed a positive relationship between vessel size (mean lumen area and diameter) and main stem carbon biomass; trees with larger conduits stored more stem carbon. This linkage can be explained mechanistically through the Hagen–Poiseuille law, which states that hydraulic conductance scales with the fourth power of the vessel radius (Tyree et al. 1994; Fan et al. 2012). Consequently, even a modest increase in vessel diameter produces a disproportionately large gain in conductive capacity. Despite having fewer xylem vessels, the wider conduits in park trees may therefore provide higher hydraulic conductivity than the numerous narrower vessels in street trees. Greater hydraulic efficiency allows for higher stomatal conductance, sustained transpiration, and increased photosynthetic carbon assimilation, which collectively promote biomass and carbon accumulation (Hoeber et al. 2014; Rodríguez-Gamir et al. 2016).

This relationship between hydraulic capacity and carbon accumulation can be understood through both the pipe model theory (Shinozaki et al. 1964) and metabolic scaling theory (West et al. 1997). The pipe model theory suggests a proportional relationship between conductive tissue area and supported leaf area. Trees with larger conduits may support a greater effective leaf area or higher leaf-level fluxes, enhancing carbon assimilation and stem carbon storage. Meanwhile, metabolic scaling theory states that plant growth depends on the efficiency of internal transport networks supplying water and nutrients to active tissues. As trees grow larger, maintaining efficient hydraulic pathways becomes crucial to reducing transport resistance and sustaining metabolic demands. Our results support MST predictions: individuals with more efficient vascular systems (larger conduits) showed greater carbon accumulation, indicating hydraulic

capacity matched photosynthetic needs. However, this increased efficiency comes with higher hydraulic risk.

Wider vessels are more vulnerable to cavitation caused by drought or freeze–thaw cycles (Pittermann et al. 2006; Christman et al. 2012). The significantly higher vulnerability index seen in park trees reflects a reliance on large conduits, which could increase susceptibility to hydraulic failure during extreme events.

Overall, our vessel trait differences are consistent with an efficiency–safety shift between parks and streets, and the modest correlations with main stem carbon suggest hydraulically mediated growth effects may contribute to carbon storage differences, but multivariate models controlling for tree size and direct measures of site water stress are needed for better understanding of vessel traits as a predictive indicator in urban carbon assessments.

2.5 Conclusions

This study shows how species characteristics and urban growing conditions influence the carbon storage potential of urban trees. The findings emphasize the importance of incorporating species-specific carbon concentrations, particularly in mixed urban forests containing both angiosperm and gymnosperm species, and recognizing that stressful urban environments, such as streets, can limit carbon accumulation by constraining tree growth. From a management perspective, improving street-tree growing conditions, such as increasing soil volume, reducing compaction, and enhancing water availability, may help increase long-term carbon storage. Additionally, incorporating species- and site-specific wood properties into urban forest inventories could reduce uncertainty in carbon estimates. Future research should expand these analyses to more species, develop urban-specific allometric equations that account for growth

forms in built environments, and evaluate how long-term urban stress affects wood carbon concentration, growth trajectories, and hydraulic structure.

References

Abegg, M., R. Boesch, M. E. Schaepman, and F. Morsdorf. 2021. Impact of Beam Diameter and Scanning Approach on Point Cloud Quality of Terrestrial Laser Scanning in Forests. *IEEE Transactions on Geoscience and Remote Sensing* 59(10):8153–8167. https://doi.org/10.1109/TGRS.2020.3037763.

Alonzo, M., P. C. Ibsen, and D. H. Locke. 2025. Urban Trees and Cooling: A Review of the Recent Literature (2018 to 2024). *Arboriculture & Urban Forestry* 51(5):420–444. https://doi.org/10.48044/JAUF.2025.023.

Altman, J., J. Doležal, and L. Čížek. 2016. Age estimation of large trees: New method based on partial increment core tested on an example of veteran oaks. *Forest Ecology and Management* 380:82–89. https://doi.org/10.1016/J.FORECO.2016.08.033.

Arseniou, G., D. W. MacFarlane, and P. Raumonen. 2025. A new approach for quantification of total above-ground heartwood and sapwood volume of trees. *Trees - Structure and Function* 39(1), 24-. https://doi.org/10.1007/s00468-024-02597-4

Arseniou, G., D. W. MacFarlane, K. Calders, and M. Baker. 2023. Accuracy differences in aboveground woody biomass estimation with terrestrial laser scanning for trees in urban and rural forests and different leaf conditions. *Trees - Structure and Function* 37(3):761–779. https://doi.org/10.1007/S00468-022-02382-1.

Arseniou, G., D. W. MacFarlane, and D. Seidel. 2021. Measuring the Contribution of Leaves to the Structural Complexity of Urban Tree Crowns with Terrestrial Laser Scanning. *Remote Sensing* 13(14). https://doi.org/10.3390/rs13142773.

Bengtsson, A., J. Bengtsson, M. Sedin, and E. Sjöholm. 2019. Carbon Fibers from Lignin-Cellulose Precursors: Effect of Stabilization Conditions. *ACS Sustainable Chemistry & Engineering* 7(9):8440–8448. https://doi.org/10.1021/ACSSUSCHEMENG.9B00108.

Bird, M., C. Keitel, and W. Meredith. 2017. Analysis of biochars for C, H, N, O and S by elemental analyser. *Biochar: A guide to analytical methods* :39–50.

Brodribb, T. J., and T. S. Feild. 2000. Stem hydraulic supply is linked to leaf photosynthetic capacity: Evidence from New Caledonian and Tasmanian rainforests. *Plant, Cell and Environment* 23(12):1381–1388. https://doi.org/10.1046/J.1365-3040.2000.00647.X.

Brzostek, E. R., D. Dragoni, H. P. Schmid, A. F. Rahman, D. Sims, C. A. Wayson, D. J. Johnson, and R. P. Phillips. 2014. Chronic water stress reduces tree growth and the carbon sink of deciduous hardwood forests. *Global Change Biology* 20(8):2531–2539. https://doi.org/10.1111/GCB.12528.

Calders, K., J. Adams, J. Armston, H. Bartholomeus, S. Bauwens, L. P. Bentley, J. Chave, et al. 2020. Terrestrial laser scanning in forest ecology: Expanding the horizon. *Remote Sensing of Environment* 251:112102. https://doi.org/10.1016/J.RSE.2020.112102.

Calders, K., N. Origo, A. Burt, M. Disney, J. Nightingale, P. Raumonen, M. Åkerblom, Y. Malhi, and P. Lewis. 2018. Realistic Forest Stand Reconstruction from Terrestrial LiDAR for Radiative Transfer Modelling. *Remote Sensing* 10(6). https://doi.org/10.3390/rs10060933.

Carlquist, S. 1977. ECOLOGICAL FACTORS IN WOOD EVOLUTION: A FLORISTIC APPROACH. *American Journal of Botany* 64(7):887–896. https://doi.org/10.1002/J.1537-2197.1977.TB11932.X.

Castagneri, D., P. Fonti, G. Von Arx, and M. Carrer. 2017. How does climate influence xylem morphogenesis over the growing season? Insights from long-term intra-ring anatomy in Picea abies. *Annals of Botany* 119(6):1011–1020. https://doi.org/10.1093/AOB/MCW274.

Castagneri, D., A. L. Prendin, R. L. Peters, M. Carrer, G. von Arx, and P. Fonti. 2020. Long-Term Impacts of Defoliator Outbreaks on Larch Xylem Structure and Tree-Ring Biomass. *Frontiers in Plant Science* 11:541137. https://doi.org/10.3389/FPLS.2020.01078/.

Chave, J., M. Réjou-Méchain, A. Búrquez, E. Chidumayo, M. S. Colgan, W. B. C. Delitti, A. Duque, T. Eid, P. M. Fearnside, and R. C. Goodman. 2014. Improved allometric models to

estimate the aboveground biomass of tropical trees. *Global change biology* 20(10):3177–3190.

Chen, Z., S. Li, X. Wan, and S. Liu. 2022. Strategies of tree species to adapt to drought from leaf stomatal regulation and stem embolism resistance to root properties. *Frontiers in Plant Science* 13:926535. https://doi.org/10.3389/FPLS.2022.926535/FULL.

Choat, B., S. Jansen, T. J. Brodribb, H. Cochard, S. Delzon, R. Bhaskar, S. J. Bucci, et al. 2012. Global convergence in the vulnerability of forests to drought. *Nature 2012* 491(7426):752–755. https://doi.org/10.1038/nature11688.

Christman, M. A., J. S. Sperry, and D. D. Smith. 2012. Rare pits, large vessels and extreme vulnerability to cavitation in a ring-porous tree species. *New Phytologist* 193(3):713–720. https://doi.org/10.1111/j.1469-8137.2011.03984.x.

Crippa, M., D. Guizzardi, E. Pisoni, E. Solazzo, A. Guion, M. Muntean, A. Florczyk, M. Schiavina, M. Melchiorri, and A. F. Hutfilter. 2021. Global anthropogenic emissions in urban areas: patterns, trends, and challenges. *Environmental Research Letters* 16(7):074033. https://doi.org/10.1088/1748-9326/AC00E2.

Czaja, M., A. Kołton, and P. Muras. 2020. The Complex Issue of Urban Trees—Stress Factor Accumulation and Ecological Service Possibilities. *Forests 2020, Vol. 11, Page 932* 11(9):932. https://doi.org/10.3390/F11090932.

Demol, M., P. Wilkes, P. Raumonen, S. M. K. Moorthy, K. Calders, B. Gielen, and H. Verbeeck. 2022. Volumetric overestimation of small branches in 3D reconstructions of Fraxinus excelsior. *Silva Fennica* 56(1). https://doi.org/10.14214/sf.10550.

DESA, U. N. United nations, department of economic and social affairs, population division. 2018. world urbanization prospects: The 2018 revision. *Online Edition*.

Deslauriers, A., J. G. Huang, L. Balducci, M. Beaulieu, and S. Rossi. 2016. The Contribution of Carbon and Water in Modulating Wood Formation in Black Spruce Saplings. *Plant Physiology* 170(4):2072–2084. https://doi.org/10.1104/PP.15.01525.

Disney, M., A. Burt, P. Wilkes, J. Armston, and L. Duncanson. 2020. New 3D measurements of large redwood trees for biomass and structure. *Scientific Reports 2020* 10(1):1–11. https://doi.org/10.1038/s41598-020-73733-6.

Disney, M. I., M. Boni Vicari, A. Burt, K. Calders, S. L. Lewis, P. Raumonen, and P. Wilkes. 2018. Weighing trees with lasers: advances, challenges and opportunities. *Interface Focus* 8(2). https://doi.org/10.1098/RSFS.2017.0048.

Doraisami, M., G. M. Domke, and A. R. Martin. 2024. Improving wood carbon fractions for multiscale forest carbon estimation. *Carbon Balance and Management* 19(1):1–10. https://doi.org/10.1186/S13021-024-00272-2.

Egerer, M., J. M. Schmack, K. Vega, C. O. Barona, and S. Raum. 2024. The challenges of urban street trees and how to overcome them. *Frontiers in Sustainable Cities* 6:1394056. https://doi.org/10.3389/frsc.2024.1394056.

Escobedo, F. J., T. Kroeger, and J. E. Wagner. 2011. Urban forests and pollution mitigation: Analyzing ecosystem services and disservices. *Environmental Pollution* 159(8–9):2078–2087. https://doi.org/10.1016/J.ENVPOL.2011.01.010.

Fan, Z. X., S. B. Zhang, G. Y. Hao, J. W. Ferry Slik, and K. F. Cao. 2012. Hydraulic conductivity traits predict growth rates and adult stature of 40 Asian tropical tree species better than wood density. *Journal of Ecology* 100(3):732–741. https://doi.org/10.1111/J.1365-2745.2011.01939.X.

Fonti, P., G. Von Arx, I. García-González, B. Eilmann, U. Sass-Klaassen, H. Gärtner, and D. Eckstein. 2010. Studying global change through investigation of the plastic responses of xylem anatomy in tree rings. *New Phytologist* 185(1):42–53. https://doi.org/10.1111/J.1469-8137.2009.03030.X.

Fonti, P., and I. García-González. 2004. Suitability of chestnut earlywood vessel chronologies for ecological studies. *New Phytologist* 163(1):77–86. https://doi.org/10.1111/J.1469-8137.2004.01089.X.

Gao, B., A. R. Taylor, H. Y. H. Chen, and J. Wang. 2016. Variation in total and volatile carbon concentration among the major tree species of the boreal forest. *Forest Ecology and Management* 375:191–199. https://doi.org/10.1016/J.FORECO.2016.05.041.

Gregg, J. W., C. G. Jones, and T. E. Dawson. 2003. Urbanization effects on tree growth in the vicinity of New York City. *Nature 2003 424:6945* 424(6945):183–187. https://doi.org/10.1038/nature01728.

Hacke, U. G., R. Spicer, S. G. Schreiber, and L. Plavcová. 2017. An ecophysiological and developmental perspective on variation in vessel diameter. *Plant Cell and Environment* 40(6):831–845. https://doi.org/10.1111/PCE.12777.

Hoeber, S., C. Leuschner, L. Köhler, D. Arias-Aguilar, and B. Schuldt. 2014. The importance of hydraulic conductivity and wood density to growth performance in eight tree species from a tropical semi-dry climate. *Forest Ecology and Management* 330:126–136. https://doi.org/10.1016/J.FORECO.2014.06.039.

Hook, D. D. 1984. Waterlogging Tolerance of Lowland Tree Species of the South[1]. *Southern Journal of Applied Forestry* 8(3):136–149. https://doi.org/10.1093/SJAF/8.3.136.

Hoover, K., and A. A. Riddle. 2020. *Forest carbon primer*. Congressional Research Service Washington, DC, USA.

Hutt-Taylor, K., C. G. Bassett, R. P. Kinnunen, B. Frei, and C. D. Ziter. 2024. Existing evidence on the effect of urban forest management in carbon solutions and avian conservation: a systematic literature map. *Environmental Evidence 2024* 13(1):23-. https://doi.org/10.1186/s13750-024-00344-3.Iakovoglou, V., J. Thompson, L. Burras. 2002. Characteristics of Trees According to Community Population Level and By Land Use in the U.S. Midwest. *Arboriculture & Urban Forestry* 28(2):59–69. https://doi.org/10.48044/jauf.2002.008.

Iakovoglou, V., J. Thompson, L. Burras, and R. Kipper. 2001. Factors related to tree growth across urban-rural gradients in the Midwest, USA. *Urban Ecosystems* 5(1):71–85. https://doi.org/10.1023/A:1021829702654.

Ipcc, I. 2006. Guidelines for national greenhouse gas inventories. *Prepared by the National Greenhouse Gas Inventories Programme. Eggleston HS, Buendia L, Miwa K, Ngara T, Tanabe K, editors. Published: IGES, Japan*.

(IPCC), I. P. on C. C., ed. 2023. Urban Systems and Other Settlements. P. 861–952 in *Climate Change 2022 - Mitigation of Climate Change: Working Group III Contribution to the Sixth Assessment Report of the Intergovernmental Panel on Climate Change*, Cambridge University Press, Cambridge. https://doi.org/10.1017/9781009157926.010.

Klein, L. J., W. Zhou, and C. M. Albrecht. 2021. Quantification of Carbon Sequestration in Urban Forests.

Krause, P., B. Forbes, A. Barajas-Ritchie, M. Clark, M. Disney, P. Wilkes, and L. P. Bentley. 2023. Using terrestrial laser scanning to evaluate non-destructive aboveground biomass allometries in diverse Northern California forests. *Frontiers in Remote Sensing* 4:1132208. https://doi.org/10.3389/FRSEN.2023.1132208.

Kükenbrink, D., O. Gardi, F. Morsdorf, E. Thürig, A. Schellenberger, and L. Mathys. 2021. Above-ground biomass references for urban trees from terrestrial laser scanning data. *Annals of Botany* 128(6):709–724. https://doi.org/10.1093/AOB/MCAB002.

Lamlom, S. H., and R. A. Savidge. 2003. A reassessment of carbon content in wood: variation within and between 41 North American species. *Biomass and Bioenergy* 25(4):381–388. https://doi.org/10.1016/S0961-9534(03)00033-3.

Lee, J.-M., H.-S. Kim, B. Choi, J.-Y. Jung, S. Lee, H. Jo, G. Kim, et al. 2025. Enhanced Accuracy in Urban Tree Biomass Estimation: Developing Allometric Equations with Land Use Classifications. *Forests 2025, Vol. 16,* 16(5). https://doi.org/10.3390/F16050841.

Lin, J., Q. Ma, Y. Ju, H. Zhang, Q. Wang, and B. Huang. 2022. Relationships between urbanization, tree morphology, and carbon density: An integration of remote sensing, allometric models, and field survey. *Urban Forestry & Urban Greening* 76:127725. https://doi.org/10.1016/j.ufug.2022.127725.

Liang, X., V. Kankare, J. Hyyppä, Y. Wang, A. Kukko, H. Haggrén, X. Yu, et al. 2016. Terrestrial laser scanning in forest inventories. *ISPRS Journal of Photogrammetry and Remote Sensing* 115:63–77. https://doi.org/10.1016/J.ISPRSJPRS.2016.01.006.

Ma, S. H., A. Eziz, D. Tian, Z. B. Yan, Q. Cai, M. W. Jiang, C. J. Ji, J. Y. Fang, and O. J. Sun. 2020. Size- and age-dependent increases in tree stem carbon concentration: implications for forest carbon stock estimations. *Journal of Plant Ecology* 13(2):233–240. https://doi.org/10.1093/JPE/RTAA005.

Martin, A. R., S. Gezahegn, and S. C. Thomas. 2015. Variation in carbon and nitrogen concentration among major woody tissue types in temperate trees. *Canadian Journal of Forest Research* 45(6):744–757. https://doi.org/10.1139/CJFR-2015-0024.

Martin, A. R., and S. C. Thomas. 2011. A Reassessment of Carbon Content in Tropical Trees. *PLOS ONE* 6(8):e23533. https://doi.org/10.1371/JOURNAL.PONE.0023533.

McClung, T., and I. Ibáñez. 2017. Quantifying the synergistic effects of impervious surface and drought on radial tree growth. *Urban Ecosystems 2017* 21(1):147–155. https://doi.org/10.1007/S11252-017-0699-5.

McHale, M. R., I. C. Burke, M. A. Lefsky, P. J. Peper, and E. G. McPherson. 2009. Urban forest biomass estimates: is it important to use allometric relationships developed specifically for urban trees? *Urban Ecosystems* 12(1):95–113. https://doi.org/10.1007/s11252-009-0081-3.

McPherson, E. G., Q. Xiao, and E. Aguaron. 2013. A new approach to quantify and map carbon stored, sequestered and emissions avoided by urban forests. *Landscape and Urban Planning* 120:70–84. https://doi.org/10.1016/J.LANDURBPLAN.2013.08.005.

McPherson, E. G., N. S. van Doorn, and P. J. Peper. 2016. Urban tree database and allometric equations. https://doi.org/10.2737/PSW-GTR-253.

Meineke, E. K., and S. D. Frank. 2018. Water availability drives urban tree growth responses to herbivory and warming. *Journal of Applied Ecology* 55(4):1701–1713. https://doi.org/10.1111/1365-2664.13130.

Miles, P. D., and W. Brad. Smith. 2009. *Specific gravity and other properties of wood and bark for 156 tree species found in North America*. U.S. Department of Agriculture, Forest Service, Northern Research Station. https://doi.org/10.2737/nrs-rn-38.

Moore, G. M., A. Fitzgerald, P. B. May, G. M. Moore, A. Fitzgerald, and P. B. May. 2019. Soil Compaction Affects the Growth and Establishment of Street Trees in Urban Australia. *Arboriculture & Urban Forestry* 45(6):239–253. https://doi.org/10.48044/jauf.2019.020.

Morales, A., and D. W. MacFarlane. 2025a. Reducing tree volume overestimation in quantitative structure models using modeled branch topology and direct twig measurements. *Forestry: An International Journal of Forest Research* 98(3):394–409. https://doi.org/10.1093/forestry/cpae046.

Morales, A., and D. W. MacFarlane. 2025b. rTwig: An R package to correct overestimated small branches and twigs in quantitative structure models of trees. *Science of Remote Sensing* 12:100284. https://doi.org/10.1016/J.SRS.2025.100284.

Mullaney, J., T. Lucke, and S. J. Trueman. 2015. A review of benefits and challenges in growing street trees in paved urban environments. *Landscape and Urban Planning* 134:157–166. https://doi.org/10.1016/J.LANDURBPLAN.2014.10.013.

Muller-Feuga, A. 2024. The Recognition of Carbon Capture and Storage by Plants. *Journal of Agricultural Science* 16(7):1. https://doi.org/10.5539/JAS.V16N7P1.

Nations, U. 2012. The millennium development goals report 2012. *Millennium development goals report*.

Ngo, K. M., and S. Lum. 2018. Aboveground biomass estimation of tropical street trees. *Journal of Urban Ecology* 4(1). https://doi.org/10.1093/jue/jux020.

Niinemets, Ü., and F. Valladares. 2006. Tolerance to shade, drought, and waterlogging of temperate northern hemisphere trees and shrubs. *Ecological Monographs* 76(4):521–547. https://doi.org/10.1890/0012-9615(2006)076[0521:TTSDAW]2.0.CO;2.

North, E. A., A. W. D'Amato, and M. B. Russell. 2018. Performance Metrics for Street and Park Trees in Urban Forests. *Journal of Forestry* 116(6):547–554. https://doi.org/10.1093/JOFORE/FVY049.

Nowak, D. J., and D. E. Crane. 2002. Carbon storage and sequestration by urban trees in the USA. *Environmental Pollution* 116(3):381–389. https://doi.org/10.1016/S0269-7491(01)00214-7.

Nowak, D. J., E. J. Greenfield, R. E. Hoehn, and E. Lapoint. 2013. Carbon storage and sequestration by trees in urban and community areas of the United States. *Environmental Pollution* 178:229–236. https://doi.org/10.1016/J.ENVPOL.2013.03.019.

Parhizgar, L., N. Pattnaik, H. Yazdi, S. Qiguan, S. Pauleit, M. A. Rahman, F. Ludwig, H. Pretzsch, and T. Rötzer. 2025. Branch biomass allometries for urban tree species based on terrestrial laser scanning (TLS) data. *Trees - Structure and Function* 39(4):1–16. https://doi.org/10.1007/S00468-025-02637-7.

Patel, V. V., S. Vishwakarma, and R. Gangwar. 2024. Urban Tree Selection and Management Strategies for Climate Adaptation. *Urban Forests, Climate Change and Environmental Pollution* :391–415. https://doi.org/10.1007/978-3-031-67837-0_19.

Pittermann, J., J. S. Sperry, J. K. Wheeler, U. G. Hacke, and E. H. Sikkema. 2006. Mechanical reinforcement of tracheids compromises the hydraulic efficiency of conifer xylem. *Plant, Cell and Environment* 29(8):1618–1628. https://doi.org/10.1111/J.1365-3040.2006.01539.X.

Pivovaroff, A. L., S. C. Pasquini, M. E. De Guzman, K. P. Alstad, J. S. Stemke, and L. S. Santiago. 2016. Multiple strategies for drought survival among woody plant species. *Functional Ecology* 30(4):517–526. https://doi.org/10.1111/1365-2435.12518.

Pretzsch, H., P. Biber, E. Uhl, J. Dahlhausen, G. Schütze, D. Perkins, T. Rötzer, et al. 2017. Climate change accelerates growth of urban trees in metropolises worldwide. *Scientific Reports* 7(1). https://doi.org/10.1038/s41598-017-14831-w.

Quigley, M. F. 2004. Street trees and rural conspecifics: Will long-lived trees reach full size in urban conditions? *Urban Ecosystems* 7(1):29–39. https://doi.org/10.1023/b:ueco.0000020170.58404.e9.

Radtke, P., D. Walker, J. Frank, A. Weiskittel, C. DeYoung, D. MacFarlane, G. Domke, C. Woodall, J. Coulston, and J. Westfall. 2017. Improved accuracy of aboveground biomass

and carbon estimates for live trees in forests of the eastern United States. *Forestry: An International Journal of Forest Research* 90(1):32–46. https://doi.org/10.1093/FORESTRY/CPW047.

Randrup, T. B., E. G. McPherson, and L. R. Costello. 2001. A review of tree root conflicts with sidewalks, curbs, and roads. *Urban Ecosystems 2001* 5(3):209–225. https://doi.org/10.1023/A:1024046004731.

Raumonen, P., M. Kaasalainen, M. Åkerblom, S. Kaasalainen, H. Kaartinen, M. Vastaranta, M. Holopainen, M. Disney, and P. Lewis. 2013. Fast Automatic Precision Tree Models from Terrestrial Laser Scanner Data. *Remote Sensing* 5(2):491–520. https://doi.org/10.3390/rs5020491.

Rissanen, K., V. Vitali, D. Kneeshaw, and A. Paquette. 2025. Vessel anatomy of urban Celtis occidentalis trees varies to favour safety or efficiency depending on site conditions. *Trees 2025 39:1* 39(1):1–15. https://doi.org/10.1007/S00468-025-02603-3.

Rodríguez-Gamir, J., E. Primo-Millo, and M. Á. Forner-Giner. 2016. An Integrated View of Whole-Tree Hydraulic Architecture. Does Stomatal or Hydraulic Conductance Determine Whole Tree Transpiration? *PLOS ONE* 11(5):e0155246. https://doi.org/10.1371/JOURNAL.PONE.0155246.

Rompato, B., L. Mondanelli, E. Lo Piccolo, C. Cocozza, G. Mastrolonardo, L. Giagnoni, G. Fantoni, et al. 2025. Cork and Compost as Mitigators of Soil Compaction from Trampling in Urban Green Areas: Effects on Plant Growth and Soil Functionality. *Urban Science* 9(1):5. https://doi.org/10.3390/urbansci9010005.

Roy, S., J. Byrne, and C. Pickering. 2012. A systematic quantitative review of urban tree benefits, costs, and assessment methods across cities in different climatic zones. *Urban Forestry & Urban Greening* 11(4):351–363. https://doi.org/10.1016/J.UFUG.2012.06.006.

Sanders, J. R., and J. C. Grabosky. 2014. 20 years later: Does reduced soil area change overall tree growth? *Urban Forestry & Urban Greening* 13(2):295–303. https://doi.org/10.1016/j.ufug.2013.12.006.

Santiago, L. S., K. Kitajima, S. J. Wright, and S. S. Mulkey. 2004. Coordinated changes in photosynthesis, water relations and leaf nutritional traits of canopy trees along a precipitation gradient in lowland tropical forest. *Oecologia 2004* 139(4):495–502. https://doi.org/10.1007/S00442-004-1542-2.

Sarah, P., H. M. Zhevelev, and A. Oz. 2015. Urban Park Soil and Vegetation: Effects of Natural and Anthropogenic Factors. *Pedosphere* 25(3):392–404. https://doi.org/10.1016/S1002-0160(15)30007-2.

Savi, T., S. Bertuzzi, S. Branca, M. Tretiach, and A. Nardini. 2015. Drought-induced xylem cavitation and hydraulic deterioration: Risk factors for urban trees under climate change? *New Phytologist* 205(3):1106–1116. https://doi.org/10.1111/NPH.13112.

Seidel, D., S. Fleck, and C. Leuschner. 2012. Analyzing forest canopies with ground-based laser scanning: A comparison with hemispherical photography. *Agricultural and Forest Meteorology* 154–155:1–8. https://doi.org/10.1016/J.AGRFORMET.2011.10.006.

Shinozaki, K., K. Hozumi, and T. Kira. 1964. A quantitative analysis of plant form-the pipe model theory: II. Further evidence of the theory and its application in forest ecology. *Japanese Journal of Ecology* 14(4):133–139. https://doi.org/10.18960/SEITAI.14.4_133.

Speak, A. F., and F. Salbitano. 2023. The impact of pruning and mortality on urban tree canopy volume. *Urban Forestry & Urban Greening* 79(4):127810. https://doi.org/10.1016/j.ufug.2022.127810.

Sperry J. S., and N. Z. Saliendra. 1994. Intra- and inter-plant variation in xylem cavitation in Betula occidentalis. *Plant, Cell & Environment* 17(11):1233–1241. https://doi.org/10.1111/J.1365-3040.1994.TB02021.X

Tang, L., G. Shao, and P. M. Groffman. 2024. Urban trees: how to maximize their benefits for humans and the environment. *Nature* 626(7998):261. https://doi.org/10.1038/D41586-024-00300-8

Tyree, M. T., S. D. Davis, and H. Cochard. 1994. Biophysical Perspectives of Xylem Evolution: is there a Tradeoff of Hydraulic Efficiency for Vulnerability to Dysfunction? *IAWA Journal* 15(4):335–360. https://doi.org/10.1163/22941932-90001369.

Von Arx, G., A. Crivellaro, A. L. Prendin, K. Čufar, and M. Carrer. 2016. Quantitative wood anatomy—practical guidelines. Frontiers in Plant Science 7(JUNE2016):197139. https://doi.org/10.3389/fpls.2016.00781.

Vorster, A. G., P. H. Evangelista, A. E. L. Stovall, and S. Ex. 2020. Variability and uncertainty in forest biomass estimates from the tree to landscape scale: the role of allometric equations. *Carbon Balance and Management 2020 15:1* 15(1):8-. https://doi.org/10.1186/s13021-020-00143-6.

Wang, Z., G. Li, H. Sun, L. Ma, Y. Guo, Z. Zhao, H. Gao, and L. Mei. 2018. Effects of drought stress on photosynthesis and photosynthetic electron transport chain in young apple tree leaves. *Biology Open* 7(11). https://doi.org/10.1242/BIO.035279/2013.

Warton, D. I., R. A. Duursma, D. S. Falster, and S. Taskinen. 2012. smatr 3- an R package for estimation and inference about allometric lines. *Methods in Ecology and Evolution* 3(2):257–259. https://doi.org/10.1111/J.2041-210X.2011.00153.X.

Wei, W., W. Li, Y. Deng, and S. Yang. 2018. Intraseasonal variation of the summer rainfall over the Southeastern United States. *Climate Dynamics 2018 53:1* 53(1):1171–1183. https://doi.org/10.1007/s00382-018-4345-6.

Weiskittel, A. R., D. W. MacFarlane, P. J. Radtke, D. L. R. Affleck, H. Temesgen, C. W. Woodall, J. A. Westfall, and J. W. Coulston. 2015. A Call to Improve Methods for Estimating Tree Biomass for Regional and National Assessments. *Journal of Forestry* 113(4):414–424. https://doi.org/10.5849/JOF.14-091.

West, G. B., J. H. Brown, and B. J. Enquist. 1997. A general model for the origin of allometric scaling laws in biology. *Science* 276(5309):122–126. https://doi.org/10.1126/science.276.5309.122.

West, R. M. 2021. Best practice in statistics: Use the Welch t-test when testing the difference between two groups. *Annals of Clinical Biochemistry* 58(4):267–269. https://doi.org/10.1177/0004563221992088.

Wilkes, P., M. Disney, M. B. Vicari, K. Calders, and A. Burt. 2018. Estimating urban above ground biomass with multi-scale LiDAR. *Carbon Balance and Management* 13(1). https://doi.org/10.1186/S13021-018-0098-0.

Wilkes, P., A. Lau, M. Disney, K. Calders, A. Burt, J. Gonzalez de Tanago, H. Bartholomeus, B. Brede, and M. Herold. 2017. Data acquisition considerations for Terrestrial Laser Scanning of forest plots. *Remote Sensing of Environment* 196:140–153. https://doi.org/10.1016/J.RSE.2017.04.030.

Williams, R. H., and B. Applegate. 1992. Tukey-like pairwise comparisons among variances. *Behavior Research Methods, Instruments, & Computers 1992* 24(3):494–495. https://doi.org/10.3758/bf03203589.

Williamson, G. B., and M. C. Wiemann. 2010. Measuring wood specific gravity...correctly. *American Journal of Botany* 97(3):519–524. https://doi.org/10.3732/ajb.0900243.

Wu, H., W. Xiang, X. Fang, P. Lei, S. Ouyang, and X. Deng. 2017. Tree functional types simplify forest carbon stock estimates induced by carbon concentration variations among species in a subtropical area. *Scientific Reports* 7(1):1–11. https://doi.org/10.1038/s41598-017-05306-z.

Zhao, M., Z. hong Kong, F. J. Escobedo, and J. Gao. 2010. Impacts of urban forests on offsetting carbon emissions from industrial energy use in Hangzhou, China. *Journal of Environmental Management* 91(4):807–813. https://doi.org/10.1016/J.JENVMAN.2009.10.010.

CHAPTER 3

Enhancing the quantification of urban tree carbon stocks with the use of terrestrial laser scanning technology.

Abstract

Quantifying the aboveground carbon biomass (AGC) of urban trees is essential for supporting climate change adaptation efforts in urban areas. However, their complex, open-grown structure cannot be accurately quantified with traditional allometric equations developed for natural forests. Terrestrial laser scanning (TLS) provides a non-destructive approach to capture three-dimensional tree structure in detail. In this study, we used TLS to quantify aboveground carbon biomass and carbon allocation in urban trees, and we compared TLS-based AGC with *i-Tree Eco* estimates, a publicly available tool for urban canopy assessments developed by the U.S. Forest Service. We laser-scanned 90 urban trees of three species (*Quercus falcata*, *Quercus lyrata*, and *Taxodium distichum*) in leaf-on and leaf-off conditions and generated quantitative structure models (QSMs) to estimate woody volume. We estimated TLS-derived above-ground carbon (AGC) using four volume-to-carbon conversion approaches: (1) published basic wood density values combined with a fixed 50% carbon concentration of woody biomass; (2) directly measured basic wood density from increment core samples combined with a fixed 50% carbon concentration; (3) published basic wood density values combined with directly measured carbon concentration determined by elemental analysis of increment cores; and (4) directly measured basic wood density combined with directly measured carbon concentration from elemental analysis. Leaf-on and leaf-off TLS-based AGC estimates were strongly correlated, but leaf-on scans yielded lower AGC estimates for *Q. lyrata* and *T.*

distichum; applying *rTwig* reduced overestimation of small-branch volume, thereby compressing the upper range of AGC estimates. It was found that carbon biomass allocation in the main stem and branches of the study trees varied among species, with *Q. lyrata* trees showing higher branch carbon biomass relative to stem carbon biomass compared to *Q. falcata* and *T. distichum* trees. Across all study trees, branch carbon biomass decreased with branch order and was mainly accumulated on a small number of large, low-order branches. Branch carbon biomass increased with branch-base diameter and was concentrated in the lower- to mid-crown height, with relatively small contributions from upper-crown branches. The i-Tree AGC estimates were strongly correlated with TLS-derived AGC across all species, and overall agreement was highest when i-Tree was run without the crown light exposure adjustment (CLE; open-grown adjustment), although the effect of CLE was species dependent. Collectively, these results demonstrate that TLS combined with measured wood traits can provide robust AGC estimates and detailed allocation patterns that are useful for validating large-tree carbon assessments and developing improved urban-specific allometric models.

3.1 Introduction

The role of urban forests in climate change mitigation and adaptation efforts has been increasingly recognized as trees store carbon in woody biomass and continue to sequester carbon as they grow (Nowak et al. 2013; Jenerette and Herrmann 2023). In the United States, a national synthesis estimated that trees in urban areas store approximately 643 million tons of carbon and sequester approximately 25.6 million tons of atmospheric carbon dioxide per year, highlighting both the magnitude and policy relevance of urban tree carbon stocks and fluxes (Nowak et al. 2013). However, the credibility of urban tree carbon accounting is constrained by methodological uncertainty: carbon estimates of urban trees can differ substantially depending on

how biomass is inferred and how biomass is converted to carbon biomass (McHale et al. 2009; Kükenbrink et al. 2021). Because large trees disproportionately contribute to total carbon storage, systematic bias, rather than random error, can propagate into city-scale inventories and distort comparisons across time, neighborhoods, or management scenarios (Calders et al. 2015).

Most urban forest carbon inventories rely on allometric equations that use easily measured tree variables (typically diameter at breast height and total height) to produce above-ground biomass (AGB) estimates-the total dry mass of all living and dead organic matter above the soil surface, including the stem, branches, bark, and foliage-which are then converted to carbon (Chave et al. 2014; McPherson et al. 2016; Arseniou et al. 2023). These allometric relationships are often developed for trees grown in forest stands, where competition, canopy structure, and management differ fundamentally from those in urban environments. Urban trees usually grow in open conditions with reduced competition, they experience pruning and infrastructure conflicts and can exhibit an architecture with distinct height–diameter relationships, all of which can alter biomass allocation patterns and violate the assumptions embedded in forest-derived allometries (Zhou et al. 2015; MacFarlane and Kane 2017; Arseniou and MacFarlane 2021; Muscas et al. 2023). Empirical comparisons demonstrate that biomass predictions can vary substantially when equations developed outside urban contexts are applied to urban trees, with variability exceeding 300% at the individual tree scale in some cases, underscoring the need for more direct, structure-based approaches or urban-specific calibration (McHale et al. 2009).

The *i-Tree Eco* is a peer-reviewed urban forest assessment software developed by the United States Forest Service and partners within the *i-Tree suite,* which uses urban forest field inventories to estimate tree biomass, carbon storage, and other ecosystem services using a

published methods framework (Nowak 2024). In *i-Tree Eco*, crown light exposure (CLE) is used to determine whether a biomass adjustment factor (BAF) is applied. CLE is a categorical index ranging from 0 to 5 that quantifies the number of sides of a tree's crown receiving direct sunlight. Trees recorded with a CLE class 4 or 5 (i.e., crowns receiving sunlight from all sides, typical of open-grown urban trees) receive a 0.8 BAF multiplier applied to biomass estimates, while other trees are estimated without that reduction (Nowak 2024). This CLE-based adjustment is intended to account for the premise that many biomass equations are derived from natural forests and tend to overestimate the biomass of open-grown urban trees (McPherson et al. 1994; McHale et al. 2009). Yet the underlying ecological premise is unlikely to be uniform across species, sizes, and architectural forms, and the urban-specific validity of a single multiplier factor remains an open question, particularly when independent structure-based estimates are available for benchmarking (McHale et al. 2009; Kükenbrink et al. 2021; Krause et al. 2023).

Even if biomass could be perfectly estimated, converting biomass to carbon introduces additional uncertainty because carbon concentration (the proportion of dry biomass that is carbon) is often assumed to be constant (approximately 50%) in many carbon accounting workflows, including *i-Tree* software (Doraisami et al. 2024; Nowak 2024). Large syntheses show that woody tissue carbon concentration varies substantially across species, biomes, and taxonomic groups, with reported values spanning a broad range (e.g., 28–65% of woody biomass in a global compilation), implying that a universal 50 % carbon concentration can create systematic bias (Martin et al. 2018). Similarly, wood density is a key conversion factor in biomass estimation when wood volume is known. It is frequently sourced from global wood trait databases rather than measured locally, even though density can vary among species, and within trees and sites. i-Tree documentation provides extensive wood density values derived from

global compilations, illustrating both the operational dependence on published densities and the importance of understanding how those values influence carbon estimates (Chave et al. 2009; McPherson et al. 2016; Nowak 2024).

Terrestrial laser scanning (TLS) offers a complementary approach to estimating tree structure by acquiring high-density three-dimensional point clouds of trees. TLS is an active remote sensing technology that emits laser energy and measures backscattered returns to map trees in 3D, producing point clouds in which each return has X, Y, Z coordinates (Wilkes et al. 2017; Calders et al. 2020). Most TLS instruments estimate range using either time-of-flight (pulse travel time) or phase-shift (phase difference of modulated signals), enabling rapid collection of millions of points per scan (Calders et al. 2020).

Quantitative structure models (QSMs) reconstruct tree architecture from TLS point clouds by fitting geometric primitives (e.g., cylinders), providing explicit estimates of woody volume and branching topology that can be used to quantify tree-component biomass and carbon biomass. *TreeQSM* is one of the most widely used QSM algorithms (Raumonen et al. 2013). It requires that input point clouds contain only woody points and limited noise because leaves can be misinterpreted as woody surfaces and bias the reconstructed wood volumes (Raumonen et al. 2013; Calders et al. 2015). Importantly, TLS has repeatedly produced accurate, non-destructive AGB estimates with quantifiable uncertainties, outperforming standard allometries (Disney et al. 2018; Calders et al. 2022; Arseniou et al. 2023). Many TLS-based studies have used published wood density values for volume to biomass conversion, although wood density varies within and among trees and across growing conditions (Arseniou et al. 2023; Krause et al. 2023; Demol et al. 2021).

Extracting increment core samples is an effective method to measure actual wood density with minimal impact on trees (Williamson and Wiemann 2010). The same core samples can be combusted in an elemental analyzer, which quantifies woody core carbon concentration as a percentage of its biomass (Bird et al. 2017). Using measured wood density together with measured carbon concentration enables accurate conversion of TLS-derived volume to total above-ground carbon biomass (AGC, kg), reducing reliance on published density values and the default 50% carbon concentration when higher accuracy is required.

Beyond estimating total above-ground carbon biomass, TLS can be used to quantify how trees allocate carbon biomass within their above-ground structure, partitioning in between the main stem and branches, and across different branch orders, branch size classes, and crown heights (Lau et al. 2018; Arseniou et al. 2021). This is important from both ecological and methodological perspectives because carbon biomass allocation reflects life history strategies, constraints to growth, and crown architecture patterns, while the size distribution of woody structure components (stems and branches) often determine modelling uncertainty (Calders et al. 2015; Demol et al. 2022a; Morhart et al. 2024). These insights are particularly valuable for urban forest biomass and carbon assessment, where destructive sampling of urban trees is typically infeasible due to safety concerns, permitting requirements, public acceptance, and logistical constraints (McHale et al. 2009; Lee et al. 2025). In this context, TLS provides a practical non-destructive alternative for deriving detailed, tree-level carbon estimates, helping overcome limitations of allometries developed largely from rural forest trees and reducing reliance on destructive approaches (Weiskittel et al. 2015; Disney et al. 2018; Arseniou et al. 2023).

In this study, we integrated TLS-derived measurements with direct measurements of wood properties (wood density and carbon concentration) to quantify above-ground urban tree

carbon biomass. Specifically, we aimed to: (i) assess how conversion approaches affect TLS-derived total above-ground carbon estimates, (ii) quantify how urban trees allocate carbon biomass in their above-ground components, and (iii) compare TLS-based carbon biomass estimates with i-Tree-based estimates. By addressing these objectives, our study provides new insights into urban tree carbon allocation that can be used to refine urban forest carbon accounting through improved allometric models that guide the application of urban forest carbon estimation methods.

3.2 Materials and Methods

3.2.1 Study Area

The study was conducted in Auburn, Alabama, USA. We sampled 90 urban trees across three species, with 30 trees representing each species: Southern red oak (*Quercus falcata*), overcup oak (*Quercus lyrata*), and bald cypress (*Taxodium distichum*). Within each species, individuals were chosen to represent a wide range of stem diameters at breast height (DBH) and total tree heights (see Table 3.1). All sampled trees were healthy, with no visible disease, pest, or structural defects (e.g., decay).

Table 3.1 Summary statistics of the size of study trees.

Species	Height(m) (mean [min, max])	DBH (m) (mean [min, max])
Quercus falcata	18.58 [7.18, 29.15]	0.67 [0.21, 1.35]
Quercus lyrata	12.51 [7.75, 18.89]	0.51 [0.32, 1.13]
Taxodium distichum	12.32 [5.90, 27.51]	0.38 [0.21, 0.82]

3.2.2 Wood density and carbon content calculation from cores

For every study tree, a 5.15 mm diameter increment core was extracted at breast height (1.37 m) using an increment borer. The samples were then immediately placed in sealed, labeled bags to prevent moisture loss. The diameter of the cores was measured using a caliper with 0.01mm precision, and the length with a standard engineer's ruler. The green volume of each core sample was then calculated assuming a cylinder's volume. Allcores were oven-dried at 100°C for 24 hours and weighed to measure dry mass. Basic wood density (ρ) was calculated using equation (1).

$$\rho_{measured} = \frac{oven\ dry\ mass\ of\ increment\ core\ sample\ (g)}{green\ volume\ of\ increment\ core\ sample\ (cm^3)} \quad (1)$$

We determined the carbon concentration (C%) of each wood core through elemental analysis. Each dried core was divided into three segments along its radius: near the pith, the middle of the core, and near the bark. From each segment, a ~2–3 mg subsample of wood was encapsulated in a tin capsule. Carbon content (C% by mass) was measured using a FlashSmart CHNS/O elemental analyzer, which combusts the sample at high temperature and quantifies C% via a thermal conductivity detector (Bird et al. 2017).

Because bark can have a different carbon concentration than wood, we calculated a weighted average carbon concentration for each core, combining wood and bark contributions. Using species-specific bark volume fractions from Miles and Smith (2009), we weighted the carbon concentrations of wood versus bark as:

$$C_{measured}\ (\%) = (C_{wood} \times \%Vol_{wood}) + (C_{bark} \times \%Vol_{bark}) \quad (2)$$

where,

$C_{measured}$ = weighted average carbon concentration of a woody core,

C_{wood} = average carbon concentration at the core center and pith,

C_{bark} = carbon concentration of the bark,

$\%Vol_{wood}$ = percentage of wood volume [80% for *T. distichum*; 78% for *Q. falcata* and *Q. lyrata* (Miles and Smith 2009)]

$\%Vol_{bark}$ = percentage of bark volume [20% for *T. distichum*; 22% for *Q. falcata* and *Q. lyrata* (Miles and Smith 2009)]

3.2.3 Terrestrial Laser Scanning (TLS) and Quantitative Structure Models Generation

All study trees were scanned using a FARO Focus Premium terrestrial laser scanner (FARO Technologies, 2024). Each tree was scanned in leaf-on and leaf-off conditions to evaluate the influence of foliage state on carbon biomass estimation. Scans were conducted under mild wind conditions to reduce noise and occlusion due to swaying stems and branches.

Each tree was scanned from 4–6 positions, with scan locations distributed across multiple angles to minimize occlusion (Wilkes et al. 2017). We began with two close-range scans from opposing directions to capture detailed stem and primary branch geometry. We then conducted two additional scans on perpendicular direction to the initial pair at a distance that allowed a clear view of the entire tree crown. Additional scans were collected for large trees with dense crowns.

To enable co-registration of scans acquired from multiple positions, four identical spherical targets were placed around each tree so that they were visible across adjacent scans. All individual scans were co-registered to create a single point cloud per study tree with *FARO Scene*

2023.1.0. Individual tree point clouds were isolated from the surrounding environment. Finally, we removed noise from the individual tree point clouds using the statistical outlier removal tool in *CloudCompare v2.13.2* (http://www.cloudcompare.org/).

For leaf-on point clouds, it is necessary to virtually remove the leaf component before generating QSMs to produce wood volume estimates. The *GBSeparation* algorithm was applied to the leaf-on point clouds to separate the leaf and wood components (Tian and Li 2022). It is a graph-based algorithm that uses shortest-path graph theory to identify cylindrical or linear features as woody structures in point clouds and separate them from the leaf component. In experiments, *GBSeparation* consistently outperformed other widely used leaf separation techniques for both broadleaf trees and conifers (Arrizza et al. 2024; Chen et al. 2025).

Quantitative structure models (QSMs) were generated from leaf-off and leaf-removed point clouds using *TreeQSM* 3.4.1. The algorithm first partitions the point cloud into small surface patches using a cover-set strategy that groups points by proximity and local surface geometry (Raumonen et al. 2013; Calders et al. 2018). The model then identifies the main stem (e.g., dominant vertical axis with low curvature) and reconstructs the branching topology by tracing connectivity among components (Arseniou et al. 2021). Cylinders are subsequently fit to the stem and branches by least-squares optimization, proceeding from the base upward while enforcing continuity and biological tapering. Due to the inherent stochasticity of the *TreeQSM* algorithm, multiple reconstructions are produced for different parameter settings, and the optimal QSM reconstruction is selected (Raumonen et al. 2013).

Inherent limitations of terrestrial laser scanning, like laser beam divergence, occlusion, and co-registration errors, prevent the accurate reconstruction of small branches and twigs (Morales and MacFarlane 2025a). Due to these limitations, QSMs tend to overestimate the

volume of small branches and twigs, resulting in a substantial overestimation of total above-ground wood volume (Demol et al. 2022b). To address this issue, Morales and MacFarlane (2025b) proposed a new method, *rTwig*, which integrates species-specific twig radius measurements to model biologically accurate branch tapering. Hence, in this study, optimal QSMs were allometrically corrected using *rTwig*. After applying *rTwig*, the final QSM provided the volume of each tree's woody components (main stem and branches).

From each QSM, we extracted the volume of the main stem and all branches to analyze carbon biomass allocation in these components. Branches are hierarchically categorized in a QSM. (Order 1: first-order branches that are directly attached to the main stem; Order 2: second-order branches that are attached to first-order branches, and so on). Furthermore, for every branch in a QSM, we can retrieve its base diameter and the height of its origin on the tree. This analysis allowed us to quantify how carbon was distributed by branch size and branching order, as well as vertically within the tree's crown.

3.2.4 TLS-based total above-ground carbon estimates

We computed each tree's above-ground carbon biomass (AGC) by multiplying TLS-based above-ground volume by basic wood density and the carbon concentration. To explore the effect of the conversion parameter, we estimated TLS-based carbon biomass under four different scenarios:

i. Scenario A: Published basic wood density ($\rho_{published}$) (Miles and Smith 2009) and 50% carbon concentration (0.50 C)
ii. Scenario B: Published basic wood density ($\rho_{published}$) (Miles and Smith 2009) and measured carbon concentration ($C_{measured}$)

iii. Scenario C: Measured basic wood density ($\rho_{measured}$) and 50% carbon concentration (0.50 C)

iv. Scenario D: Measured basic wood density ($\rho_{measured}$) and measured carbon concentration ($C_{measured}$)

The last scenario, where all conversion parameters were measured, should provide the most accurate estimate of a tree's carbon biomass, so we treated it as a reference.

3.2.5 i-Tree Carbon Estimation

For each study tree, we recorded species, DBH, and total height following the standard *i-Tree Eco* inventory protocols (Nowak 2024). We also visually assessed the Crown Light Exposure (CLE) for each tree on a 1–5 scale, where 1 indicates that the crown receives direct light from only one side and 5 indicates unobstructed light capture from above and all four sides. Using *i-Tree Eco v6.0.36*, we generated two carbon biomass estimates for each study tree:

(i) i-Tree without CLE: For trees classified as open-grown (CLE class = 4 or 5), biomass was estimated using allometric equations, with no adjustment factor applied for open-grown tree structure.

(ii) i-Tree with CLE applied: For trees classified as open-grown, biomass estimates were multiplied by 0.8 to account for open-grown tree structure.

In both cases, i-Tree converts the estimated biomass to carbon biomass by multiplying by 0.5 (Nowak 2024). These two scenarios allowed us to examine i-Tree's sensitivity to the CLE adjustment.

3.2.6 Statistical analyses

We compared TLS-based leaf-on and leaf-off total above-ground tree carbon biomass (AGC) estimates using simple regression analysis, performed both before and after applying the *rTwig* allometric correction. Agreement between leaf-on and leaf-off AGC estimates was evaluated using Pearson's correlation coefficient (r) and the concordance correlation coefficient (CCC), calculated separately for each species and for all species combined, both with and without *rTwig* correction. For each tree, the AGC difference was calculated as:

$$d_i = AGC_{leaf-off,i} - AGC_{leaf-on,i}$$

where $AGC_{\text{leaf-off},i}$ is the leaf-off TLS-derived AGC estimate for the tree i, and $AGC_{\text{leaf-on},i}$ is the corresponding leaf-on TLS-derived AGC estimate. Based on these differences, the following error metrics were calculated:

- Mean relative difference (MRD; %):

$$\text{MRD} = \frac{100}{n} \sum_{i=1}^{n} \frac{| d_i |}{AGC_{\text{leaf-off},i}}$$

- Root mean square error (RMSE; kg):

$$\text{RMSE} = \sqrt{\frac{1}{n} \sum_{i=1}^{n} d_i^2}$$

- Percent RMSE (%RMSE):

$$\%\text{RMSE} = \frac{RMSE}{AGC_{\text{leaf-off. mean}}} \times 100$$

where n is the number of trees and $AGC_{\text{leaf-off. mean}}$ is the mean leaf-off AGC estimate for the group being analyzed. All other analyses used leaf-off, *rTwig*-corrected TLS-based AGC estimates unless specified otherwise.

To quantify the influence of conversion parameters on TLS-derived carbon biomass, we treated Scenario D (measured basic wood density and measured carbon concentration) as a reference. Bias induced in Scenarios A–C was quantified as a within-tree percent difference relative to Scenario D:

$$\Delta_s(\%) = \frac{AGC\ (x) - AGC\ (D)}{AGC\ (D)} \times 100\% \qquad x \in \{A, B, C\} \qquad (3)$$

where,

AGC (x) = Total above-ground carbon biomass estimated under scenario x (i.e., scenarios A-C)

AGC (D) = Total above-ground carbon biomass estimated under scenario D

All conversions in the remaining analyses were performed using the measured parameters (Scenario D) unless otherwise specified.

To quantify how trees allocate above-ground carbon biomass in their main stem and branches, we examined the relationship between total branch carbon biomass and main stem carbon biomass using simple linear regression.

To evaluate differences in mean branch carbon biomass among branching classes, we grouped branches by *TreeQSM* branch order and branch-base diameter class and summarized branch-level carbon biomass. Because variances differed among classes, we used Welch's one-way

ANOVA applied to tree-level analyses. Group-wise distributional assumptions were evaluated using Q–Q plots, and statistical significance was assessed at $\alpha = 0.05$.

To examine the relationship between i-Tree and TLS-based carbon biomass estimates, we used linear regression and calculated Pearson's correlation coefficient (r). Agreement between the two methods was quantified using the concordance correlation coefficient (CCC). To further compare the two types of tree carbon biomass estimates the following error metrics were calculated:

- AGC difference for each tree (d; kg):

$$\mathrm{d} = AGC_{TLS} - AGC_{i-Tree}$$

- Mean relative difference (MRD; %):

$$\mathrm{MRD} = \frac{100}{n}\sum_{i=1}^{n}\frac{|\ d_i\ |}{AGC_{TLS,i}}$$

- Root mean square error (RMSE; kg):

$$\mathrm{RMSE} = \sqrt{\frac{1}{n}\sum_{i=1}^{n}(\ d_i)^2}$$

- Percent RMSE (%):

$$\%\mathrm{RMSE} = \frac{\mathrm{RMSE}}{AGC_{TLS.mean}} \times 100\%$$

where, AGC_{TLS} denotes the TLS reference carbon biomass estimate (Scenario D), $AGC_{TLS.mean}$ denotes its mean value across trees, AGC_{i-Tree} is the i-Tree-based carbon biomass estimate (with CLE or without CLE, depending on the comparison).

All comparisons were computed separately for i-Tree estimates generated with CLE and without the CLE parameter. Finally, all statistical analyses were done in R version 4.3.1 (R Core Team, 2023).

3.3 Results

3.3.1 Measured Wood Properties

Increment core analyses showed clear species differences in the two conversion parameters that link TLS-derived woody volume to above-ground carbon biomass (AGC) (see Table 3.2). Both oak species had high basic wood density (mean $\rho_{measured}$ = 0.62–0.63 g cm^{-3}), whereas *T. distichum* had substantially lower density (mean $\rho_{measured}$= 0.41 g cm^{-3}). Published wood density values from Miles and Smith (2009) differed from these measurements: the published value for both oaks was lower ($\rho_{published}$= 0.56 g cm^{-3}), while the published wood density value for *T. distichum* was higher ($\rho_{published}$= 0.44 g cm^{-3}) (see Table 3.2).

Measured carbon concentration also differed from the common 50% of dry biomass assumption: the oak trees averaged 45.5–45.7% C, while *T. distichum* averaged 49.8% C.

Table 3.2 Summary of wood trait values used for TLS volume to carbon conversion.

Species	$mean\ \rho_{measured}$ (g/cm^3)	$\rho_{published}$ (g/cm^3)	$mean\ C_{measured}$ (%)
Quercus falcata	0.62 ± 0.05	0.56	45.52 ± 0.53
Quercus lyrata	0.63 ± 0.04	0.56	45.67 ± 0.70
Taxodium distichum	0.41 ±0.04	0.44	49.82 ± 0.66

Note:

Basic wood density ($\rho_{measured}$): computed from increment cores as oven-dry mass / green volume (g cm^{-3}).

Carbon concentration ($C_{measured}$): percent carbon by dry mass measured via elemental analysis (CHNS/O).

Published density ($\rho_{published}$): species-average basic wood density from Miles and Smith (2009); used to represent a "published default" parameterization.

3.3.2 Effect of conversion parameters on TLS-based AGC

AGC estimates derived from TLS were sensitive to the selected conversion parameters, with both the direction and magnitude of bias varying across species. (see Figure 3.1). Compared with the reference scenario that used measured wood density and measured carbon concentration (Scenario D), the alternative parameterizations resulted in the following mean differences:

- *Quercus falcata*: Scenario C ($\rho_{measured}$ & 50% C) estimated 9.8% more AGC; Scenario B ($\rho_{published}$ & $\%C_{measured}$) estimated 9.1% less AGC; Scenario A ($\rho_{published}$ & 50% C) showed the smallest deviation from Scenario D, estimating 0.2% less AGC.
- *Quercus lyrata*: Scenario B and Scenario A estimated 10.5% and 2.1% less AGC respectively, while Scenario C estimated 9.4% more AGC.
- *Taxodium distichum*: All alternative scenarios estimated more AGC. The greatest over estimation occured under Scenario A (+14.2%), followed by Scenario B (+9.1%), while Scenario C produced the smallest (+4.7%).

Overall, these patterns indicate that the effects of the conversion parameter were species dependent. Importantly, the relatively small deviation of Scenario A from Scenario D in the two oak species should not be interpreted as evidence that this published parameterization was accurate; rather, it reflects counter-balancing errors, whereby the lower published wood density offset the upward bias introduced by the 50% carbon concentration.

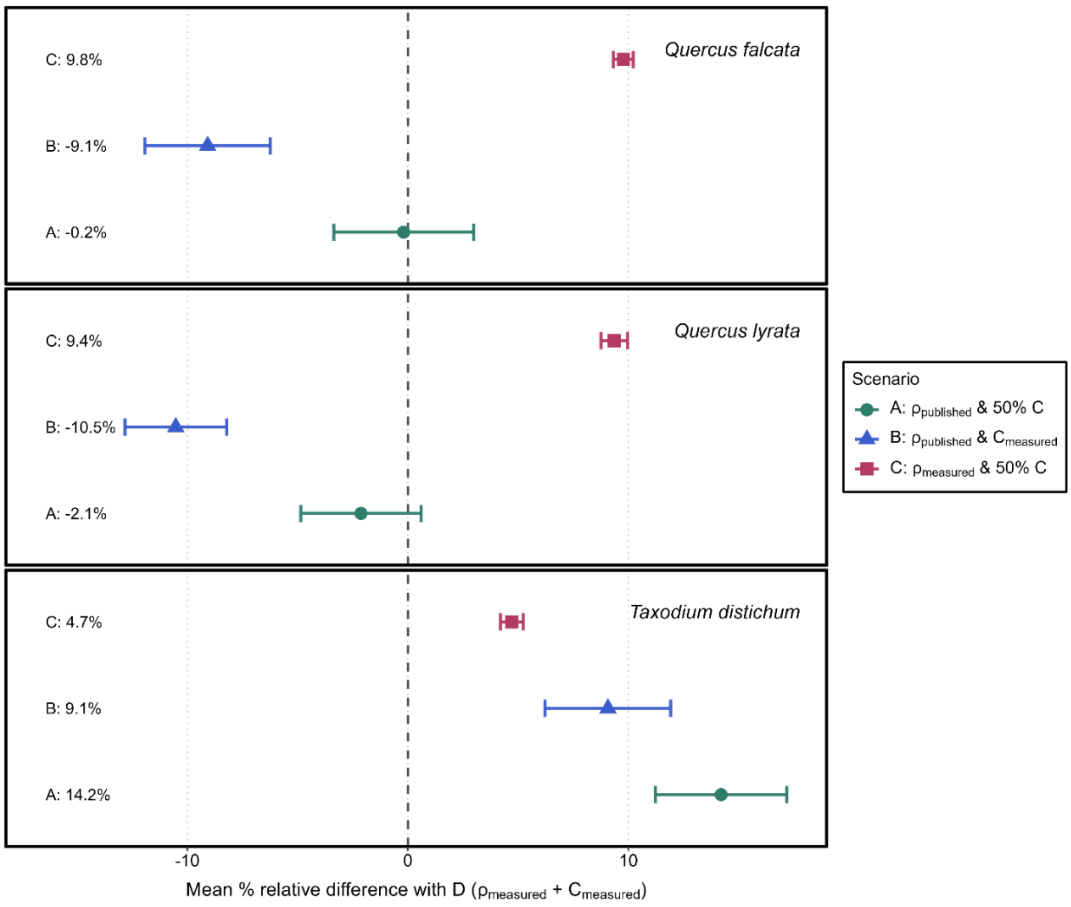

Figure 3.1 Species-specific sensitivity of TLS-derived above-ground carbon biomass (AGC) to conversion parameters. Points show the mean percent difference in AGC, with standard deviations, for Scenarios A–C relative to Scenario D (measured wood density and measured carbon concentration). The dashed vertical line indicates zero difference from Scenario D.

3.3.3 Leaf-off versus leaf-on TLS-based carbon estimates and rTwig correction

Across species, Pearson's correlation coefficients remained high with and without *rTwig*, but CCC, RMSE, and MRD revealed that systematic differences between leaf-on and leaf-off AGC estimates persisted (see Table 3.3). Applying *rTwig* did not substantially alter the overall linear relationship between leaf-on and leaf-off estimates, but it reduced the upper-end spread in AGC values (see Figure 3.2). Across all species combined, *rTwig* reduced RMSE, RMSE(%),

and MRD(%), indicating improved overall error relative to the uncorrected models, while CCC remained unchanged. The effect of *rTwig* was, nevertheless, species dependent. For *Q. falcata* and *T. distichum*, *rTwig* generally improved the comparison with leaf-off estimates, whereas for *Q. lyrata* the effect remained mixed: RMSE was reduced, but concordance and relative error metrics did not improve consistently. Leaf-off TLS-based AGC estimates remained higher than leaf-on estimates for *Q. lyrata* and *T. distichum*, regardless of whether *rTwig* was applied, whereas the difference between scan conditions was smaller for *Q. falcata* (see Figure 3.2).

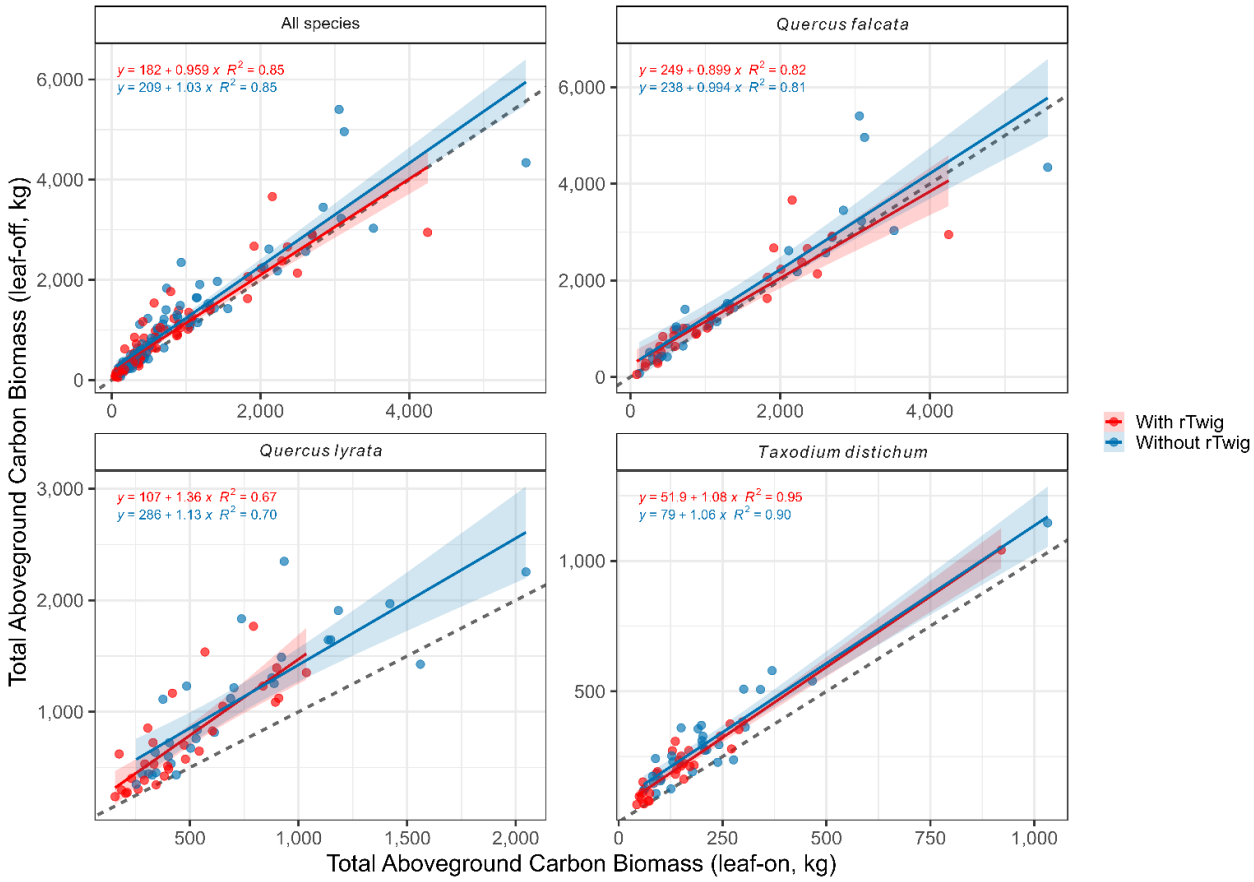

Figure 3.2 Leaf-on vs leaf-off TLS-based above-ground carbon (AGC) estimates with and without rTwig correction, shown for all species combined and by each species separately. Points indicate individual trees; red color indicates the use of rTwig, blue color indicates no use of

rTwig. Solid lines represent linear regressions with 95% confidence intervals plotted around them. The dashed line indicates the 1:1 relationship.

Table 3.3 Comparison of leaf-on versus leaf-off TLS-derived above-ground carbon biomass (AGC) estimates with and without rTwig correction for each species and across all species combined

Metric	*Quercus falcata*		*Quercus lyrata*		*Taxodium distichum*		Combined	
	with rTwig	without rTwig	with rTwig	without rTwig	with rTwig	without rTwig	with rTwig	without rTwig
RMSE (kg)	438.44	653.52	378.40	502.74	78.26	111.99	337.41	480.41
RMSE(%)	32.62	36.48	50.64	45.70	33.62	36.02	43.55	45.00
MRD(%)	20.38	19.63	33.32	33.84	30.47	32.54	28.06	28.67
CCC*	0.90	0.88	0.55	0.63	0.90	0.85	0.90	0.90
Pearson's r*	0.91	0.90	0.82	0.84	0.97	0.95	0.93	0.92

* All CCC and Pearson's r values were statistically significant ($p<0.01$).

3.3.4 Total above-ground carbon biomass in main stem and branches

In this analysis, TLS-based AGC estimates were generated from leaf-off tree point clouds. Across all species, total branch carbon biomass increased with main stem carbon biomass (see Figure 3.3). For all species combined, the main stem accumulated more carbon biomass than branches. Species-level relationships differed, with *Q. lyrata* showing higher branch carbon biomass relative to main stem carbon biomass as opposed to *Q. falcata* and *T. distichum* (see Figure 3.3).

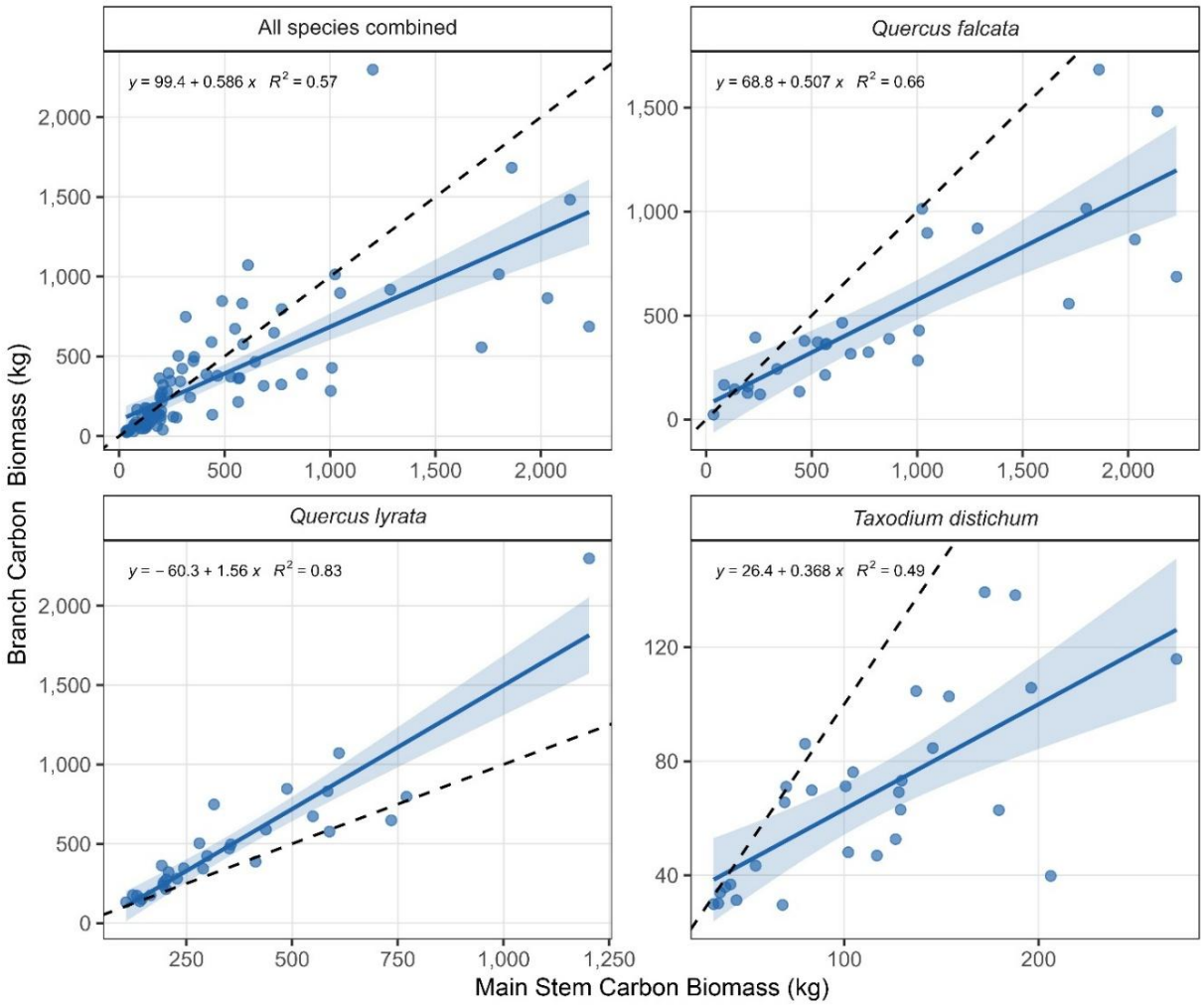

Figure 3.3 Relationship between main-stem carbon biomass and total branch carbon biomass for all species combined and for individual species separately. The 95% confidence interval is plotted around the regression lines. Dashed lines indicate the 1:1 relationship.

3.3.5 Carbon biomass distribution in branches

We also examined how branch carbon biomass is distributed within tree crowns, with respect to branch order, branch-base diameter, and the vertical position of branch origin, all derived from QSMs. Branch carbon biomass differed among branch orders across all study species combined and for each species separately ($p<0.05$; Figure 3.4). Carbon biomass was

mainly allocated in lower branch orders, and this carbon biomass distribution was positively skewed, with a small number of low-order branches containing most of the carbon biomass (see Figure 3.4). Specifically, first- and second-order branches accounted for the largest share of total branch carbon biomass, while higher-order branches accumulated less carbon biomass.

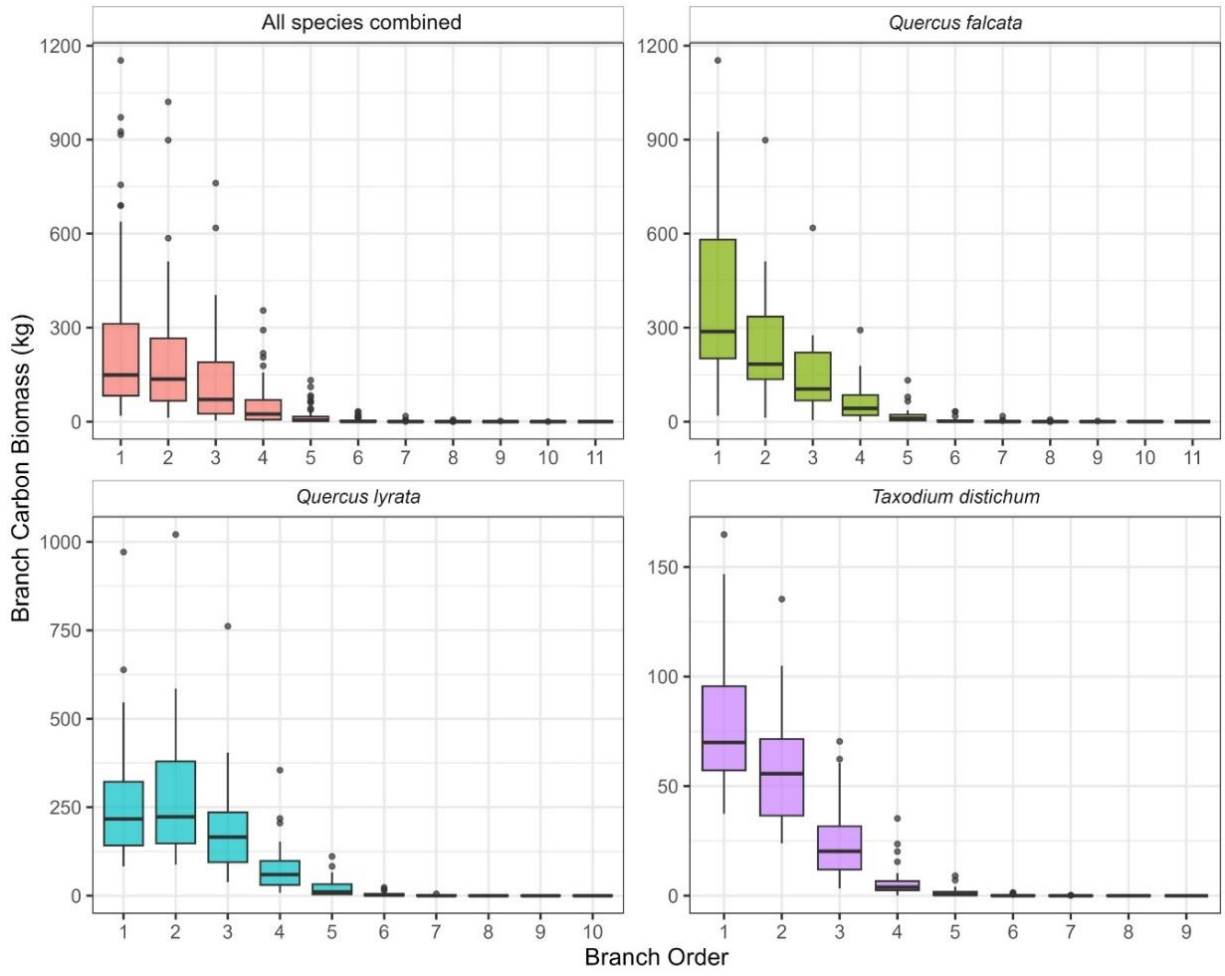

Figure 3.4 Distribution of branch carbon biomass per branch order for all species combined and for individual species.

Branch carbon biomass differed significantly among branch-base diameter classes when all species were combined and when each species was analyzed separately ($p < 0.001$; Figure 3.5). The distribution of carbon biomass by branch-base diameter was positively skewed: small

diameter classes contained many branches with relatively low carbon biomass, whereas mid- and large-diameter classes had fewer branches but disproportionately higher carbon biomass. Both oak species exhibited much larger branch-base diameters and a marked increase in carbon biomass in the upper diameter classes (particularly >25 cm). In contrast, *T. distichum* trees had smaller branch-base diameters (≤ ~22 cm) and showed a unimodal distribution, with peak branch carbon biomass occurring in medium branch diameters (~8–12 cm).

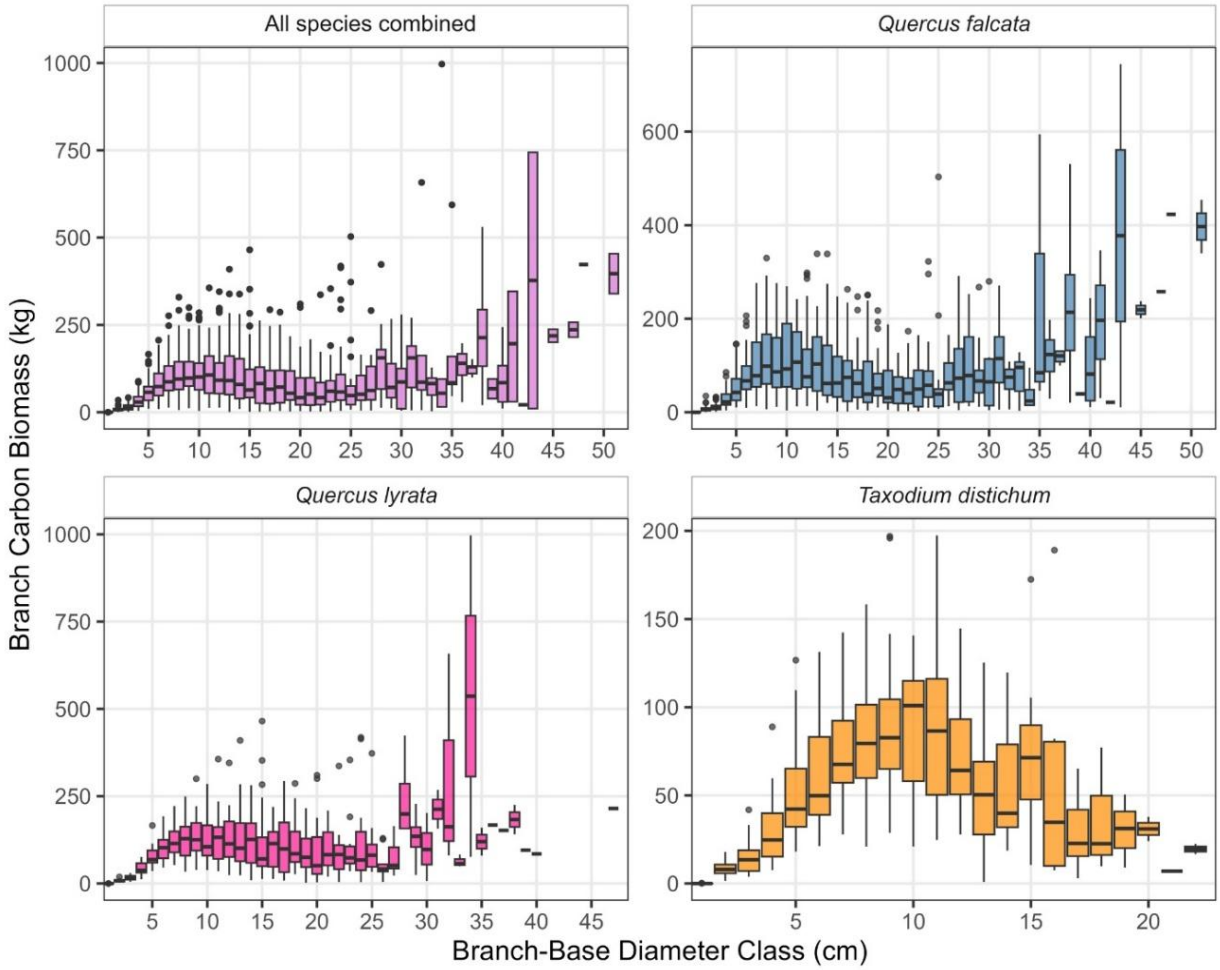

Figure 3.5 Distribution of branch carbon biomass across branch base diameter classes, shown for all species combined and for each species separately.

We also examined the relative vertical distribution (branch base height divided by total tree height) of branch carbon biomass (proportion of total branch carbon biomass) within crowns. We found that relative branch carbon biomass was unevenly distributed along the vertical profile of tree crowns, showing a parabolic distribution (see Figure 3.6). Across all species, relative branch carbon biomass was mainly concentrated in the lower to mid-crown levels, with reduced accumulation toward the upper crown.

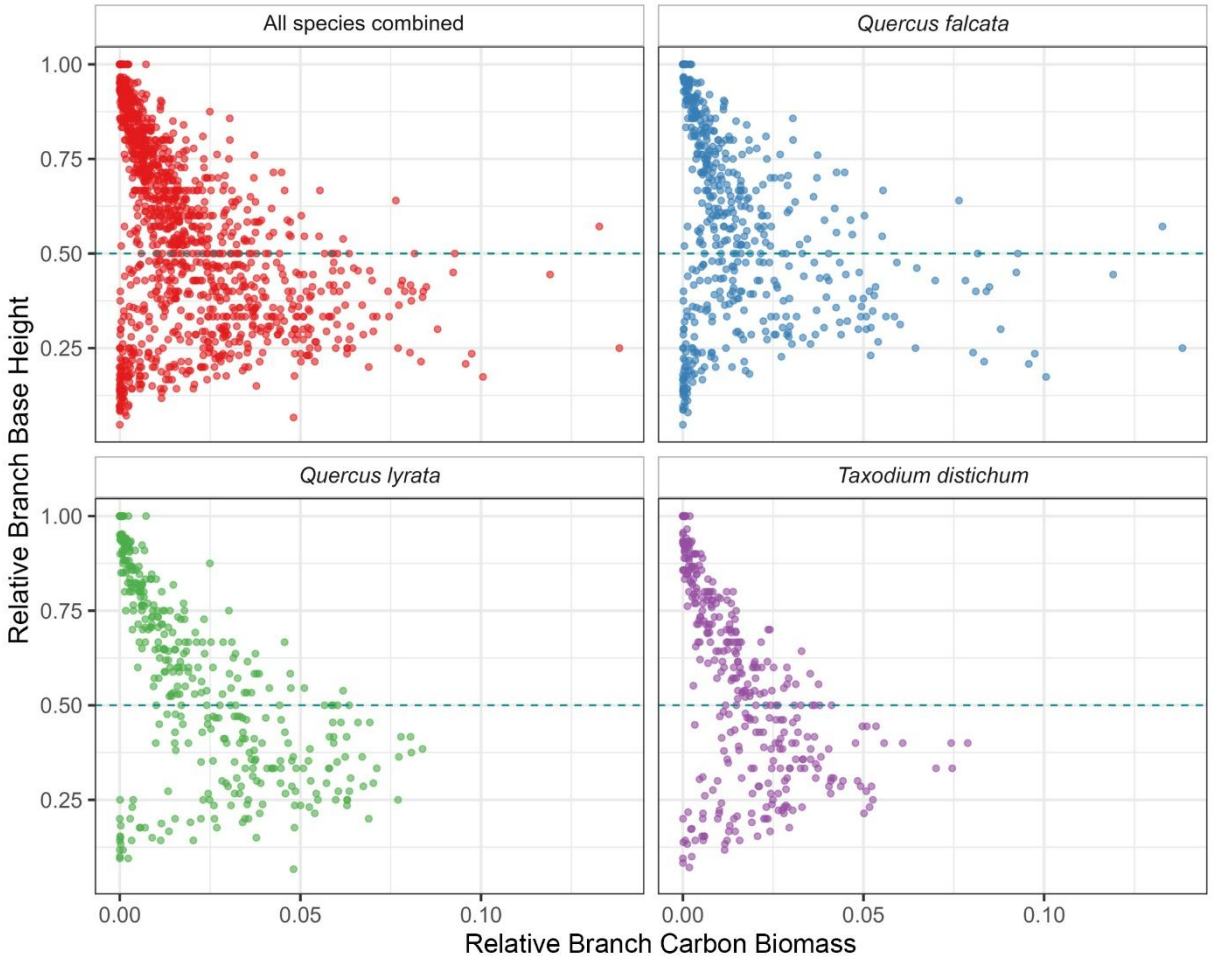

Figure 3.6 Relative vertical distribution (branch base height divided by total tree height) of branch carbon biomass (proportion of total branch carbon biomass) within crowns, shown for all trees combined and by species. The dashed horizontal line marks the mid-crown.

3.3.6 i-Tree versus -TLS-based carbon biomass estimates

We found a strong positive relationship between TLS-based and i-Tree-based carbon biomass estimates across all species (see Figure 3.7). However, the effect of the Crown Light Exposure (CLE) adjustment on agreement with TLS-based AGC estimates was inconsistent across species (see Table 3.4).

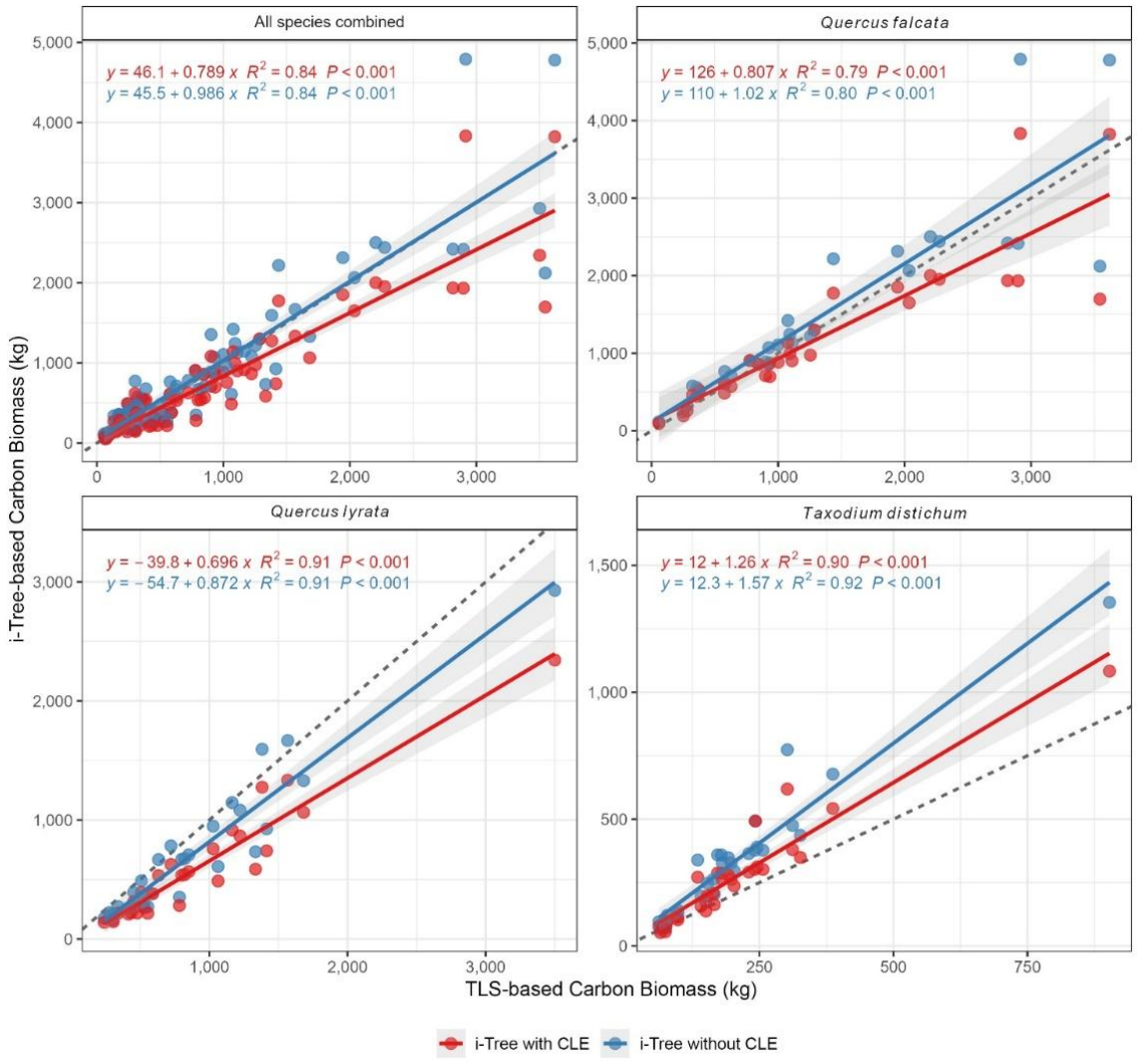

Figure 3.7 Regression comparisons of above-ground carbon biomass estimate from i-Tree versus TLS-derived estimates shown for all trees combined and by species. Blue points and lines indicate i-Tree estimates without the CLE adjustment; red points and lines indicate i-Tree

estimates with the CLE adjustment. Solid lines are fitted linear regressions with 95% confidence intervals plotted around them. The dashed black line indicates the 1:1 relationship.

Table 3.4 Comparison statistics between TLS-based above-ground carbon (AGC) and i-Tree-based AGC estimates, with and without the Crown Light Exposure (CLE) adjustment.

Metric	*Quercus falcata*		*Quercus lyrata*		*Taxodium distichum*		Combined	
	with CLE	without CLE	with CLE	without CLE	with CLE	without CLE	with CLE	without CLE
RMSE (kg)	368.97	451.67	414.72	279.56	74.73	139.51	323.38	317.08
MRD (%)	18.98	22.65	36.47	24.29	19.27	39.37	24.91	28.77
RMSE (%)	27.63	33.82	48.71	32.84	32.32	60.35	40.12	39.34
CCC*	0.92	0.91	0.78	0.91	0.93	0.82	0.91	0.93
Pearson's r*	0.93	0.93	0.95	0.95	0.96	0.96	0.93	0.94

* All CCC and Pearson's r values were statistically significant (<0.01).

When all species were analyzed together, Pearson's correlation coefficients remained high regardless of whether CLE was applied ($r = 0.94$ without CLE; $r = 0.93$ with CLE; $p < 0.01$), but concordance was slightly lower with CLE (CCC = 0.93 without CLE; CCC = 0.91 with CLE), indicating that the CLE adjustment did not improve overall agreement. For *Q. falcata*, Pearson's *r* was unchanged ($r = 0.93$; $p < 0.01$), and CCC increased only slightly with CLE. For *Q. lyrata*, Pearson's *r* remained high ($r = 0.95$; $p < 0.01$), but CCC declined substantially when CLE was applied, indicating poorer agreement with TLS. In contrast, for *T. distichum*, Pearson's *r* also remained high ($r = 0.96$; $p < 0.01$), and CCC increased with CLE, indicating improved agreement for that species. Overall, these results show that the influence of CLE on i-Tree-based AGC estimates was species dependent and did not consistently improve agreement with TLS-based estimates across the dataset.

3.4 Discussion

3.4.1 Implications of wood density and carbon concentration for AGC estimation

This study demonstrates that even when using precise, structure-based TLS-based methods, the accuracy of total above-ground carbon (AGC) estimates in urban trees remains highly contingent on the accuracy of the underlying conversion parameters: wood density and carbon concentration (Demol et al. 2021; Guo et al. 2024). By isolating the effect of these parameters, our results show that improvements in quantifying tree structure do not necessarily yield an unbiased carbon estimate when generic wood property values are used.

The deviation of published wood density values from our measured values drives the bias in scenarios that relied on these defaults. This is consistent with the well-established fact that wood density is not a fixed species constant, but varies across climatic gradients, geographic locations, and local growing conditions (Wiemann and Williamson 2002). This issue is especially relevant in urban environments, where trees experience altered thermal, hydrological, and management conditions relative to forest stands, and recent evidence shows that wood specific gravity can differ both among urban site types and from forest-grown reference values (Pretzsch et al. 2017; Sonti et al. 2025). Consequently, published species means such as those compiled by Miles and Smith (2009) are useful operational reference values, but they may not adequately represent local urban wood properties when the goal is high-precision carbon estimation.

The common assumption that wood biomass contains 50% carbon remains widespread in carbon accounting, but studies show that woody tissue carbon concentration varies substantially among species and tissues (Thomas and Martin 2012; Doraisami et al. 2022). In this study, the measured carbon concentrations for the two oak species were substantially lower than 50%,

while *T. distichum* (49.8%) was very close to it. This distinction is biologically plausible because conifer wood often has a higher carbon concentration than hardwood, partly owing to higher lignin content (Lamlom and Savidge 2003; Thomas and Martin 2012).

The species-specific bias in the scenario analysis was caused by the combined effects of wood density and carbon concentration. For the oak species, Scenario A used a published wood density that was lower than the measured value, which resulted in lower AGC estimates. At the same time, it used a fixed 50% carbon concentration that was higher than the measured value, which resulted in higher AGC estimates. Because these two errors acted in opposite directions, they partly canceled each other, and Scenario A showed only a small mean difference from Scenario D. However, this should not be interpreted as evidence that the default parameterization was accurate. Instead, the apparent agreement was caused by counter-balancing errors. This pattern is not reliable and would not necessarily occur for other species, sites, or combinations of wood traits. This is illustrated by *T. distichum*, where Scenario A produced the largest overestimation because the same two factors no longer offset each other. Therefore, Scenario A may appear accurate in some cases, but that accuracy is only coincidental, making it unsuitable as a generally reliable approach for mixed-species urban carbon estimation.

An additional point is that Scenario C produced less dispersed deviations relative to the reference scenario despite remaining systematically offset. This suggests that retaining measured wood density preserved an important source of biologically meaningful variation among trees, whereas replacing measured carbon concentration with a fixed percentage imposed a more uniform scaling. The implication is methodological: a formulation can appear comparatively stable while remaining biased. Similar concerns have been raised in the allometric literature, where limited calibration or incomplete representation of key sources of variation can yield

outputs that appear coherent but remain systematically inaccurate, especially for larger trees (Duncanson et al. 2015)

These findings have a clear practical implication. While TLS effectively addresses the architectural uncertainty associated with allometric equations for open-grown urban trees (McHale et al. 2009; Tanhuanpää et al. 2017; Kükenbrink et al. 2021), our work shows that this structural precision does not guarantee an accurate carbon estimate. The remaining uncertainty shifts from tree form to wood properties. Therefore, when employing TLS as a high-accuracy reference method, for example, to calibrate urban allometries or to quantify carbon stocks in large, high-value trees, locally representative wood density and carbon concentration should be treated as part of the measurement framework (Demol et al. 2021; Kükenbrink et al. 2021). This point is further supported by Chapter 2 of this thesis, which indicates that wood carbon concentration can vary not only among species but also within urban settings, likely in response to differences in local site conditions and stress exposure. While not without its own limitations, using increment cores to measure wood density and carbon concentration represents a substantial improvement over relying on generic, often geographically mismatched, published values (Sonti et al. 2025; Demol et al. 2021).

3.4.2 Leaf-on versus leaf-off AGC estimates

The strong relationship between leaf-on and leaf-off AGC estimates indicates that both scan conditions captured the major structural differences among trees, even though leaf condition can influence QSM reconstruction and biomass estimation from TLS data (Arseniou et al. 2023). However, the degree of agreement between the two scan conditions depended on how completely the woody structure could be captured and retained from leaf-on point clouds. In leaf-on workflows, woody volume may be reduced both because foliage occludes stems and

branches and because leaf–wood separation algorithms can remove points belonging to fine twigs and distal branches (Hartley et al. 2024; Chen et al. 2025). Recent studies show that QSM-based biomass derived from leaf-removed leaf-on point clouds often underestimates reference biomass relative to both destructive measurements and leaf-off reconstructions, indicating that leaf removal improves the usability of leaf-on scans but does not fully eliminate underestimation bias (Chen et al. 2025).

The species-specific patterns in our study are consistent with these mechanisms. For *Q. lyrata* and *T. distichum*, leaf-off AGC was higher than leaf-on AGC, whereas this pattern was less evident for *Q. falcata*. *Q. lyrata* has broader leaves and large scaffold branches (Solomon 1990), which likely increase crown occlusion during leaf-on scanning and may also increase the chance that woody points adjacent to leaves are removed during the separation step. In contrast, *Q. falcata* generally has narrower leaves and more often maintains a longer trunk with major branches that are more widely spaced (Jensen 1989). A crown architecture with broader internal branching likely increases self-occlusion during leaf-on scanning, thereby reducing the completeness of woody surface capture (Hartley et al. 2024; Chen et al. 2025)

T. distichum, as a deciduous conifer with needle-like foliage closely associated with fine woody elements, presents a structurally intricate outer crown in which leaves and woody axes are difficult to separate cleanly from leaf-on TLS data (Gilman and Watson 1994; Chen et al. 2025). This is particularly relevant for graph-based separation approaches, which rely on geometric connectivity and shortest-path relationships within the point cloud to identify woody structure; when needles and fine shoots are closely associated, true woody points may be more difficult to retain (Chen et al. 2025; Tian and Li 2022). Recent studies support this interpretation, showing that leaf–wood separation generally performs less effectively in coniferous trees than in

broadleaved trees and that biomass estimates from leaf-removed conifer point clouds are more sensitive to classification error (Chen et al. 2025). Thus, in *T. distichum*, the lower leaf-on AGC likely reflects loss of fine woody structure during the separation stage rather than crown occlusion alone.

The application of the *rTwig* correction reduced the upper range of AGC estimates and improved overall error across all species combined, indicating that correction of inflated small-branch radii enhanced the consistency of leaf-on estimates with the leaf-off reference. Small branches and twigs lie close to the effective resolution limit of TLS because beam divergence, point density limitations, scattering, and co-registration error all reduce the reliability of fine-scale reconstruction, making distal cylinders especially prone to radius inflation in QSMs (Wilkes et al. 2017; Disney et al. 2018). Morales and MacFarlane (2025b) developed *rTwig* specifically to address this problem by using measured twig diameters to model realistic taper along branch paths, and their validation showed a major improvement in biomass estimation after correction. This matters because small-branch errors accumulate across many distal cylinders throughout the tree (Millan et al. 2024). Demol et al. (2022b) showed that branches < 5 cm diameter accounted for more than 80% of branch volume overestimation in destructively validated ash trees and produced whole-tree overestimation of 38–52%.

The leaf-removal algorithm can affect the performance of *rTwig*. The correction can only be applied to the woody structure that remains after leaf removal and QSM reconstruction. If the leaf-removal step removes distal twig points together with leaves, then *rTwig* is effectively applied lower on the branch system, at a thicker point below the missing twigs (Morales and MacFarlane, 2025a). Under those conditions, *rTwig* cannot recover the lost distal structure; instead, it may further reduce the estimated volume of the retained distal branch segment by

imposing taper below the true twig position. Collectively, these results suggest that leaf-on TLS can preserve relative differences among trees but may be less consistent than leaf-off TLS for AGC estimation when leaf-removal errors reduce the retention of fine woody structure.

3.4.3 Stem–branch carbon allocation

The study result showed strong species-specific divergence in branch versus stem carbon biomass allocation, even though the overall relationship indicates that the main stem accumulates more carbon biomass than the branch.

The greater branch carbon biomass allocation in *Q. lyrata* aligns with previous studies showing that open-grown trees may allocate more biomass in their branches due to their squat form (short trunk and large crown), allowing them to optimize light capture and maintain their balance against wind loads in urban settings (MacFarlane and Kane 2017). However, the observed pattern for *Q. falcata* and *T. distichum* was unexpected, given their open-grown form. For *Q. falcata*, higher stem carbon biomass likely reflects species-specific architecture together with the relatively large DBH of the sampled individuals. This species typically maintains a straight, prominent bole with major branches that are relatively well (Jensen 1989). Because woody biomass scales strongly with diameter, the comparatively large DBH of these trees would increase stem cross-sectional area and bole volume, reinforcing carbon biomass accumulation in the main stem. For *T. distichum*, stem dominance is mostly explained by its excurrent form. This species maintains strong apical dominance compared to broadleaf species (Brown et al. 1967), and this apical control suppresses lateral branch growth, thereby increasing the stem fraction of above-ground biomass (Wilson 2000). In addition, *T. distichum* trees typically develop basal buttressing that further increases stem biomass (Walsh and Dawson 2014; Pietrzykowski et al. 2015). In urban settings, these inherent species differences may be reinforced by management,

because routine pruning can reduce branch biomass and alter branch–stem allometry over time (Speak and Salbitano 2023).

The accumulation of carbon biomass in a small number of large, low-order branches is consistent with the fractal-like organization of tree crowns and can be interpreted through theories of tree form and resource transport (Arseniou et al. 2021). Pipe model theory proposes that proximal woody axes must contain sufficient conductive and supporting tissue to supply the distal foliage they subtend, so branch cross-sectional area should increase toward the crown base where each axis supports a larger downstream crown system (Shinozaki et al. 1964; Lehnebach et al. 2018). The West–Brown–Enquist framework extends this logic by viewing trees as hierarchically organized, self-similar transport networks in which branch size, path length, and resource flux scale systematically across branch orders (West et al. 1997). Together, these frameworks suggest that first- and second-order branches should contain disproportionate woody volume and carbon biomass because they integrate the hydraulic and mechanical demands of much larger distal subnetworks, whereas higher-order branches become progressively smaller and contribute less carbon biomass per branch.

This interpretation also matches the vertical pattern in our data. Branches originating in the lower to mid-crown are more likely to represent persistent scaffold axes supporting large crown subnetworks, whereas upper-crown insertions are more often composed of shorter, higher-order branches that are younger and less woody, so their contribution to total branch carbon biomass is smaller (Ishii and Mcdowell 2002). It is also consistent with TLS-based studies of urban trees, which show that branch allocation varies with branch order, branch-base diameter, branch-base height, structural complexity, and path-length distributions (Zheng et al. 2025; Parhizgar et al. 2025; Arseniou et al. 2021).

3.4.4 TLS versus i-Tree-based carbon estimates

Across all trees, TLS- and i-Tree-based AGC estimates were strongly correlated, indicating that both approaches captured relative differences in carbon biomass among individuals. However, absolute agreement varied by species and by whether the open-grown Crown Light Exposure (CLE) adjustment was applied. This pattern is consistent with previous studies showing that urban-tree biomass estimates can differ substantially depending on the allometric equations used, particularly because equations developed from forest-grown trees may not always represent the architecture of open-grown urban trees well (McHale et al. 2009; Aguaron and McPherson, 2012).

The CLE adjustment in i-Tree Eco assumes that open-grown trees generally have less above-ground biomass than forest-grown trees because open urban growing conditions often promote broader crowns, larger branches, and shorter, more spreading forms (McHale et al. 2009; MacFarlane and Kane, 2017). Our results suggest that this generalized adjustment is too simplistic for consistent use across species. Although i-Tree and TLS remained strongly correlated regardless of whether CLE was applied, the inclusion of CLE did not improve overall agreement across the full dataset. McHale et al. (2009) reported that forest-derived equations could overpredict urban-tree biomass in some cases and underpredict it in others, demonstrating that the bias is not constant enough to be corrected reliably with a single fixed reduction factor. Therefore, while a 20% reduction may be reasonable as a broad average assumption, it is unlikely to be appropriate for all species or tree forms.

The pattern observed for *T. distichum* is especially important for interpreting the CLE adjustment. This species showed the clearest improvement when CLE was applied, yet *T. distichum* generally maintains an upright, excurrent crown form with strong apical dominance,

even in open-grown settings, rather than developing the broad, spreading architecture that the CLE correction is intended to approximate (Gilman and Watson, 1994; Brown et al. 1967; Wilson, 2000). Thus, the species showing the clearest apparent benefit from CLE was not the one for which the biological rationale of the correction is strongest. This weakens the argument for treating CLE as a generally applicable open-grown biomass adjustment and suggests instead that its effects are species dependent and not consistently explained by the crown-form mechanism it is intended to represent.

More broadly, these findings highlight a general limitation of allometric biomass estimation in urban trees. Urban carbon models often rely on forest-derived equations or compiled literature values rather than on destructively sampled, open-grown urban trees that span the wide range of crown forms and size classes found in cities (McHale et al. 2009; McPherson et al. 2016). This matters because allometric bias is not constant across tree size, and model error can increase substantially when large trees are poorly represented in calibration datasets (Duncanson et al. 2015). Recent work has similarly emphasized that urban biomass equations should be developed from datasets spanning broad size distributions and urban growing conditions, because stem and branch allocation vary strongly within species and across urban settings (Lee et al. 2025; Parhizgar et al. 2025).

Accordingly, i-Tree Eco remains valuable for operational, city-scale inventories because it is accessible, standardized, and widely used, and published sensitivity analyses confirm that its outputs respond strongly to several tree- and crown-related inputs, including CLE (Lin et al. 2021; Lin et al. 2020). However, the present results indicate that the current allometric formulations and generalized CLE-based correction remain a limitation when higher-accuracy AGC estimates are needed for large, structurally complex urban trees. In such cases, TLS

provides a practical non-destructive reference because it measures tree structure directly and can support the development and validation of urban-specific allometries without requiring destructive harvest (Kükenbrink et al. 2021; Krause et al. 2023; Parhizgar et al. 2025).

3.5 Conclusions

This study demonstrates that TLS, combined with locally measured wood density and carbon concentration, provides a reliable non-destructive reference for estimating above-ground carbon (AGC) in urban trees and for quantifying carbon allocation between stems and crowns. This is particularly valuable for large urban trees, which dominate city-scale carbon stocks but are rarely represented in destructive datasets used to develop biomass allometries. Our findings also show that the use of published wood density values and a fixed 50% carbon concentration can introduce species-dependent bias, highlighting the importance of locally measured wood traits when high-precision estimates are required. Although i-Tree Eco captured relative variation in AGC well, the CLE open-grown adjustment did not consistently improve agreement with TLS-based estimates across species. Taken together, these results provide little support for CLE as a general biomass correction for urban trees and instead emphasize the need for species-specific urban allometries or TLS-based calibration datasets when greater accuracy is required. Future work should expand TLS reference datasets to include a broader range of species, tree sizes, and management histories to strengthen urban forest carbon estimation across spatial and temporal scales.

References

Aguaron, E., and E. G. McPherson. 2012. Comparison of methods for estimating carbondioxide storage by sacramento's urban forest. *Carbon Sequestration in Urban Ecosystems* :44–71. https://doi.org/10.1007/978-94-007-2366-5_3.

Arrizza, S., S. Marras, R. Ferrara, and G. Pellizzaro. 2024. Terrestrial Laser Scanning (TLS) for tree structure studies: a review of methods for wood-leaf classifications from 3D point clouds. *Remote Sensing Applications: Society and Environment* 36:101364. https://doi.org/10.1016/J.RSASE.2024.101364.

Arseniou, G., and D. W. MacFarlane. 2021. Fractal dimension of tree crowns explains species functional-trait responses to urban environments at different scales. *Ecological Applications* 31(4):e02297. https://doi.org/10.1002/EAP.2297.

Arseniou, G., D. W. MacFarlane, K. Calders, and M. Baker. 2023. Accuracy differences in aboveground woody biomass estimation with terrestrial laser scanning for trees in urban and rural forests and different leaf conditions. *Trees - Structure and Function* 37(3):761–779. https://doi.org/10.1007/S00468-022-02382-1/.

Arseniou, G., D. W. Macfarlane, and D. Seidel. 2021. Woody Surface Area Measurements with Terrestrial Laser Scanning Relate to the Anatomical and Structural Complexity of Urban Trees. *Remote Sensing 2021, Vol. 13,* 13(16). https://doi.org/10.3390/RS13163153.

Bird, M., C. Keitel, and W. Meredith. 2017. Analysis of biochars for C, H, N, O and S by elemental analyser. *Biochar: A guide to analytical methods* :39–50.

Brown, C. L., R. G. McAlpine, and P. P. Kormanik. 1967. APICAL DOMINANCE AND FORM IN WOODY PLANTS: A REAPPRAISAL. *American Journal of Botany* 54(2):153–162. https://doi.org/10.1002/j.1537-2197.1967.tb06904.x.

Calders, K., N. Origo, A. Burt, M. Disney, J. Nightingale, P. Raumonen, M. Åkerblom, Y. Malhi, and P. Lewis. 2018. Realistic Forest Stand Reconstruction from Terrestrial LiDAR for Radiative Transfer Modelling. *Remote Sensing* 10(6). https://doi.org/10.3390/rs10060933.

Calders, K., J. Adams, J. Armston, H. Bartholomeus, S. Bauwens, L. P. Bentley, J. Chave, et al. 2020. Terrestrial laser scanning in forest ecology: Expanding the horizon. *Remote Sensing of Environment* 251:112102. https://doi.org/10.1016/J.RSE.2020.112102.

Calders, K., G. Newnham, A. Burt, S. Murphy, P. Raumonen, M. Herold, D. Culvenor, et al. 2015. Nondestructive estimates of above-ground biomass using terrestrial laser scanning. *Methods in Ecology and Evolution* 6(2):198–208. https://doi.org/10.1111/2041-210X.12301.

Calders, K., H. Verbeeck, A. Burt, N. Origo, J. Nightingale, Y. Malhi, P. Wilkes, P. Raumonen, R. G. H. Bunce, and M. Disney. 2022. Laser scanning reveals potential underestimation of biomass carbon in temperate forest. *Ecological Solutions and Evidence* 3(4):e12197. https://doi.org/10.1002/2688-8319.12197.

Chave, J., D. Coomes, S. Jansen, S. L. Lewis, N. G. Swenson, and A. E. Zanne. 2009. Towards a worldwide wood economics spectrum. *Ecology Letters* 12(4):351–366. https://doi.org/10.1111/J.1461-0248.2009.01285.X.

Chave, J., M. Réjou-Méchain, A. Búrquez, E. Chidumayo, M. S. Colgan, W. B. C. Delitti, A. Duque, T. Eid, P. M. Fearnside, and R. C. Goodman. 2014. Improved allometric models to estimate the aboveground biomass of tropical trees. *Global change biology* 20(10):3177–3190.

Chen, S., H. Verbeeck, L. Terryn, W. A. J. Van den Broeck, M. B. Vicari, M. Disney, N. Origo, et al. 2025. The impact of leaf-wood separation algorithms on aboveground biomass estimation from terrestrial laser scanning. *Remote Sensing of Environment* 318:114581. https://doi.org/10.1016/J.RSE.2024.114581.

Demol, M., K. Calders, S. M. Krishna Moorthy, J. Van den Bulcke, H. Verbeeck, and B. Gielen. 2021. Consequences of vertical basic wood density variation on the estimation of aboveground biomass with terrestrial laser scanning. *Trees - Structure and Function* 35(2):671–684. https://doi.org/10.1007/S00468-020-02067-7/.

Demol, M., H. Verbeeck, B. Gielen, J. Armston, A. Burt, M. Disney, L. Duncanson, et al. 2022a. Estimating forest above-ground biomass with terrestrial laser scanning: Current status and future directions. *Methods in Ecology and Evolution* 13(8):1628–1639. https://doi.org/10.1111/2041-210X.13906.

Demol, M., P. Wilkes, P. Raumonen, S. M. K. Moorthy, K. Calders, B. Gielen, and H. Verbeeck. 2022b. Volumetric overestimation of small branches in 3D reconstructions of Fraxinus excelsior. *Silva Fennica* 56(1). https://doi.org/10.14214/sf.10550.

Disney, M. I., M. Boni Vicari, A. Burt, K. Calders, S. L. Lewis, P. Raumonen, and P. Wilkes. 2018. Weighing trees with lasers: advances, challenges and opportunities. *Interface Focus* 8(2). https://doi.org/10.1098/RSFS.2017.0048.

Doraisami, M., G. M. Domke, and A. R. Martin. 2024. Improving wood carbon fractions for multiscale forest carbon estimation. *Carbon Balance and Management* 19(1):1–10. https://doi.org/10.1186/S13021-024-00272-2/.

Duncanson, L., O. Rourke, and R. Dubayah. 2015. Small Sample Sizes Yield Biased Allometric Equations in Temperate Forests. *Scientific Reports 2015* 5(1):17153-. https://doi.org/10.1038/srep17153.

Gilman, E. F., and D. G. Watson. 1994. Taxodium distichum–baldcypress. *Department of Agriculture, Forest Service, Southern Group of State Foresters, Fact Sheet ST-620*.

Guo, P., X. Zhao, X. Wang, Q. Feng, X. Li, and Y. Tan. 2024. Wood Density and Carbon Concentration Jointly Drive Wood Carbon Density of Five Rosaceae Tree Species. *Forests 2024, Vol. 15,* 15(7). https://doi.org/10.3390/f15071102.

Hartley, R. J. L., S. Jayathunga, J. Morgenroth, and G. D. Pearse. 2024. Tree Branch Characterisation from Point Clouds: a Comprehensive Review. *Current Forestry Reports* 10(5):360–385. https://doi.org/10.1007/s40725-024-00225-5.

Ishii, H., and N. Mcdowell. 2002. Age-related development of crown structure in coastal Douglas-fir trees. *Forest Ecology and Management* 169:257–270.

Jenerette, G. D., and D. L. Herrmann. 2023. A global synthesis of reported urban tree carbon production rates and approaches. *Frontiers in Ecology and Evolution* 11:1244418. https://doi.org/10.3389/FEVO.2023.1244418/.

Jensen, R. J. 1989. The Quercus falcata Michx. complex in Land Between The Lakes, Kentucky and Tennessee: a study of morphological variation. *American Midland Naturalist* 121(2):245–255. https://doi.org/10.2307/2426028.

Krause, P., B. Forbes, A. Barajas-Ritchie, M. Clark, M. Disney, P. Wilkes, and L. P. Bentley. 2023. Using terrestrial laser scanning to evaluate non-destructive aboveground biomass allometries in diverse Northern California forests. *Frontiers in Remote Sensing* 4:1132208. https://doi.org/10.3389/FRSEN.2023.1132208/BIBTEX.

Kükenbrink, D., O. Gardi, F. Morsdorf, E. Thürig, A. Schellenberger, and L. Mathys. 2021. Above-ground biomass references for urban trees from terrestrial laser scanning data. *Annals of Botany* 128(6):709–724. https://doi.org/10.1093/AOB/MCAB002.

Lamlom, S. H., and R. A. Savidge. 2003. A reassessment of carbon content in wood: variation within and between 41 North American species. *Biomass and Bioenergy* 25(4):381–388. https://doi.org/10.1016/S0961-9534(03)00033-3.

Lau, A., L. P. Bentley, C. Martius, A. Shenkin, H. Bartholomeus, P. Raumonen, Y. Malhi, T. Jackson, and M. Herold. 2018. Quantifying branch architecture of tropical trees using terrestrial LiDAR and 3D modelling. *Trees 2018 32:5* 32(5):1219–1231. https://doi.org/10.1007/S00468-018-1704-1.

Lee, J. M., H. S. Kim, B. Choi, J. Y. Jung, S. Lee, H. Jo, G. Kim, et al. 2025. Enhanced Accuracy in Urban Tree Biomass Estimation: Developing Allometric Equations with Land Use Classifications. *Forests 2025, Vol. 16,* 16(5). https://doi.org/10.3390/f16050841.

Lehnebach, R., R. Beyer, V. Letort, and P. Heuret. 2018. The pipe model theory half a century on: a review. *Annals of Botany* 121(5):773–795. https://doi.org/10.1093/aob/mcx194.

Lin, Jian, Kroll, Charles N, Nowak, and David J. 2020. Ecosystem service-based sensitivity analyses of i-Tree Eco. *Arboriculture and Urban Forestry* 46:287–306.

Lin, J., C. N. Kroll, and D. J. Nowak. 2021. An uncertainty framework for i-Tree eco: A comparative study of 15 cities across the United States. *Urban Forestry & Urban Greening* 60:127062. https://doi.org/10.1016/j.ufug.2021.127062.

Ma, S. H., A. Eziz, D. Tian, Z. B. Yan, Q. Cai, M. W. Jiang, C. J. Ji, J. Y. Fang, and O. J. Sun. 2020. Size- and age-dependent increases in tree stem carbon concentration: implications for forest carbon stock estimations. *Journal of Plant Ecology* 13(2):233–240. https://doi.org/10.1093/jpe/rtaa005.

MacFarlane, D. W., and B. Kane. 2017. Neighbour effects on tree architecture: functional trade-offs balancing crown competitiveness with wind resistance. *Functional Ecology* 31(8):1624–1636. https://doi.org/https://doi.org/10.1111/1365-2435.12865.

Martin, A. R., M. Doraisami, and S. C. Thomas. 2018. Global patterns in wood carbon concentration across the world's trees and forests. *Nature Geoscience* 11(12):915–920. https://doi.org/10.1038/S41561-018-0246-X.

McHale, M. R., I. C. Burke, M. A. Lefsky, P. J. Peper, and E. G. McPherson. 2009. Urban forest biomass estimates: is it important to use allometric relationships developed specifically for urban trees? *Urban Ecosystems* 12(1):95–113. https://doi.org/10.1007/s11252-009-0081-3.

McPherson, E. G., D. J. Nowak, and R. A. Rowntree. 1994. *Chicago's urban forest ecosystem: Results of the Chicago Urban Forest Climate Project.(Includes executive summary). Forest Service general technical report (Final)*. Forest Service, Delaware, OH (United States). Northeastern Forest Experiment ….

McPherson, E. G., N. S. van Doorn, and P. J. Peper. 2016. Urban tree database and allometric equations. https://doi.org/10.2737/PSW-GTR-253.

Miles, P. D., and W. Brad. Smith. 2009. *Specific gravity and other properties of wood and bark for 156 tree species found in North America*. U.S. Department of Agriculture, Forest Service, Northern Research Station. https://doi.org/10.2737/nrs-rn-38.

Millan, M., A. Bonnet, J. Dauzat, and R. Vezy. 2024. Advancing fine branch biomass estimation with lidar and structural models. *Annals of Botany* 134(3):455–466. https://doi.org/10.1093/aob/mcae083.

Morales, A., and D. W. MacFarlane. 2025a. Reducing tree volume overestimation in quantitative structure models using modeled branch topology and direct twig measurements. *Forestry: An International Journal of Forest Research* 98(3):394–409. https://doi.org/10.1093/forestry/cpae046.

Morales, A., and D. W. MacFarlane. 2025b. rTwig: An R package to correct overestimated small branches and twigs in quantitative structure models of trees. *Science of Remote Sensing* 12:100284. https://doi.org/10.1016/J.SRS.2025.100284.

Morhart, C., Z. Schindler, J. Frey, J. P. Sheppard, K. Calders, M. Disney, F. Morsdorf, P. Raumonen, and T. Seifert. 2024. Limitations of estimating branch volume from terrestrial laser scanning. *European Journal of Forest Research* https://doi.org/10.1007/s10342-023-01651-z.

Muscas, D., M. Fornaciari, C. Proietti, L. Ruga, and F. Orlandi. 2023. Tree growth rate under urban limiting conditions. *European Journal of Forest Research* 142(6):1423–1437. https://doi.org/10.1007/S10342-023-01599-0/.

Nowak, D. J. 2024. *Understanding i-Tree: 2023 summary of programs and methods*. https://doi.org/10.2737/NRS-GTR-200-2023.

Nowak, D. J., E. J. Greenfield, R. E. Hoehn, and E. Lapoint. 2013. Carbon storage and sequestration by trees in urban and community areas of the United States. *Environmental Pollution* 178:229–236. https://doi.org/10.1016/J.ENVPOL.2013.03.019.

Parhizgar, L., N. Pattnaik, H. Yazdi, S. Qiguan, S. Pauleit, M. A. Rahman, F. Ludwig, H. Pretzsch, and T. Rötzer. 2025. Branch biomass allometries for urban tree species based on terrestrial laser scanning (TLS) data. *Trees - Structure and Function* 39(4):1–16. https://doi.org/10.1007/S00468-025-02637-7/.

Pietrzykowski, M., W. L. Daniels, and S. C. Koropchak. 2015. Microtopographic effects on growth of young bald cypress (Taxodium distichum L.) in a created freshwater forested wetland in southeastern Virginia. *Ecological Engineering* 83:135–143. https://doi.org/10.1016/j.ecoleng.2015.06.024.

Pretzsch, H., P. Biber, E. Uhl, J. Dahlhausen, G. Schütze, D. Perkins, T. Rötzer, et al. 2017. Climate change accelerates growth of urban trees in metropolises worldwide /631/158/858 /704/158/2165 article. *Scientific Reports* 7(1). https://doi.org/10.1038/s41598-017-14831-w.

Raumonen, P., M. Kaasalainen, M. Åkerblom, S. Kaasalainen, H. Kaartinen, M. Vastaranta, M. Holopainen, M. Disney, and P. Lewis. 2013. Fast Automatic Precision Tree Models from Terrestrial Laser Scanner Data. *Remote Sensing* 5(2):491–520. https://doi.org/10.3390/rs5020491.

Shinozaki, K., K. Hozumi, T. Kira. 1964. A QUANTITATIVE ANALYSIS OF PLANT FORM-THE PIPE MODEL THEORY : II. FURTHER EVIDENCE OF THE THEORY AND ITS APPLICATION IN FOREST ECOLOGY. *JAPANESE JOURNAL OF ECOLOGY* 14(4):133–139. https://doi.org/10.18960/SEITAI.14.4_133.

Solomon, J. D. 1990. Quercus lyrata Walt. overcup oak. *Silvics of North America* 2:681–685.

Sonti, N. F., J. A. Westfall, M. C. Wiemann, and T. L. Eberhardt. 2025. Influence of site type on wood specific gravity and ash content for urban-grown hardwoods. *Urban Ecosystems 2025 28:3* 28(3):122-. https://doi.org/10.1007/s11252-025-01735-1.

Speak, A. F., and F. Salbitano. 2023. The impact of pruning and mortality on urban tree canopy volume. *Urban Forestry & Urban Greening* 79:127810. https://doi.org/10.1016/j.ufug.2022.127810.

Thomas, S. C., and A. R. Martin. 2012. Carbon Content of Tree Tissues: A Synthesis. *Forests 2012, Vol. 3, Pages 332-352* 3(2):332–352. https://doi.org/10.3390/f3020332.

Tian, Z., and S. Li. 2022. Graph-Based Leaf-Wood Separation Method for Individual Trees Using Terrestrial Lidar Point Clouds. *IEEE Transactions on Geoscience and Remote Sensing* 60. https://doi.org/10.1109/TGRS.2022.3218603.

Walsh, C., and J. O. Dawson. 2014. Variation in Buttressing Form and Stem Volume Ratio of Baldcypress Trees. *Transactions of the Illinois State Academy of Science* 107:5–11.

Weiskittel, A. R., D. W. MacFarlane, P. J. Radtke, D. L. R. Affleck, H. Temesgen, C. W. Woodall, J. A. Westfall, and J. W. Coulston. 2015. A Call to Improve Methods for Estimating Tree Biomass for Regional and National Assessments. *Journal of Forestry* 113(4):414–424. https://doi.org/10.5849/JOF.14-091.

West, G. B., J. H. Brown, and B. J. Enquist. 1997. A general model for the origin of allometric scaling laws in biology. *Science* 276(5309):122–126. https://doi.org/10.1126/science.276.5309.122.

Wiemann, M. C., and G. B. Williamson. 2002. Geographic Variation in Wood Specific Gravity: Effects of Latitude, Temperature, and Precipitation. *Wood and Fiber Science* :96–107.

Wilkes, P., A. Lau, M. Disney, K. Calders, A. Burt, J. Gonzalez de Tanago, H. Bartholomeus, B. Brede, and M. Herold. 2017. Data acquisition considerations for Terrestrial Laser Scanning of forest plots. *Remote Sensing of Environment* 196:140–153. https://doi.org/10.1016/J.RSE.2017.04.030.

Williamson, G. B., and M. C. Wiemann. 2010. Measuring wood specific gravity...correctly. *American Journal of Botany* 97(3):519–524. https://doi.org/10.3732/ajb.0900243.

Wilson, B. F. 2000. Apical control of branch growth and angle in woody plants. *American Journal of Botany* 87(5):601–607. https://doi.org/10.2307/2656846.

Zheng, C., W. Guo, S. Huang, X. Xiao, G. Guo, X. Lian, and C. Lai. 2025. Branching pattern and branch biomass allocation of three widely used urban greening Ficus Linnaeus species in Southern China. *Tropical Ecology 2025 66:2* 66(2):228–239. https://doi.org/10.1007/s42965-025-00381-0.

Zhou, X., M. M. Schoeneberger, J. R. Brandle, T. N. Awada, J. Chu, D. L. Martin, J. Li, Y. Li, and C. W. Mize. 2015. Analyzing the Uncertainties in Use of Forest-Derived Biomass Equations for Open-Grown Trees in Agricultural Land. *Forest Science* 61(1):144–161. https://doi.org/10.5849/forsci.13-071.

CHAPTER 4

OVERALL DISCUSSION AND CONCLUSIONS

4.1 Discussion

The main question addressed in this thesis was how aboveground carbon storage in urban trees is shaped by both biological variation and methodological choices, and how these sources of variation can be integrated to improve carbon accounting. The results show that accurate carbon estimation in urban trees cannot rely on a single simplification, whether that is a forest-derived allometric equation, a published wood density value, or a fixed assumption that dry biomass is 50% carbon. Instead, urban tree carbon reflects the combined effects of tree architecture, wood properties, species identity, and growing environment. This is particularly important in urban forests because open-grown trees often differ structurally from forest-grown trees, and urban site conditions can alter both growth and wood traits in ways that generalized methods do not capture (McHale et al. 2009; Weiskittel et al. 2015; Kükenbrink et al. 2021)

A key synthesis from this work is that urban tree carbon storage depends on both the amount of woody structure produced and the carbon concentration of that structure. Chapter 2 showed that species and growing environment influenced wood carbon concentration, growth through time, and xylem anatomical traits. Chapter 3 showed that carbon estimates remained sensitive to the wood density and carbon concentration values used to convert TLS-derived volume into carbon biomass. Together, these findings indicate that uncertainty in urban tree carbon estimates does not end with biomass estimation; it continues through the full volume-to-carbon conversion chain. In this sense, the study extends the usual view of carbon estimation as

mainly a biomass problem and shows that it is also a wood-trait problem, especially in mixed-species urban forests and across heterogeneous urban sites.

The biological findings further indicate that growing environment matters not only because it influences tree size, but also because it affects how trees function. Park trees generally accumulated more carbon biomass over time than street trees, and the anatomical results for the two oak species suggest that this difference is linked to contrasting hydraulic strategies. Park-grown oaks exhibited vessel traits associated with greater hydraulic efficiency, whereas street-grown oaks exhibited traits associated with greater hydraulic safety. This pattern is consistent with the well-established efficiency–safety trade-off in xylem structure, in which larger conduits increase water transport efficiency and potentially support greater carbon gain, while smaller conduits reduce cavitation risk under chronic stress (Hacke et al. 2017; Rissanen et al. 2025). The importance of this result is not that xylem anatomy alone fully predicts carbon storage, but that it provides a physiological explanation for why trees growing in constrained urban sites may store less carbon even within the same species.

This interpretation also clarifies the relationship between tree growth and carbon content. Trees growing in more favorable urban environments are not simply larger because they have more space or time; they may also maintain hydraulic systems that better support stomatal conductance, carbon assimilation, and sustained wood formation. In contrast, trees exposed to stronger urban stress may shift toward safer but less efficient hydraulic strategies, which can limit long-term carbon accumulation. This interpretation agrees with broader evidence that urban stressors such as restricted soil volume, compaction, impervious cover, and altered water supply can suppress growth and modify wood formation (McHale et al. 2009; Sonti et al. 2025). Urban

carbon storage, therefore, should not be viewed only as a consequence of tree size, but as the outcome of linked structural and physiological responses to site conditions.

From a methodological perspective, this thesis confirms that terrestrial laser scanning (TLS) represents a major advance for urban tree carbon estimation because it measures tree structure directly. This is especially valuable for urban trees, whose open-grown architecture often differs markedly from that of forest-grown trees. Previous studies have shown that biomass estimates based on equations developed outside urban environments can vary substantially, with error at the individual-tree level sometimes exceeding 300% (McHale et al. 2009). By contrast, TLS-derived biomass estimates have shown strong agreement with destructive reference data for urban trees and have consistently outperformed conventional allometric approaches (Kükenbrink et al. 2021; Arseniou et al. 2023). The present study supports that broader conclusion and extends it by showing that TLS not only improves whole-tree carbon estimation but also reveals how carbon is distributed among stems and branches within urban tree crowns.

At the same time, improved structural measurement does not automatically produce an unbiased carbon estimate. Once woody volume is measured more accurately, the remaining uncertainty shifts to the factors used to convert volume to biomass and biomass to carbon. This is why the scenario analysis in Chapter 3 is important. It showed that even when the same TLS-derived volume was used, carbon estimates changed meaningfully depending on whether wood density and carbon concentration were measured directly or taken from published defaults. This pattern is consistent with earlier work showing that wood density varies within and among trees and that using published values can affect TLS-based biomass estimation (Demol et al. 2021; Arseniou et al. 2023). It is also consistent with broader evidence that carbon concentration varies among species and can change with tree size and age, meaning that a fixed carbon concentration

may introduce systematic bias (Lamlom and Savidge 2003; Thomas and Martin 2012). The main methodological contribution of this thesis, therefore, is not only to show that TLS is useful, but to show that it is most effective when paired with biologically realistic wood-trait information. The species-specific sensitivity of carbon estimates to wood density and carbon concentration has important implications for urban inventories. For the two oak species in this study, measured carbon concentration was substantially lower than the commonly assumed 50%, whereas *T. distichum* was much closer to that value. This pattern is consistent with syntheses showing that conifers often have higher wood carbon concentrations than angiosperms, partly because of differences in lignin chemistry and tissue composition (Thomas and Martin 2012). In practical terms, this means that a fixed carbon concentration may appear reasonable for some species while producing systematic over- or underestimation for others. The same logic applies to wood density. Sonti et al. (2025) showed that wood specific gravity in urban-grown hardwoods can vary across urban site types and may differ from values reported for forest-grown trees. Generic defaults are therefore most problematic in the very conditions that characterize urban forests: mixed-species populations, heterogeneous site conditions, and structurally atypical trees.

The component-level analyses in Chapter 3 add another important layer to this synthesis by showing that carbon biomass allocation within urban trees is highly uneven and strongly influenced by architecture. A relatively small number of large, low-order branches contained a disproportionate share of total branch carbon biomass, and branch carbon biomass was concentrated mainly in the lower to mid-crown. This matters because open-grown urban trees often invest heavily in large scaffold branches, which are structurally and hydraulically important but are not represented explicitly in traditional allometric approaches. These patterns are broadly consistent with the logic of pipe model theory, which links supporting stem tissue to

the foliage and branch systems it supplies (Shinozaki et al. 1964), while also aligning with later work showing that such relationships vary with ontogeny and environment rather than following a universal constant form (Lehnebach et al. 2018). Likewise, branching-network theory suggests that tree structure is shaped by transport and biomechanical constraints, but that real trees often deviate from idealized symmetrical forms (West et al. 1997). In this thesis, these theories are most useful not as strict predictive laws, but as conceptual frameworks for understanding why branch carbon biomass accumulates disproportionately in the large scaffold structures that organize the urban crown.

The comparison with i-Tree Eco places these findings in a more applied context. The strong correlations between TLS- and i-Tree-based carbon estimates indicate that i-Tree captures relative differences among trees reasonably well, which helps explain its value for city-scale inventories and broad ecosystem-service assessments. However, the fact that agreement changed depending on species and on whether the Crown Light Exposure (CLE) adjustment was applied shows that a single generalized multiplier cannot fully represent the diversity of open-grown urban tree forms. This is consistent with earlier critiques of applying generalized biomass corrections to urban trees, particularly when forest-derived allometries are used for species with distinct crown architecture and branching patterns (McHale et al. 2009; Kükenbrink et al. 2021). The broader implication is that operational models such as i-Tree Eco remain useful for screening and inventory purposes, but they should not be assumed to provide equally accurate estimates across all urban species and forms. TLS is especially valuable in this context because it provides an independent, non-destructive reference against which such models can be evaluated and improved.

Overall, the findings support a broader shift in urban forest carbon accounting: from generic, equation-driven estimates toward integrated, context-sensitive estimation frameworks. Such a shift does not require destructive sampling of every tree or the abandonment of inventory tools. Rather, it requires recognizing that urban trees are both biologically and structurally diverse, and that methods should reflect that diversity where it matters most. For city-scale planning, generalized tools may still be appropriate. However, for calibrating urban allometries, evaluating large high-value trees, benchmarking carbon inventories, or improving policy-relevant estimates, direct structural measurements and locally representative wood traits are increasingly important. This is especially relevant as urban forests are more frequently included in climate mitigation strategies, greenhouse gas accounting, and ecosystem-service valuation frameworks (Weiskittel et al. 2015; Kükenbrink et al. 2021).

The management implications of this work are equally clear. If urban site conditions influence both growth and wood properties, then improving urban carbon storage is not simply a matter of planting more trees. It also requires creating conditions that allow planted trees to realize high-carbon growth trajectories over time. Street trees often grow in the very places where cooling, air-quality improvement, and climate adaptation benefits are most needed, yet they also face the strongest structural and physiological constraints. The results therefore support management strategies that increase rooting volume, reduce soil compaction, improve infiltration and water availability, and account for species-specific performance across urban settings. More broadly, reliable urban carbon accounting depends not only on how much wood a tree has, but also on how urban conditions shaped that wood and the physiology behind its formation.

4.2 Limitations and Future Research

This thesis provides an integrated assessment of urban tree carbon storage and estimation; however, several limitations should be acknowledged. The study was conducted in a single city and focused on only three species. While these species represent contrasting wood traits and ecological strategies, they do not capture the full functional diversity of urban tree populations. Expanding this work across more species, cities, and climatic regions will be necessary to determine how broadly these findings apply, particularly for diffuse-porous hardwoods, evergreen broadleaves, and other conifer taxa that may respond differently to urban stress and differ in branch architecture or wood chemistry (Weiskittel et al. 2015; Kükenbrink et al. 2021).

Wood density and carbon concentration were measured from increment cores extracted at breast height. This approach is practical and minimally destructive, but it does not capture the full within-tree variation in these traits. Both wood density and carbon concentration can vary radially, vertically, and among organs, and this variation may influence biomass-to-carbon conversion when high precision is required. Previous work has shown that vertical variation in basic wood density can affect TLS-based biomass estimation, and syntheses of carbon concentration have also highlighted variation among tissues and tree sizes (Thomas and Martin 2012; Ma et al. 2020; Demol et al. 2021). Future studies should therefore evaluate whether multi-height or multi-organ sampling improves urban carbon estimation enough to justify the added effort.

The anatomical analysis in this thesis was limited to the two ring-porous oak species. That focus was appropriate given the biological differences between vessel-bearing angiosperms and conifers, but it means that the mechanistic relationship between hydraulic design and carbon accumulation was not tested for *T. distichum*. Because conifers rely mainly on tracheids rather

than vessels, future work should examine whether tracheid dimensions, wall reinforcement, or related anatomical traits provide similar mechanistic insight into carbon accumulation across contrasting urban environments.

TLS-based estimation still has methodological limitations even when it outperforms traditional allometric approaches. Occlusion, fine-branch reconstruction error, co-registration uncertainty, and the need for leaf–wood separation in leaf-on scans can all affect QSM-derived volume estimates. Recent studies have shown that TLS-derived estimates are especially sensitive to the treatment of fine branches and to the performance of leaf–wood separation algorithms, particularly in trees with structurally complex crowns or conifer-like foliage arrangements (Arrizza et al. 2024; Chen et al. 2025). The use of *rTwig* in this study helped reduce overestimation of small branches, but continued improvement in fine-branch representation, scan registration, and classification methods remains important if TLS is to serve as a calibration standard for urban carbon accounting.

The comparison with i-Tree Eco was necessarily limited to the structure of the model and the parameterization available to the user. Because i-Tree combines multiple embedded allometries and standardized assumptions, it is difficult to isolate all sources of disagreement with an independent structural method such as TLS. The results should be interpreted as evidence that species- and architecture-specific bias can remain when broad operational models are applied to structurally diverse urban trees. Future work could build on this by using larger TLS reference datasets to test model behavior across more species, crown forms, and management histories, and to evaluate whether urban-specific corrections can outperform generalized CLE-based adjustments.

Several research directions follow directly from these limitations. A first priority is the development of larger multi-city TLS datasets paired with locally measured wood traits. Such datasets would allow testing whether wood density, carbon concentration, and carbon biomass allocation vary consistently across urban climates, soils, and management regimes. A second priority is linking component-level carbon biomass allocation to post-removal carbon pathways, since branch and stem fractions may differ in utilization, decomposition, and long-term carbon residence. A third priority is work that combines repeated TLS scanning with tree-ring and anatomical measurements to evaluate how drought, heat, pruning, and site modification alter both tree structure and wood properties over time. Together, these directions would move urban tree carbon accounting from static estimation toward a more mechanistic and dynamic understanding of urban tree carbon cycling.

4.3 Conclusions

This thesis demonstrates that accurate estimation of aboveground carbon biomass in urban trees requires an integrated approach that accounts for both structural and biological sources of variation. Species identity, growing environment, wood density, carbon concentration, and tree architecture all influenced carbon storage in this study, showing that urban tree carbon biomass cannot be represented adequately by generalized allometric equations or fixed biomass-to-carbon conversion factors alone.

Urban site conditions influenced carbon storage not only through differences in growth, but also through differences in wood chemistry and hydraulic structure. At the same time, the methodological result shows that TLS is a powerful non-destructive tool for quantifying woody volume and carbon biomass allocation in urban trees, particularly in large, open-grown individuals that are poorly represented by conventional allometries. However, structural

precision alone is not sufficient. The conversion of woody volume into carbon biomass remains sensitive to assumptions about wood density and carbon concentration, and those assumptions can introduce species-dependent bias when generic values are applied. The most reliable estimates were therefore obtained when TLS-derived volume was paired with locally measured wood traits.

From an applied perspective, the thesis supports a two-level approach to urban tree carbon accounting. Broad-scale inventory tools such as i-Tree Eco remain useful for describing broad patterns across urban tree populations, but TLS combined with measured wood traits provides a stronger reference framework when higher accuracy is required. More broadly, improving urban forest carbon storage depends not only on planting trees, but also on maintaining growing conditions that allow trees to survive, grow efficiently, and accumulate substantial woody carbon over time.

In summary, urban tree carbon estimates are most reliable when they reflect both how trees are structurally built and how urban environments shape their wood properties and growth.

References

Arrizza, S., S. Marras, R. Ferrara, and G. Pellizzaro. 2024. Terrestrial Laser Scanning (TLS) for tree structure studies: a review of methods for wood-leaf classifications from 3D point clouds. *Remote Sensing Applications: Society and Environment* 36:101364. https://doi.org/10.1016/J.RSASE.2024.101364.

Arseniou, G., D. W. MacFarlane, K. Calders, and M. Baker. 2023. Accuracy differences in aboveground woody biomass estimation with terrestrial laser scanning for trees in urban and rural forests and different leaf conditions. *Trees - Structure and Function* 37(3):761–779. https://doi.org/10.1007/S00468-022-02382-1/.

Chen, S., H. Verbeeck, L. Terryn, W. A. J. Van den Broeck, M. B. Vicari, M. Disney, N. Origo, et al. 2025. The impact of leaf-wood separation algorithms on aboveground biomass estimation from terrestrial laser scanning. *Remote Sensing of Environment* 318:114581. https://doi.org/10.1016/J.RSE.2024.114581.

Demol, M., K. Calders, S. M. Krishna Moorthy, J. Van den Bulcke, H. Verbeeck, and B. Gielen. 2021. Consequences of vertical basic wood density variation on the estimation of aboveground biomass with terrestrial laser scanning. *Trees - Structure and Function* 35(2):671–684. https://doi.org/10.1007/S00468-020-02067-7/.

Hacke, U. G., R. Spicer, S. G. Schreiber, and L. Plavcová. 2017. An ecophysiological and developmental perspective on variation in vessel diameter. *Plant Cell and Environment* 40(6):831–845. https://doi.org/10.1111/PCE.12777.

Kükenbrink, D., O. Gardi, F. Morsdorf, E. Thürig, A. Schellenberger, and L. Mathys. 2021. Above-ground biomass references for urban trees from terrestrial laser scanning data. *Annals of Botany* 128(6):709–724. https://doi.org/10.1093/AOB/MCAB002.

Lamlom, S. H., and R. A. Savidge. 2003. A reassessment of carbon content in wood: variation within and between 41 North American species. *Biomass and Bioenergy* 25(4):381–388. https://doi.org/10.1016/S0961-9534(03)00033-3.

Lehnebach, R., R. Beyer, V. Letort, and P. Heuret. 2018. The pipe model theory half a century on: a review. *Annals of Botany* 121(5):773–795. https://doi.org/10.1093/aob/mcx194.

Ma, S. H., A. Eziz, D. Tian, Z. B. Yan, Q. Cai, M. W. Jiang, C. J. Ji, J. Y. Fang, and O. J. Sun. 2020. Size- and age-dependent increases in tree stem carbon concentration: implications for forest carbon stock estimations. *Journal of Plant Ecology* 13(2):233–240. https://doi.org/10.1093/JPE/RTAA005.

McHale, M. R., I. C. Burke, M. A. Lefsky, P. J. Peper, and E. G. McPherson. 2009. Urban forest biomass estimates: is it important to use allometric relationships developed specifically for urban trees? *Urban Ecosystems* 12(1):95–113. https://doi.org/10.1007/s11252-009-0081-3.

Rissanen, K., V. Vitali, D. Kneeshaw, and A. Paquette. 2025. Vessel anatomy of urban Celtis occidentalis trees varies to favour safety or efficiency depending on site conditions. *Trees 2025 39:1* 39(1):1–15. https://doi.org/10.1007/S00468-025-02603-3.

Shinozaki, K., K. Hozumi, and T. Kira. 1964. A quantitative analysis of plant form-the pipe model theory: II. Further evidence of the theory and its application in forest ecology. *Japanese Journal of Ecology* 14(4):133–139. https://doi.org/10.18960/SEITAI.14.4_133.

Sonti, N. F., J. A. Westfall, M. C. Wiemann, and T. L. Eberhardt. 2025. Influence of site type on wood specific gravity and ash content for urban-grown hardwoods. *Urban Ecosystems 2025 28:3* 28(3):122-. https://doi.org/10.1007/s11252-025-01735-1.

Thomas, S. C., and A. R. Martin. 2012. Carbon Content of Tree Tissues: A Synthesis. *Forests 2012, Vol. 3, Pages 332-352* 3(2):332–352. https://doi.org/10.3390/f3020332.

Weiskittel, A. R., D. W. MacFarlane, P. J. Radtke, D. L. R. Affleck, H. Temesgen, C. W. Woodall, J. A. Westfall, and J. W. Coulston. 2015. A Call to Improve Methods for Estimating Tree Biomass for Regional and National Assessments. *Journal of Forestry* 113(4):414–424. https://doi.org/10.5849/JOF.14-091.

West, G. B., J. H. Brown, and B. J. Enquist. 1997. A general model for the origin of allometric scaling laws in biology. *Science* 276(5309):122–126. https://doi.org/10.1126/science.276.5309.122.